The Synthesis and Medicinal Applications of Pyrogallol[4]arenes

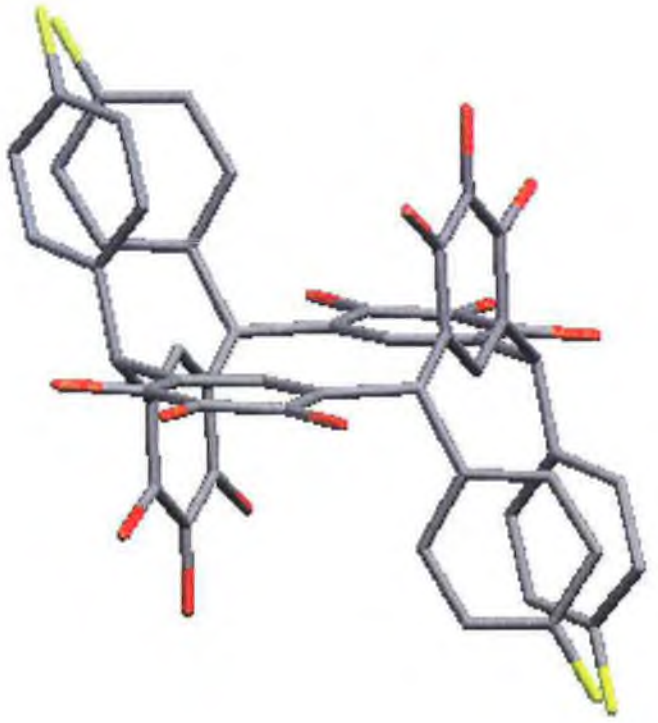

Stephen Carey
K. Nolan Research Group
August 2006

Ph.D. Thesis

DCU Science & Health Studies
Project Submission Form

Student Name:	**Stephen James Joseph Carey**
Student Number:	**98034227**
Project Title:	**The Synthesis and Medicinal Applications of Pyrogallol[4]arenes**
Module code:	**Ph.D.**
Programme:	**CHPD4 - PhD**
Lecturer:	**Dr. K. Nolan**
Project Due Date:	**25/09/2006**

Declaration

I the undersigned declare that the project material, which I now submit, is my own work. Any assistance received by way of borrowing from the work of others has been cited and acknowledged within the work. I make this declaration in the knowledge that a breach of the rules pertaining to project submission may carry serious consequences.

I am aware that the project will not be accepted unless this form has been handed in along with the project.

Signed: Stephen Carey

26/09/06

Contents:

List of Schemes, Figures and Tables:

List of Abbreviations

2-D	two dimensional
2-HOC_6H_4	ortho phenol
3-D	three dimensional
4-BrC_6H_4	para-bromo phenyl
4-$C_6H_5C_6H_4$	naphthyl
4-$H_2NC_6H_4$	para-amino phenyl
4-HOC_6H_4	para-phenol
Å	angstrom
μM	micromolar
μg/ml	microgram per millilitre
π	pi
σ	sigma
AgO_2	silver oxide
AIDS	acquired immunodeficiency syndrome
Alk	alkyl
Ar	aryl
aq	aqueous
AZT	Azidothymidine
$BaCl_2$	barium chloride
Br	bromo group

Br_2	bromine
^oC	degrees celsius
%C	percentage of carbon
$CaCl_2$	calcium chloride
CD4	T-helper cell
CD4i	induced T-helper cell
CH_3	methyl
$CH_2(CH_2)_4$	pentyl
$C_6H_5(CH_2)_2$	vinyl
$(C_6H_5)*Fe*(C_6H_4)$	ferrocenyl
$CHCl_3$	chloroform
$Cl(CH_2)_5$	1-chloro pentyl
CS_2	carbon disulphide
CsCl	caesium chloride
Cpd	compound
CuCl	copper (I) chloride
$CuCl_2$	copper (II) chloride
CV-N	cyanovirin
d	doublet
DCU	Dublin City University
DBU	1,8-diazabicyclo[5.4.0]undecene
DEAD	diazenedicarboxylic acid diethyl ester
DMF	dimethylformamide
DMSO	dimethylsulfoxide
DNA	deoxyribonucleic acid

D2S	dextran-2-sulphate
EC_{50}	median effective concentration that killed 50% of the cells
ELISA	enzyme linked immunosorbent assay
Env	envelope
eq	equivalents
[eq]	equivalent ppm difference
ESI	electrospray ionisation
et. al.	and others
EtBrOAc	ethylbromo acetate
EtOH	ethanol
expt	experiment
g	gram
g/ml	gram per millilitre
gp	glycoprotein
%H	percentage of hydrogen
HCl	hydrochloric acid
HIV	human immunodeficiency virus
^{1}H-NMR	proton nuclear magnetic resonance
H_2O	water
HOBT	hydroxy benzotriazole
$HO(CH_2)_4$	hydroxy butyl
HPLC	high performance liquid chromatography
IC_{50}	inhibitory concentration that killed 50% of the cells
IR	infrared
k	kelvin

K	equilibrium constant
KBr	potassium bromide
K_2CO_3	potassium carbonate
kD	kilodalton
KOH	potassium hydroxide
LiAlH4	lithium aluminium hydride
LiCl	lithium chloride
m-	*meta* substituent
M	molarity
M^{-1}	inverse moles (units of K (equilibrium constant))
MeOH	methanol
$MgCl_2$	magnesium chloride
$MgSO_4$	magnesium sulphate
MHz	megahertz
ml	millilitre
mmol	millimoles
MS	mass spectrometry
M/Z	mass to charge ratio
%N	percentage of nitrogen
$NaBH_4$	sodiumborohydride
NaCl	sodium chloride
$NaOCH_3$	sodium methoxide
NaOD	sodium deuteroxide
NaOH	sodium hydroxide
NBS	N-bromosuccinimide

NCSR	National Centre for Sensor Research
$NiCl_2$	nickel (II) chloride
nm	nanometre
NMR	nuclear magnetic resonance
NMR-D	diffusion nuclear magnetic resonance
NNRTI	non- nucleotide reverse transcriptase inhibitor
No	number
NO_2	nitro group
NRTI	nucleotide reverse transcriptase inhibitor
o-	*ortho* substituent
O_2	Oxygen
OEt	ethoxy
p-	*para* substituent
p	protein
PCS	photon correlation spectroscopy
PDI	protein disulphide isomerase
pK_a	acid dissociation constant
PI	protease inhibitor
PPh_3	triphenyl phosphine
ppm	parts per million
PrBrOEt	ethylbromo propionate
rccc	reference, *cis, cis, cis*
rcct	reference, *cis, cis, trans*
rctt	reference, *cis, trans, trans*
RNA	ribonucleic acid

rtct	reference, *trans, cis, trans*
RT	room temperature
s	singlet
SIV	simian immunodeficiency virus
$SnCl_2$	tin chloride
Spec	spectrometry
THF	tetrahydrofuran
TLC	thin layer chromatography
Vol	volume
$ZnCl_2$	zinc chloride

Acknowledgments

To the guys in the Lab, Shane, Pauline, Íde, Irene, Nameer, Rob and Ben, thanks for all your help, advice and support.

To the lunch/coffee break crew, Eoin, Sarah, Paula, Linda, Ciarán, James and Martina, without you guys this thesis would have been submitted months ago!!!

To my Family for putting up with me taking over rooms in the house, using up all the ink and printing paper time and time again and coping with my 'bad' days when the computer crashed, a huge and long overdue thank you!

To my supervisor, Kieran Nolan, for always being there, whenever I had a problem over the three and a bit years. Your constant support, advice and problem solving skills got me through this.

To the technical staff in Chemical Sciences and in the NCSR, if ever a problem arose with anything in either building you were always there to dig me out of a hole, thanks.

To Swapan for all his help on the PCS work, Sarah for her assistance with Hyperchem, and to Dr. Helge Müller-Bunz for his work on the X-ray crystallography thanks guys!

Also a huge thank you to my proof-reader Pauline, with my bad spelling and atrocious typing, her role was pivotal in getting this thesis out.

Finally I'd like to thank anyone else I may have forgotten who made my last 7 years in DCU both incredibly enjoyable and memorable.

Thanks.

Abstract:

To date almost all pyrogallol[4]arenes reported in the literature have been prepared from alkyl aldehydes. We were interested in preparing more pyrogallol[4]arenes from commercially available benzaldehydes. On synthesising these compounds we discovered that they are structurally unique, compared to previously reported pyrogallol[4]arenes, as they exist in a *rctt* chair conformation as determined by X-ray crystallography and ^{1}HNMR.

We also discovered from our synthetic studies that the yields for the pyrogallol[4]arenes depend strongly on the electron donating/withdrawing ability of substituents placed in the benzaldehyde, the more electron withdrawing the higher the yield. We also discovered a unique metal salt effect on the condensation of pyrogallol with 4-fluorobenzaldehyde that doubled the yields of the resulting macrocycle. Interestingly, this effect is absent with the condensation of pyrogallol with alkyl aldehydes. The role of steric effects, using bulky substituted benzaldehydes was also investigated to determine whether the stereochemical outcome for these condensation reactions could be controlled.

The further derivatisation of the pyrogallol[4]arenes was also investigated. The preparation of partially and completely alkylated derivatives of these macrocycles was of interest to us. We found that the introduction of acetate groups could be readily accomplished, however other alkyl groups could not be efficiently introduced into the pyrogallol[4]arenes. The partially and completely alkylated acetate derivatives of pyrogallol[4]arene were screened for biological activity against HIV-1. It was discovered that the partially alkylated derivatives possessed higher selectivity indexes than the completely alkylated derivatives indicating that biological activity may not be dependent on charge.

Chapter 1

Literature Survey

1.1 Resorcinarenes

In 1940, Niederl and Vogel[1] studied several condensation products previously obtained from the reaction of aliphatic aldehydes and resorcinol. From molecular weight determinations they concluded that the ratio between aldehyde and resorcinol, in the product was 1:1. They proposed a cyclic tetrameric structure (figure 1) analogous to cyclic tetrameric structures frequently found in nature, (e.g porphyrins). This structure was finally proved in 1968 by Erdtman *et al.* by a single crystal X-ray analysis[2].

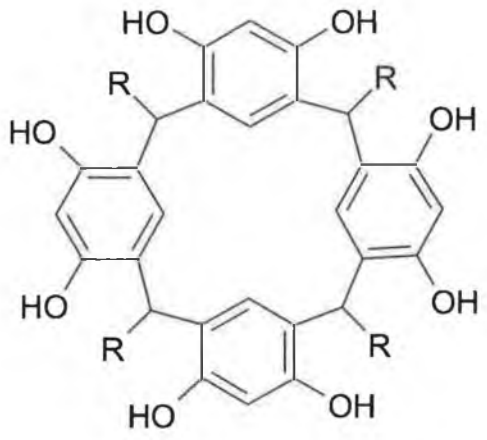

(1)

Figure 1: *General Structure of Resorcin[4]arenes*

A suitable trivial name for these molecules was never found. Gutsche and Bömher attempted to classify them as calixarenes by calling them calix[4]resorcinarenes[3] or resorcinol-derived calix[4]arenes[3,4], but totally different names like Högberg compounds[5], or simply octols[6,7] also appeared in the literature. In the mid 1990's the name resorcinarenes was suggested[8], which is widely used today.

Resorcinarenes, **1** can be prepared in reasonable to high yields *via* a simple, one-step procedure using either templates (such as metal templation see Chapter 2) or high dilution techniques. Most cases involve the acid-catalysed condensation reaction between resorcinol, **3** and an aliphatic or aromatic aldehyde.[5,6,9] The acid catalysed condensation reaction between resorcinol and an aldehyde is generally carried out by heating the constituents to reflux in a mixture of ethanol and concentrated hydrochloric acid for several hours, although for every aldehyde different optimal reaction conditions exist.[5,6,9] Usually, the cyclotetramer crystallizes from the reaction mixture but, in some cases, water should be added in order to isolate the product.[6,10]

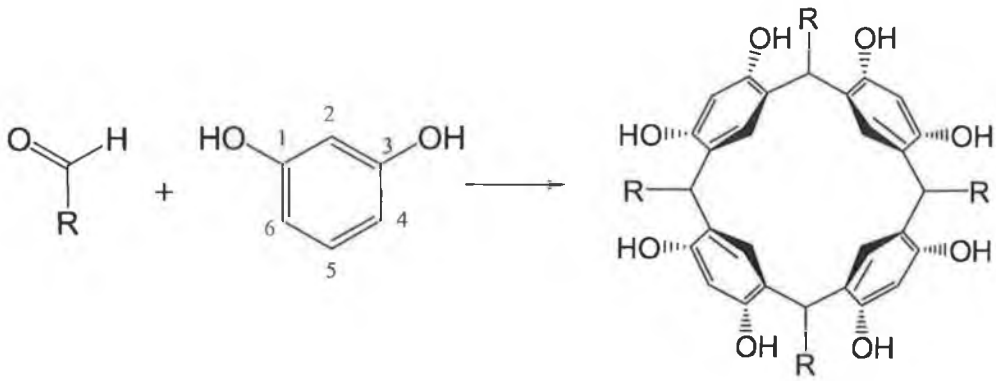

(2) (3) (1)

Scheme 1: *Preparation of Resorcin[4]arenes*

It was also found that resorcinol derivatives carrying electron withdrawing substituents like NO_2 or Br[6] at the 2-position of resorcinol, or in which the hydroxyl groups of resorcinol are partially alkylated[7] do not yield cyclomeric products due to the high electron withdrawing nature of these groups.

R Group (Scheme 2)	Yield (%)	Reference
$-CH_3$	73	7
$-(CH_2)_4CH_3$	77	6
$-(CH_2)_2C_6H_5$	69	6
$-(CH_2)_2NaO_3S$	40	11
$-(CH_2)_4HO$	80	6
$-(CH_2)_5Cl$	67	6
$2\text{-}HOC_6H_4\text{-}$	78	11
$4\text{-}BrC_6H_4\text{-}$	43	6
$4\text{-}C_6H_5C_6H_4\text{-}$	99	6
$4\text{-}H_2NC_6H_4\text{-}$	Not reported	11
$4\text{-}AcHNC_6H_4\text{-}$	52	6
$4\text{-}HOC_6H_4\text{-}$	91	11
$-(C_6H_4)*Fe*(C_6H_5)$	10	11

Table 1: *Yields of selected resorcinarenes synthesized from functionalised aliphatic or (substituted) benzaldehydes and resorcinols*

1.1.1 Structure and Conformations of Resorcinarenes

The non-planarity of resorcinarenes means that they can, in principle, exist in many different isomeric forms. The stereochemistry is generally defined as a combination of the following two stereochemical elements:

a). The conformation of the macrocyclic ring, which can adopt four symmetrical arrangements: Cone (1a), Boat (1b), Chair (1c), Saddle (1d). Below are crystal structure representations of the four conformations.

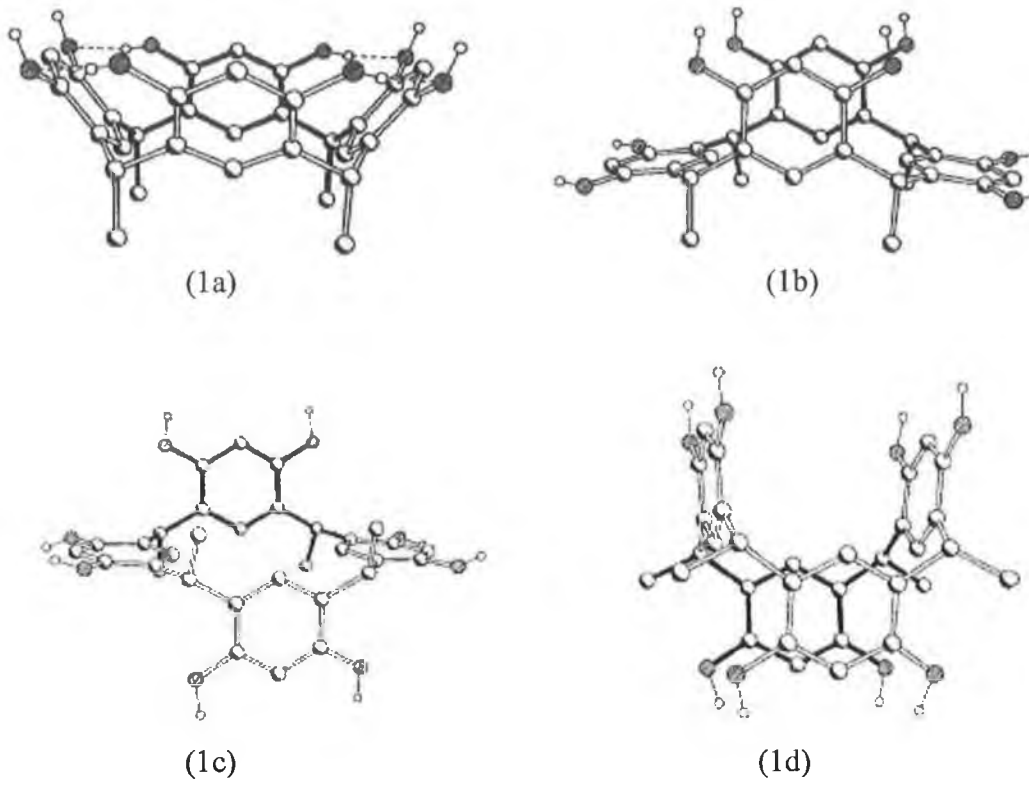

(1a) (1b)

(1c) (1d)

Figure 2: Conformations of Resorcin[4]arenes[12]

b). The relative configuration of the main substituent at the methylene bridges, gives the cis (*rccc*), cis-cis-trans (*rcct*), cis-trans-trans (*rctt*), trans-cis-trans (*rtct*).

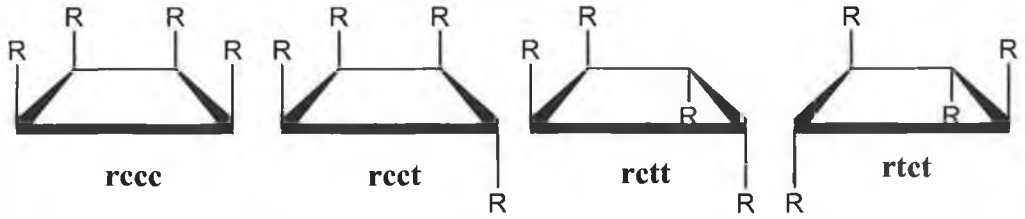

Figure 3: Configuration of substituent groups on resorcin[4]arenes

Combinations of these stereochemical elements gives rise to a vast number of possible stereoisomers. Thus far, the only four that have been found experimentally are the *rccc* cone, the *rctt* chair, the *rctt* saddle and the *rctt* boat. [11,13,14].

Typically, resorcinarenes derived from alkyl aldehydes exist in the *rccc* cone conformation (scheme 2), whereas those derived from aromatic aldehydes exist in a number of different conformations (scheme 3).

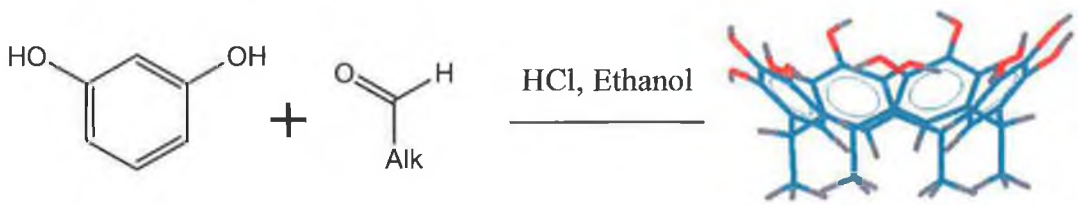

(3) (4) (1a)

Scheme 2: *Condensation of resorcinarene with an alkyl aldehyde.*

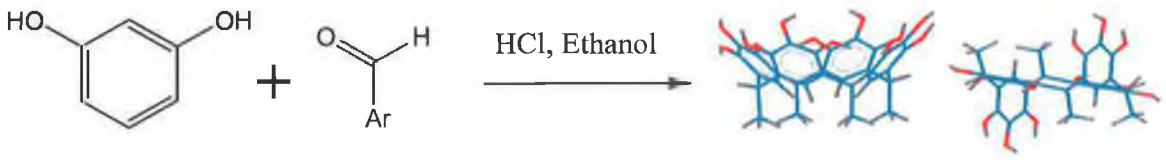

(3) (5) (1a) (1d)

Scheme 3: *Condensation of resorcinarene with an aromatic aldehyde*

1.1.2 Thermodynamic vs Kinetic formation of Resorcinarenes

In 1980 , Högberg reported that the formation of resorcinarenes was a combination of both thermodynamic and kinetic influences on the system. In a reaction of resorcinol and 4-bromobenzaldehyde, two conformations of resorcinarene were formed initially (figure 4). The first was the kinetically favoured product, **1c** the *rctt*-chair conformation and the second was the thermodynamically favoured *rccc*-boat conformation[15], **1b**.

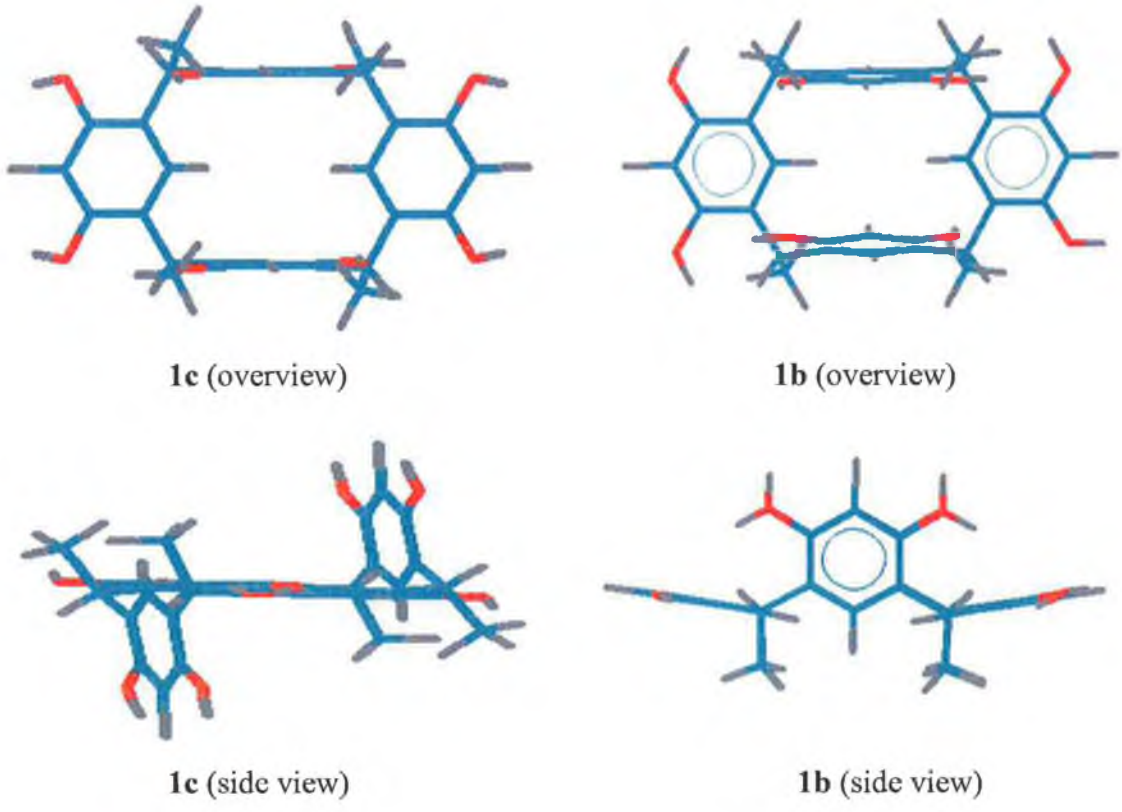

Figure 4: *(1c) rctt chair isomer; (1b) rccc boat isomer of resorcinarene.*

Högberg's study included ^{1}H-NMR, X-ray crystallography, and molecular modelling calculations. He also plotted the yields of these two conformations as a function of time (figure 5). It is clear from figure 5 that after 2 hours the maximum overall yield was reached, resulting in equal amounts of both conformations **1c** and **1b**. After a

further 8 hours of reaction time, only **1b** was present. This indicated that formation of isomer **1c** was reversible under the reaction conditions. This was subsequently confirmed by another reaction where isomer **1c** was treated under the same conditions as the condensation. After 5 hours an equal mixture of **1c** and **1b** was present, however after a further 5 hours all of **1c** was converted to **1b**.

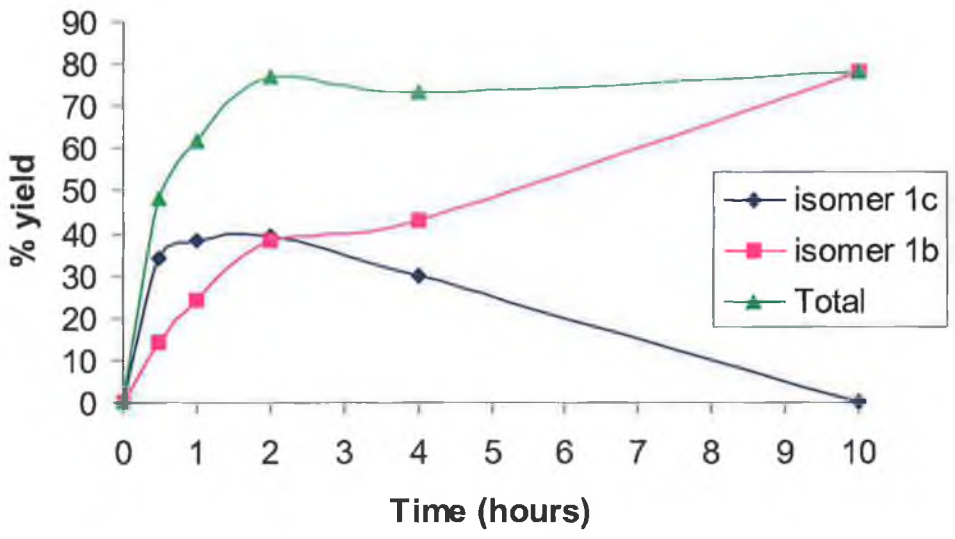

Figure 5: *Percentage Yield of isomers 1c and 1b as a function of time*[15].

Molecular modelling calculations were carried out on the octabutyrate derivatives of **1c** and **1b** and they were compared to other theoretical conformations and isomers. They were compared to the *rccc* boat with R groups in equatorial positions rather than axial positions. They were also compared to the *rccc* saddle conformation. Molecular models of stereostructures **1c** and **1b** appeared to be relatively free of steric compression and the phenyl groups are free to rotate. In the case of the other theoretical stereocentres (such as the *rccc* saddle isomer) there was an increased intramolecular steric repulsion and interlocking of the phenyl groups[15].

Anisotropic ring current effects on the proton in the 5 position of the resorcinol ring were calculated for the theoretical structures (using the Bovey-Johnson equation) and then compared to the experimental values for **1c** and **1b** (1a = 0.45ppm and 1b = 0.37ppm). The models of these stereostructures gave a value of 0.5ppm for both (these values are for the changes in chemical shift and are within acceptable limits). However the values for the other two stereocentres were not acceptable. (*rccc* boat [eq] = 0.1ppm; *rccc* saddle = 1.9ppm). This result shows that the latter two structures are unlikely[15]

1.1.3 Derivatisation of Resorcinarenes

1.1.3.1: Reaction of the Hydroxy Groups

The phenolic hydroxy groups of resorcinarenes can be completely acylated[16]. Many examples of octaesters (scheme 4)[17] of *rccc*, *rctt* and *rtct* regioisomers have been reported. The reaction proceeds with both alkyl and aromatic substituents, under basic conditions.

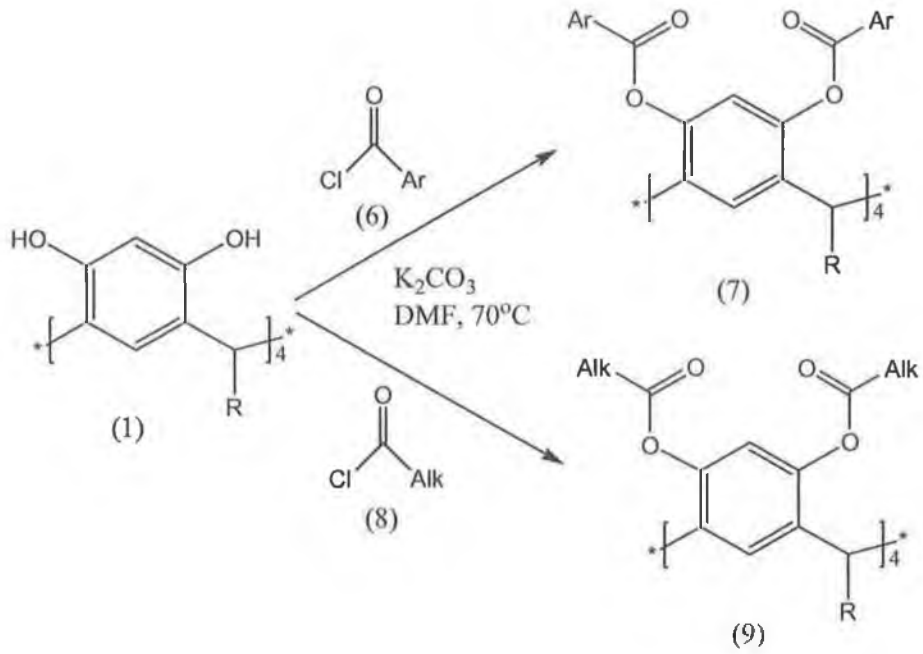

Scheme 4: *Acylation of resorcinarenes to octaesters*

The reaction of a resorcinarene with an excess of diarylchlorophosphate and diphenylchlorophosphine, gives octaphosphates[18] and octaphosphinites[19] respectively. This is shown in scheme 5, again basic conditions are used.

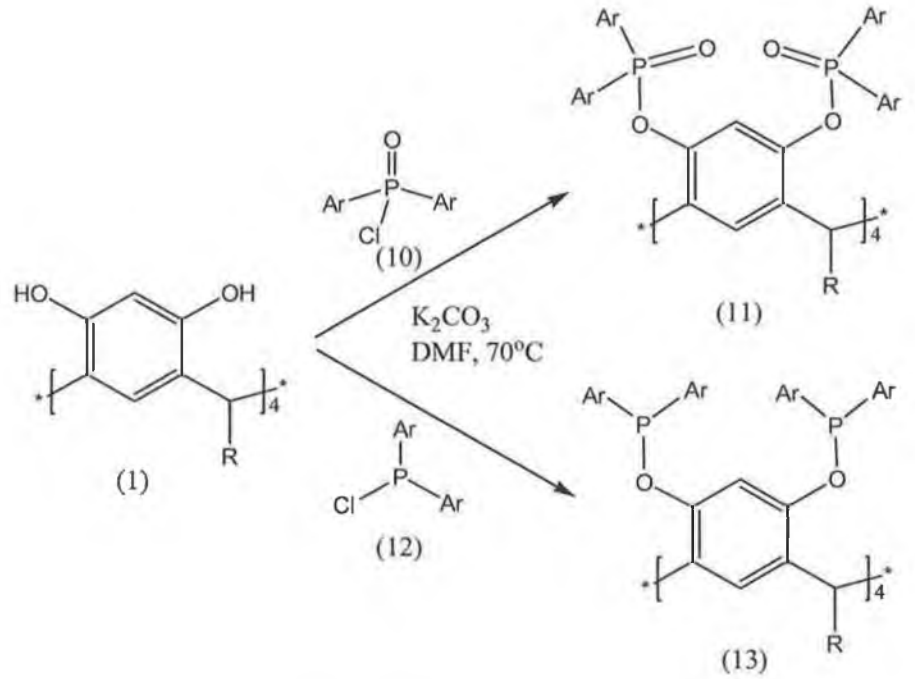

Scheme 5: *Formation of octaphosphates and octaphosphinites from resorcinarene*

The reaction of a resorcinarene with an excess of arylsulphonylchlorides gives octasulfonates[20]. Once again this reaction proceeds under basic conditions (scheme 6).

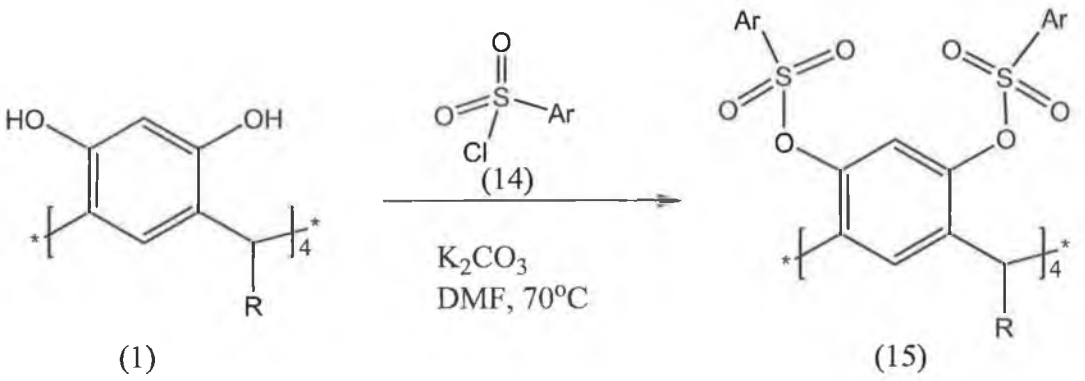

Scheme 6: *Formation of octasulfonate from resorcinarene*

The reaction of a resorcinarene with an excess of trimethylchlorosilane gives octa silyl derivatives[21]. This reaction is carried out under basic conditions, (scheme 7).

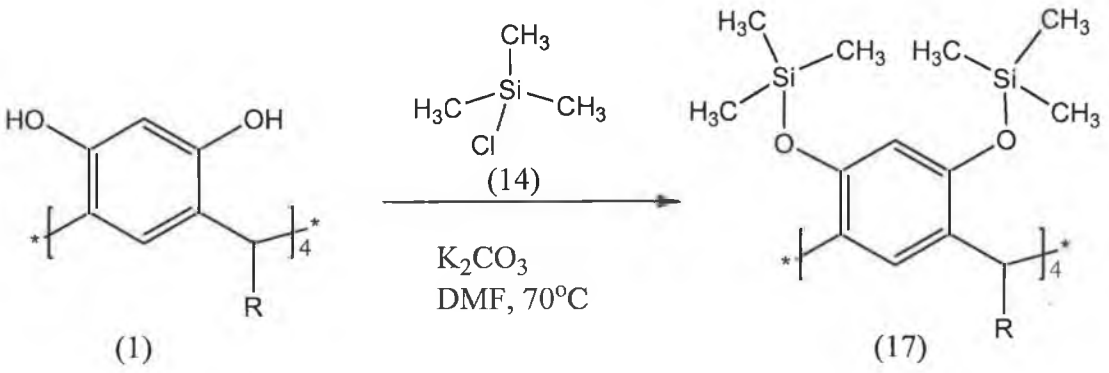

Scheme 7: *Octa silyl derivative formation from resorcinarene*

Complete O-alkylations of *rccc*-resorcinarenes result in octaethers[22] (scheme 8). The attachment of eight 3,5-dihydroxy benzyl ether groups to the *rccc*-resorcinarenes led to the first generation dendrimer, **19**.

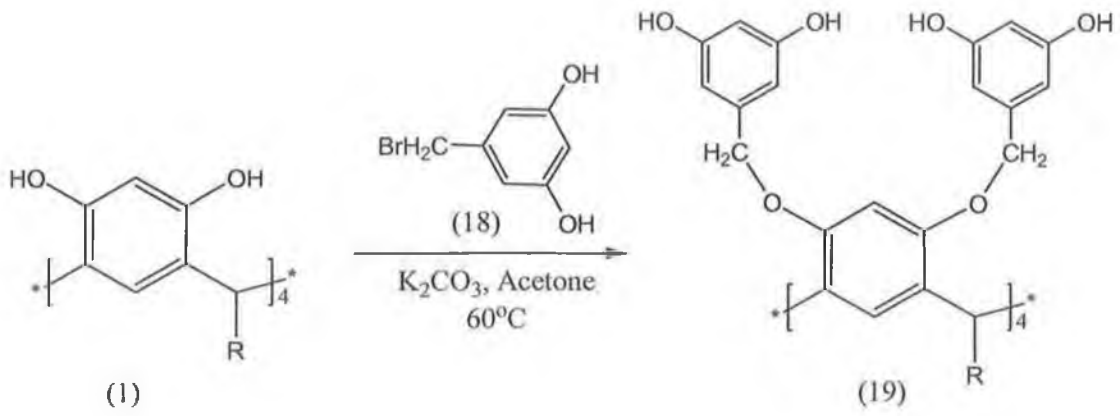

Scheme 8: *Alkylation of resorcinarene to form and octaether.*

Alkylation of a resorcinarene with excess ethylbromoacetate leads to octaesters, **21** which were then transformed into their corresponding octaacids, **22**[23] by hydrolysis. (scheme 9)

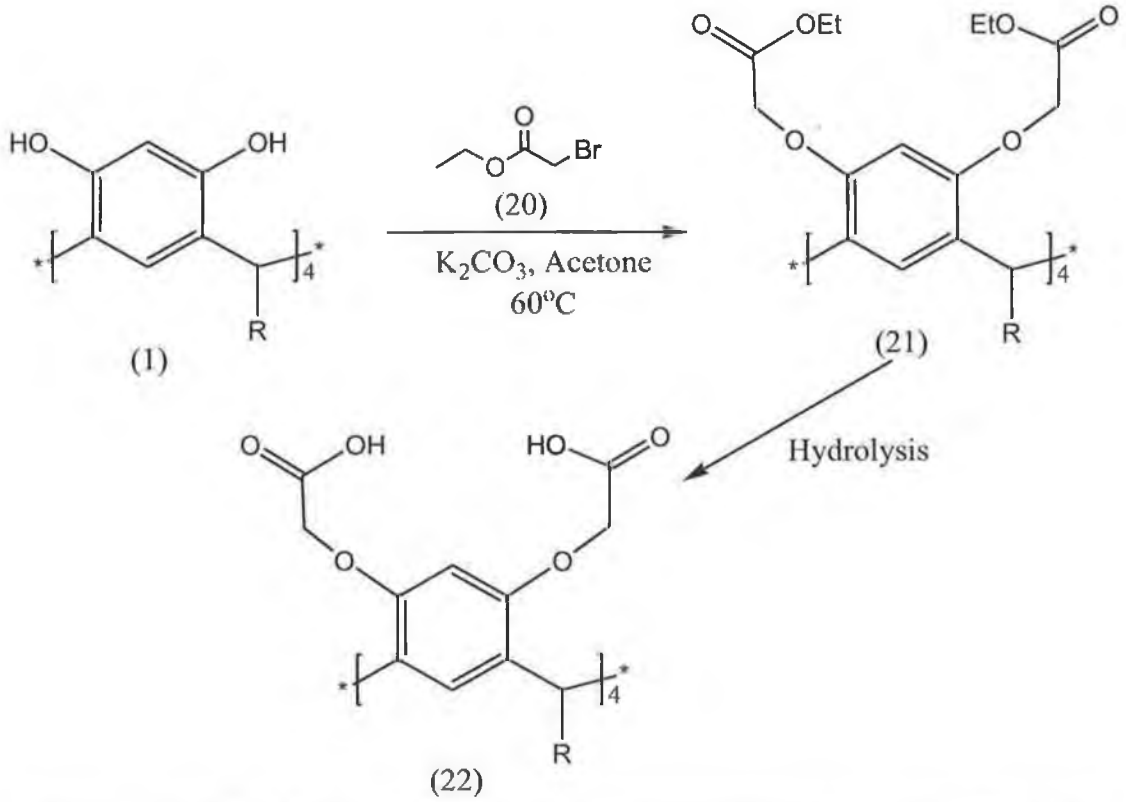

Scheme 9: *Esterification and hydrolysis of resorcinarene, to form the octaacid.*

Aminolysis of **21** with chiral amines and aminoalcohols resulted in chiral octaamide derivatives, **23**[23], as shown in scheme 10.

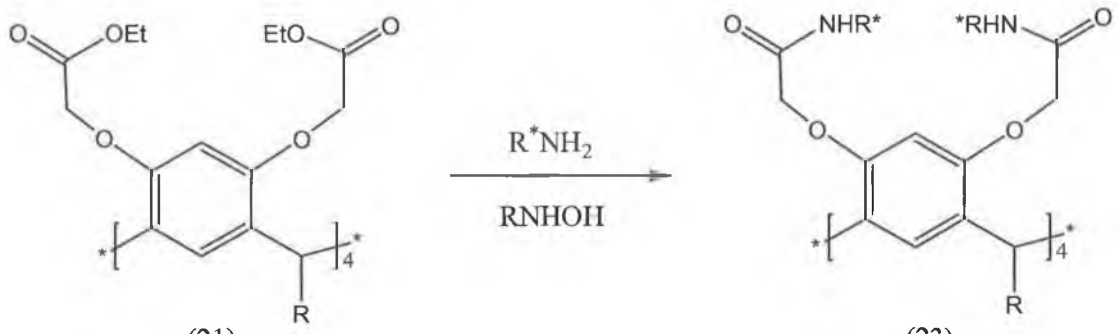

(21) (23)

Scheme 10: *Aminolysis of resorcinarene.*

Reduction of the octaester, **21,** with $LiAlH_4$ gave the octol, **24,** which underwent a Mitsunobu reaction with phthalimide, **25**, DEAD and PPh_3 to give an octaphthalimide, **26**. The hydrazinolysis of the phthalimido groups resulted in the corresponding octaamine, **27,** which was reacted with lactono-lactone to give a water soluble resorcinarene-sugar cluster (scheme 11). These sugar clusters are almost irreversibly adsorbed on the surface of a quartz plate, which acts as a simplified model of a multivalent receptor site[24]. This property has extensive application in biomimetic chemistry in mimicking enzyme interactions on a chemical scale[24].

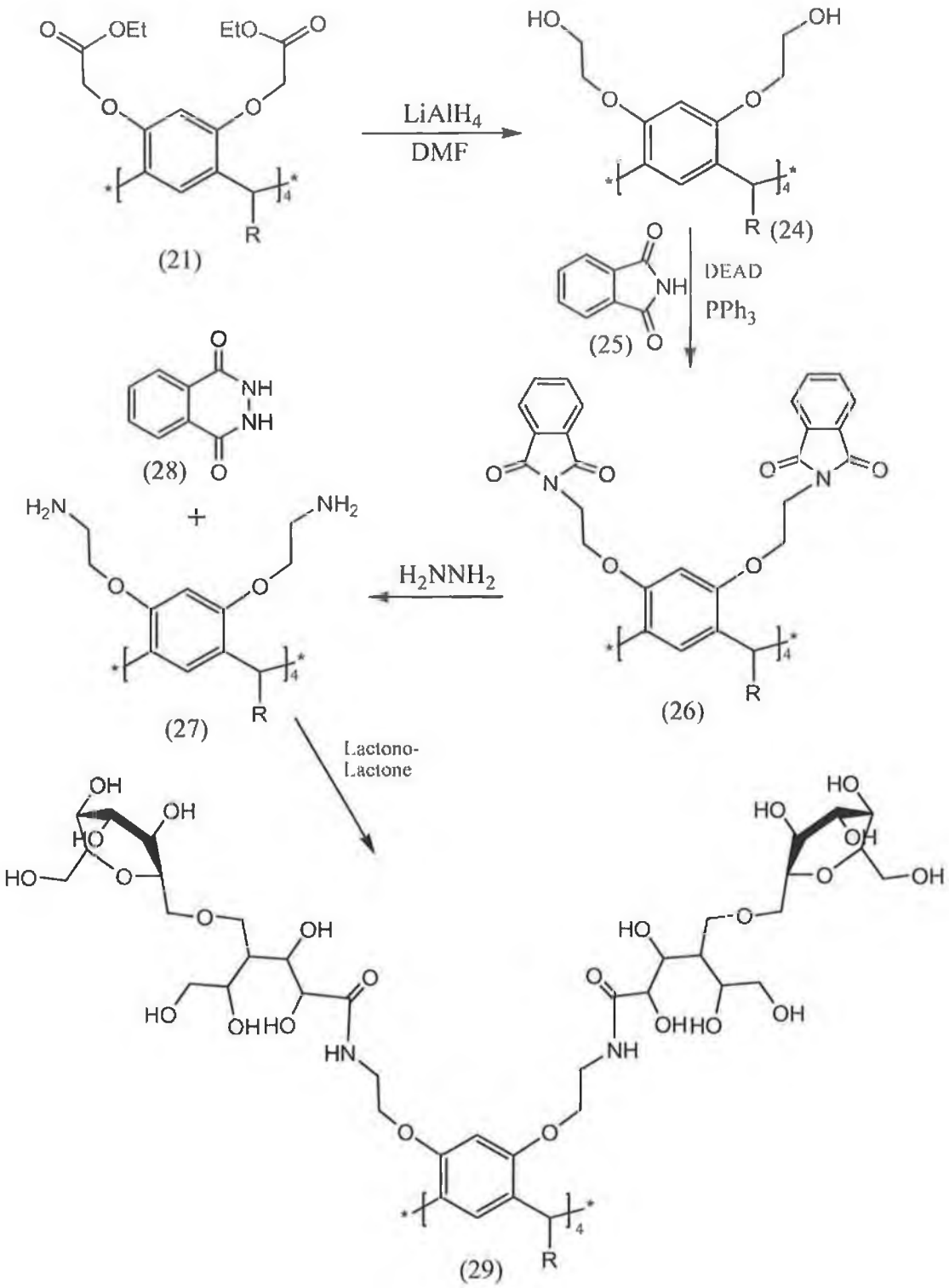

Scheme 11: *The formation of a water-soluble resorcinarene-sugar cluster via octol, octaphthalimide and octaamine intermediates, from the octaester.*

1.1.3.2 Electrophilic Substitutions at the Aromatic Rings.

The 2-position of the resorcinol rings may be substituted by mild electrophiles, for example by bromination or by coupling with diazonium salts. More severe reactions such as nitration failed probably due to the disruption of the resorcinarene skeleton. Bromination occurs at room temperature in 80% yield using excess N-bromosuccinimide as shown in scheme 12.

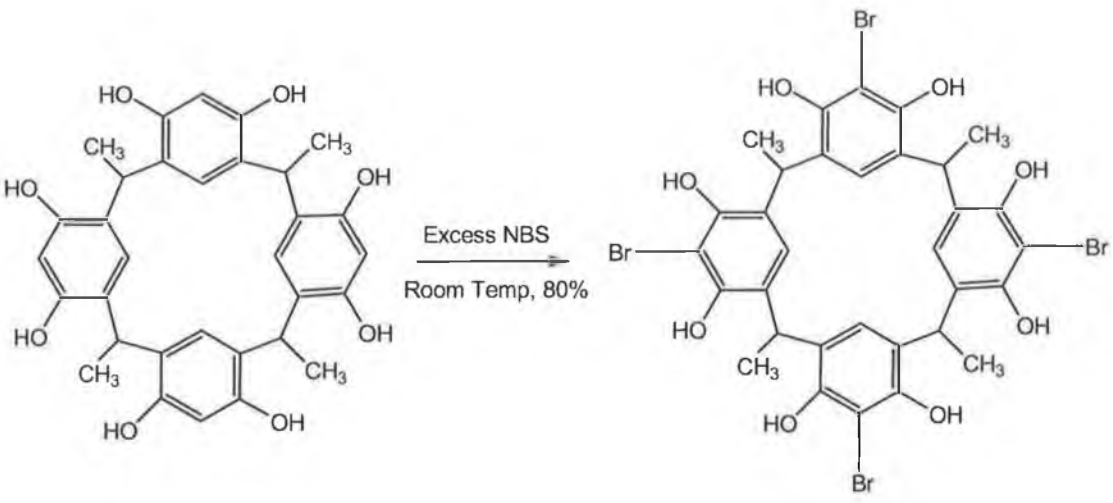

(30) (31)

Scheme 12: *Bromination of tetramethyl resorcin[4]arene using excess N-bromosuccinimide, NBS*

Aminomethylation of resorcinarenes with secondary amines and formaldehyde readily give the corresponding tetraamines, via the Mannich reaction (figure 6)[25] which exist in apolar solvents in a chiral C_4-symmetrical conformation with left or right handed orientation of the pendant hydrogen bonded amino groups[26]. In this study there were various functional groups including chiral and cation binding functions[27] that could be easily introduced to the resorcinarene platform.

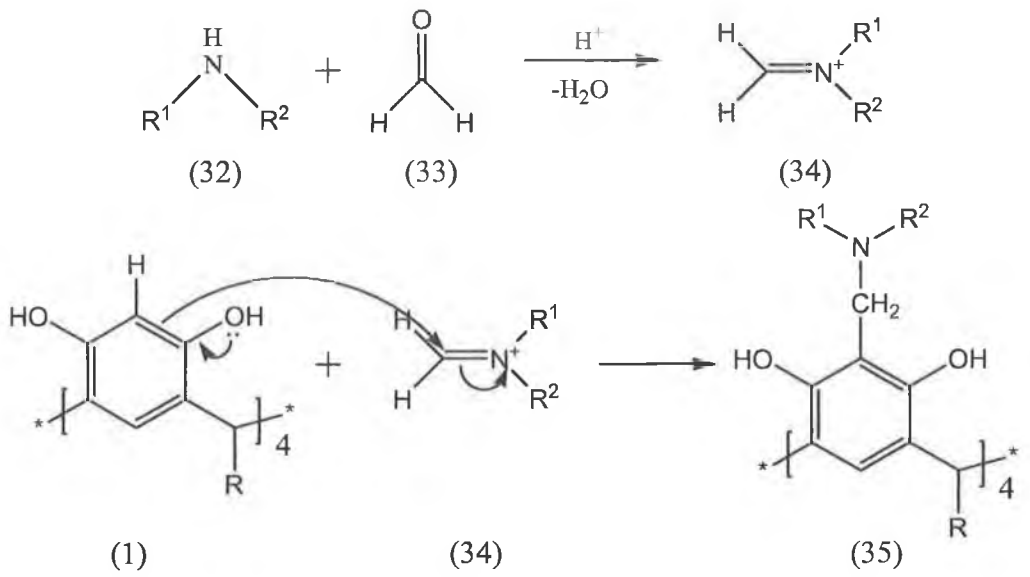

Figure 6: *Formation of a tetraamine resorcinarene via the Mannich reaction.*

1.1.3.3 Synthesis of Chiral Resorcinarenes

In the year 2005 Page et al.[28] described the first enantioselective syntheses (scheme 13) of a number of enantiomerically pure resoricinarene derivatives. The procedure enables ready access to multigram quantities of the diastereoisomerically pure tetrakis(benzoxazines) (figure 7) in a short route starting from resorcinol and dodecanal. Subsequent transformation provides C_{4n} symmetric resoricinarene derivatives as single enantiomers. The residual phenol and secondary amine groups allow for further functionalisation and the possibility of accessing a wide range of axially chiral resorcinarene derivatives. Investigations are currently underway to assess their application in the areas of chiral recognition and asymmetric catalysis.

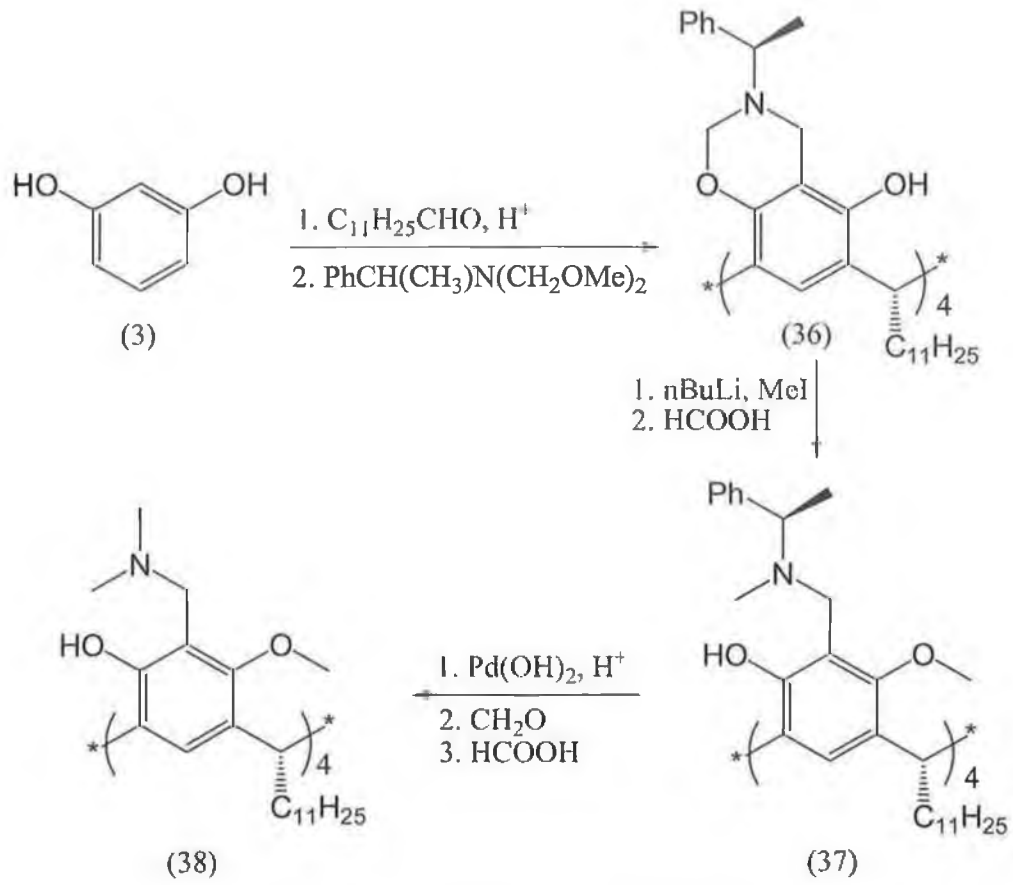

Scheme 13: *The synthesis of chiral resorcinarenes*

Almost all of these molecules adopt the cone or bowl-shape conformation. The bowl-shape of these molecules can be seen from this X-ray structure representation of a tetrakis(benzoxazine).

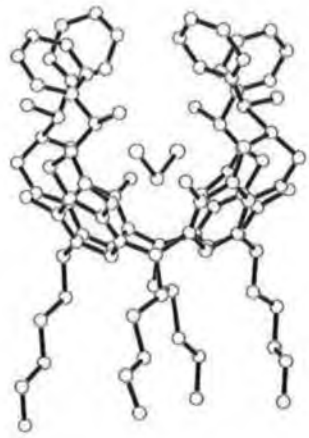

(39)

Figure 7: *X-Ray structure of 39*

1.1.4 Applications of Resorcinarenes

Resorcinarenes are highly soluble in aqueous basic solutions because of deprotonation of the phenolic hydroxyl groups. However, removal of the first four protons is much easier than the last four. Potentiomeric titrations have shown that the pK_a values for the first four protons are lower by two units than the pK_a of resorcinol, while the last four protons cannot even be removed with a strong base like $NaOCH_3$. The stability of the tetraphenolate (figure 8) is a result of the ideal geometric disposition of the O-H-O arrangement[29,30] and the possibility of delocalisation of negative charges. These factors combine to yield resorcinarenes as useful tools in cation complexation, with a possible application in sensor technology.

Tetraphenolate binds methyl trialkylammonium cations with spectacularly high binding constants ($K = 3x10^4 M^{-1}$ in 0.5N NaOD),[27,29,30] exceeding the corresponding constants in biological systems[31]. The strength of binding is only moderately affected by changing the ionic strength[32] or solvent polarity[33], indicating that the interaction is based almost exclusively on electrostatic attraction between the positively charged R_3N^+Me and the negatively charged resorcinarene[33]. In 1993, it was shown that neutral resorcinarenes are also able to complex alkylammonium cations, as was proved by a single X-ray crystal structure[34].

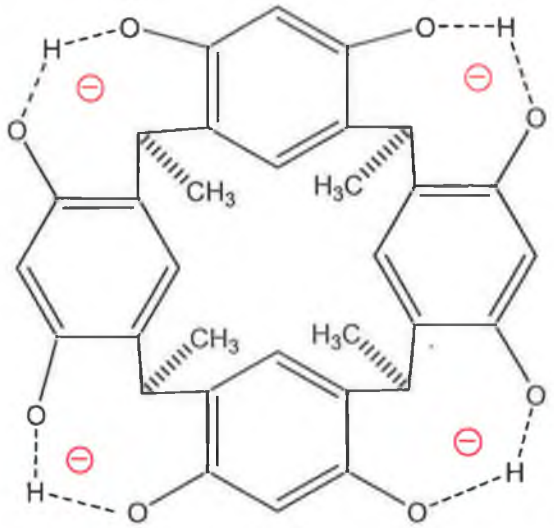

(40)

Figure 8: *Tetraphenolate resorcinarene – cation receptor*

Resorcinarenes have extensive use as host-guest receptors. One such example is illustrated in figure 9, where 6 resorcinarene molecules encapsulate a quaternary ammonium guest. Host structures held together by hydrogen bonds have quite significant lifetimes in organic solvents, long enough to directly observe the encapsulated guest by NMR spectroscopy[35].

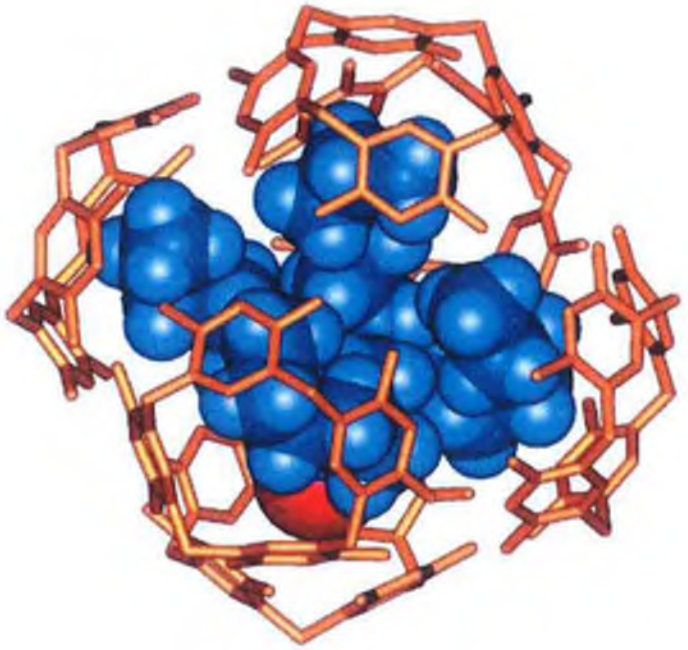

(41)

Figure 9: *Ammonium guest encapsulated by six resorcinarene molecules*[35]

1.1.5 Cram's Cavitands

Resorcinarenes can be used as the starting material in the synthesis of a class of macrocycle know as cavitands, so named by Cram in 1982.[36] Cavitands are structurally novel and have application in host-guest chemistry.

Scheme 14 outlines the synthesis of a cavitand, which has been synthesised by a covalent linkage of neighbouring hydroxyl groups of the corresponding resorcin[4]arene. The first reported synthesis outlined a reaction of a resorcinarene with excess bromochloromethane in a mixture of DMSO and DMF under basic conditions. The cavitand was recovered in 23% yield.

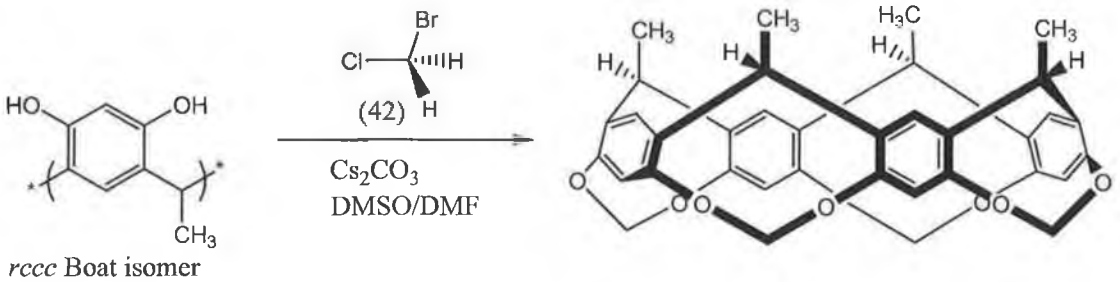

rccc Boat isomer (30)

(43)

Scheme 14: *The synthesis of the first of Cram's cavitand.*

Other cavitands contain dialkylsilicon bridges, these have been shown to be able to complex with linear guests such as CS_2, propyne (C_3H_4) and even oxygen (O_2).[37] The synthesis of this type of cavitand is outlined in scheme 15. The cavitand is synthesised, in this particular example, by treatment of a resorcinarene with dimethyldichlorosilane in THF/TEA at high dilution yielding the cavitand in 37% yield.

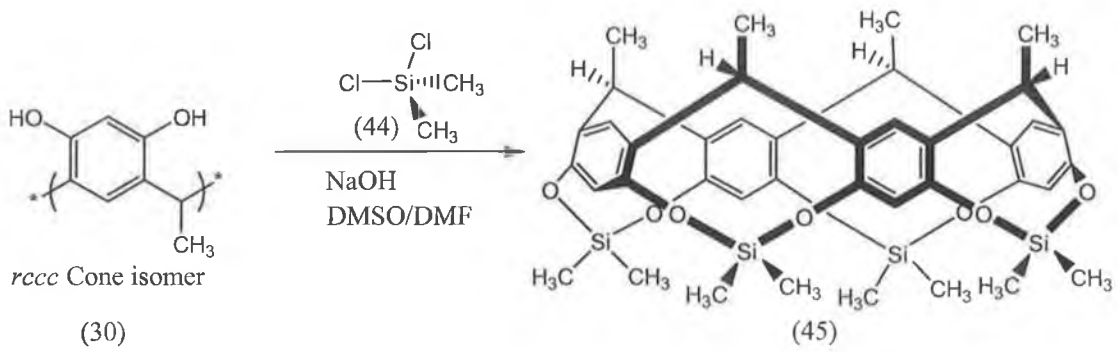

Scheme 15: *Synthesis of a dimethylsilicon bridged cavitand.*

Cavitands with phosphoryl bridges have also been reported and are a result of the reaction of a resorcinarene with dichlorophenylphosphine under basic conditions of pyridine in DMF, (scheme 16). This class of cavitand was found to have applications in both cation (specifically copper and silver) and anion (specifically chloride and iodide) binding.[38]

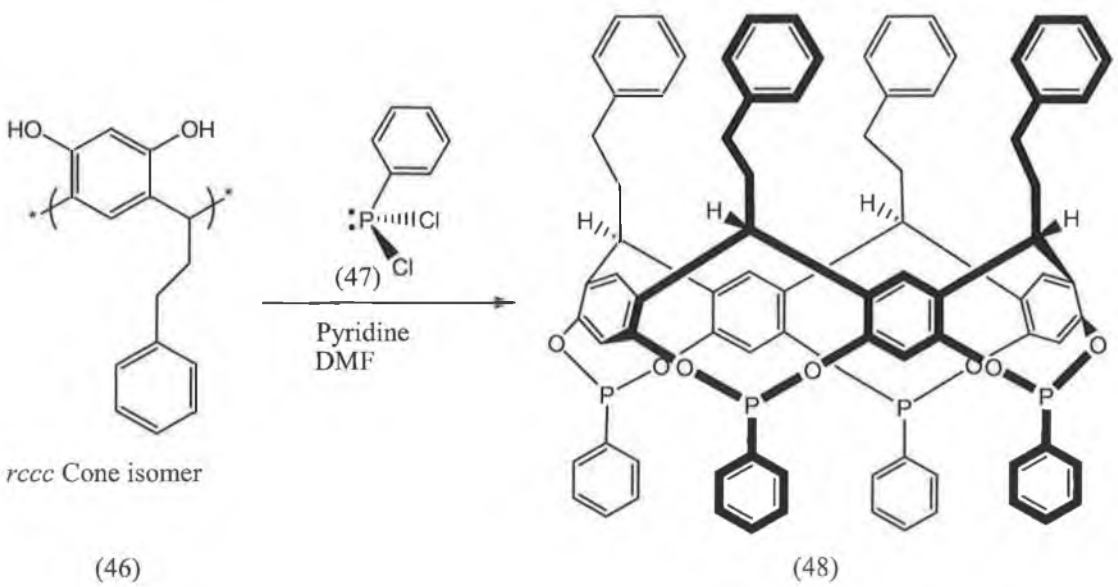

Scheme 16: *Synthesis of a phenyl phosphoryl bridged cavitand.*

Carcerands are formed from two cavitands covalenty linked *via* an oxygen (or sulphur) atom in the 2 position of the resorcinol moiety as shown in figure 10.

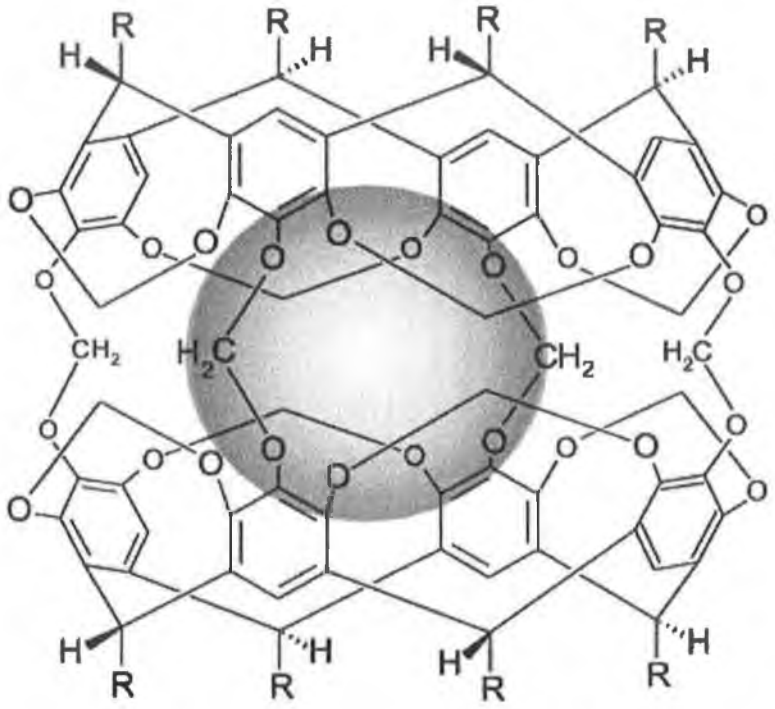

(49)

Figure 10: *General structure of a carcerand*[39].

Carcerands irrevisbly trap guests during their synthesis, which result in "carceplexes". However it is not possible for the guest molecule or ion in a carceplex to escape without rupturing covalent bonds in the shell of the host or the guest. The term "hemicarcerands" is used to describe cavitand-based hosts that possess holes large enough for guest entry or egression to occur. The term for the corresponding host-guest complex is a "hemicarceplex". Guest exchange in hemicarceplexes is in general quite slow at room temperature[39].

1.2 Pyrogallol[n]arenes

Pyrogallol[4]arenes, **51** are prepared from the condensation of pyrogallol, **50** with aldehydes, **1**, under acidic conditions. Their synthesis was first reported in the patent

literature in 1990[40]. The name pyrogallolarene was coined in a similar fashion to a resorcinarene, which was derived from rescorcinol[41]. It's structural similarity to calixarenes (Greek for Chalice "Calix" and Crater "Arene") also contributed to their name. The synthetic route used to prepare a pyrogallolarene is shown in scheme 17 and as with resorcinarines, many stereoisomers are possible (figure 2).

Pyrogallol[4]arene is the only reported product from the condensation of pyrogallol, **2** and alkyl aldehydes[42]. Theoretically, trimers, pentamers, hexamers and even higher cyclic oligomers are possible, but none have been reported to date.

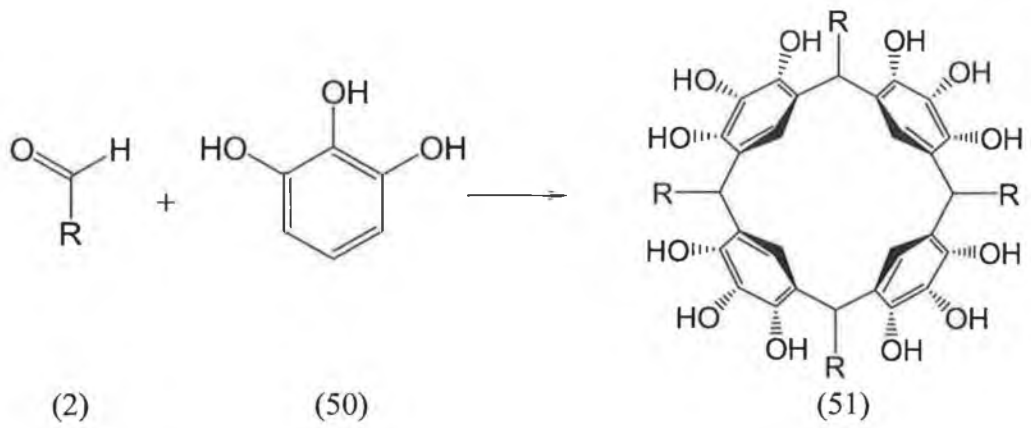

Scheme 17: *Preparation of pyrogallol[4]arene*

1.2.1 Self-Assembly of Pyrogallol[4]arenes

For the past two decades chemists have strived to design discrete spherical molecular hosts similar to those found in nature (for example spherical viruses, fullerenes). Such frameworks possess cavities capable of entrapping molecular guests and have applications in chemistry (for example, catalysis or sensors), biology (drug delivery), and materials science (molecular devices). Organic frameworks capable of such enclosure of space have been formed by synthesis and by self-assembly. Self-

assembly has proved an attractive means of constructing large, highly organized chemical entities.

The acid-catalyzed condensation of pyrogallol and long chain alkyl aldehydes yields pyrogallol[4]arenes, which associate in the form of hexameric capsules of extraordinary stability due to the presence of 48 intermolecular hydrogen bonds seaming the individual pyrogallol[4]arenes together, (scheme 18).

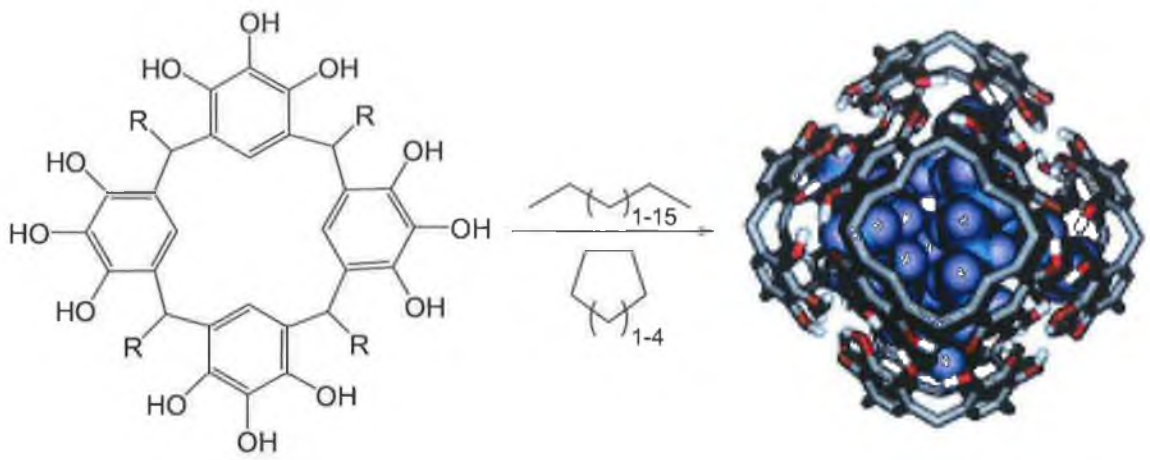

(52) (52a)

Scheme 18: *Assembly of pyrogallol[4]arenes to hexameric capsules in a variety of nonpolar liquid hydrocarbons*[43].

The use of calix[4]arenes and resorcin[4]arenes for the construction of large supramolecular assemblies has long been of interest to many researchers, such as J.L. Atwood[44]. Iwanek, Mattay and co-workers structurally characterized crystals which exhibited two different types of assembly via hydrogen bonds: wave-like 2D polymeric structures and for *C*-isobutylpyrogallol[4]arene, a spherical hexameric structure (figure 11).[45]

Unfortunately, it appears that the spherical hexamer was only obtained on one occasion.[46] The instability of hexamer **53** compared to [(*C*-methylresorcin[4]arene)$_6$(H_2O)$_8$], a very large synthetic molecular capsule,[47] was given as the explanation for the failure to obtain crystals of the spherical hexamer again. However, in view of the 48 intermolecular hydrogen bonds holding the six pyrogallol[4]arenes together, it was believed that the hexamer should be quite stable in solvents such as acetonitrile or nitrobenzene, particularly in view of the solution stability of [(*C*-methylresorcin[4]arene)$_6$(H_2O)$_8$] in such solvents.

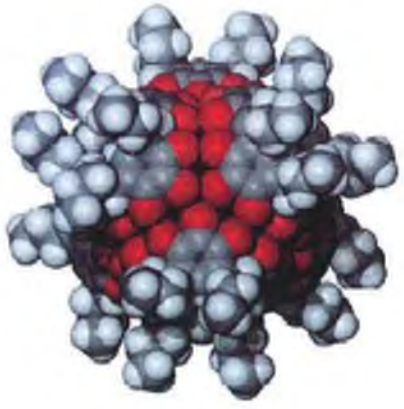

(53)

Figure 11: *Space filling representation of the C-propylpyrogallol[4]arene hexameric capsule.*

Another interesting property of compound **53** was that the hexamer crystallized in the triclinic space group P1 bar, although the illustration provided made it clear that such a hexamer could support higher symmetry. This low symmetry of such an inherently symmetric capsule could prove useful.

In the study of host-guest chemistry of [(*C*-methylresorcin[4]arene)$_6$(H_2O)$_8$], the high symmetry of the large capsule[47] has made crystallographic identification of the guests

housed within the capsule impossible. Atwood *et al* came to the conclusion that a lower symmetry capsule should make crystallographic study of the guests therein feasible.

(53a)

Figure 12: The oxygen atoms of the capsule in the space-filling metaphor

Figure 12 displays the hydrogen-bonding scheme of **53**. The oxygen atoms participating in the hydrogen bonding are found in bands, which seam the capsule together. The volume available for guests is about 1500Å^3 [48] but thus far, even with P1bar space symmetry, the guests on the interior are in each case badly disordered. Diffusion NMR was used in this study to identify the guests within their structures.

1.2.2 Host – Guest Chemistry of Pyrogallol[4]arenes

Selective binding of biorelevant molecules such as amino acids through polar interactions in nonpolar organic media is a rapidly growing area of molecular recognition.[46] Such a polar interaction, however, is far less pronounced in water. In fact, amino acid binding in aqueous media has been limited, to aromatic amino acids having good hydrophobicity as well as the capability of undergoing π-π stacking or charge transfer interaction.[49]

Kobayashi *et al.* introduced a highly electron rich aromatic cavity of water soluble pyrogallol or resorcinol cyclic tetramer and opened a newer phase of aqueous host-guest association involving highly hydrophilic guests such as sugars. It was reported that relatively hydrophobic aliphatic as well as aromatic amino acids can be bound to the pyrogallol or resorcinol cyclic tetramer (figure 13). The interaction between the host as π-base and the guests as either σ- or π-acid plays an important role.[50]

Results from this research proved that every guest is bound more tightly to the pyrogallol host than to the resorcinol host. The former having an additional hydroxy group on each of the benzene rings has a more electron-rich and less hydrophobic aromatic cavity, as compared with the latter. Thus, the π-basicity of the host is an important factor.

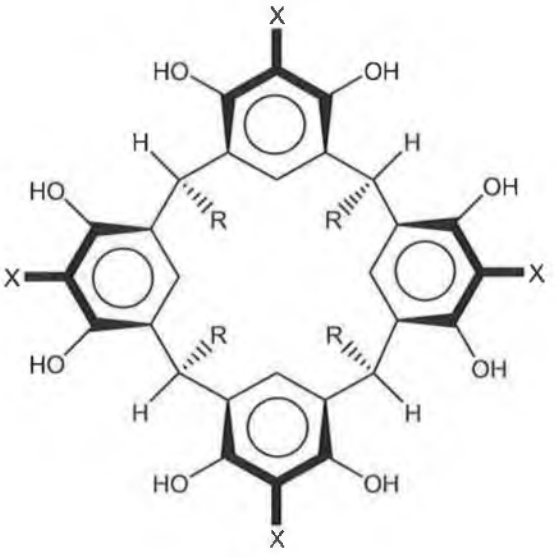

X = OH,H
R = $(CH_2)SO_3Na$

(54)

Figure 13: *Tetrasulphonated derivative of resorcin[4]arene or pyrogallol[4]arene, water soluble amino acid receptor.*

This particular result indicates that the present amino acid binding in water, as in the case of mono[51] and polyol complexation, is not simply due to the so-called

hydrophobic effect but there is substantial stabilization arising from the CH-π interaction[52] between the guests as σ-acids and the host as π-base.

1.3 The role of Gp120 in HIV infection and Gp120 inhibitors

Acquired Immunodeficiency Syndrome (AIDS) is one of the worst pandemics the world has ever known. Human Immunodeficiency Virus (HIV) the virus that causes AIDS was first discovered in 1981 in a remote area of central Africa.

HIV works by invading the cells of our immune system and reprogramming them to become HIV-producing factories. Slowly, the number of immune cells in the body dwindles and AIDS develops.[53]

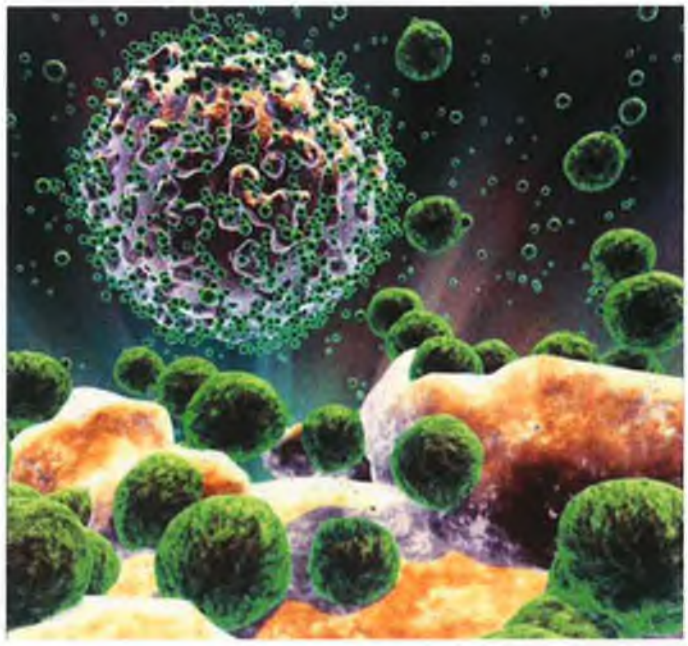

Figure 14: *HIV Cells attaching to a C4 human T-cell*[54]

HIV is a retrovirus, it uses the enzyme Reverse Transcriptase to convert RNA into DNA in the host cell.

HIV infects one particular type of immune system cell, the CD4+T cell; also known as a T-helper cell. Once infected, the T-helper cell turns into a HIV-replicating cell. HIV slowly reduces the number of T-cells until the infected individual develops AIDS. To better understand how HIV infects the body, the basic structure of the virus needs to be looked at:

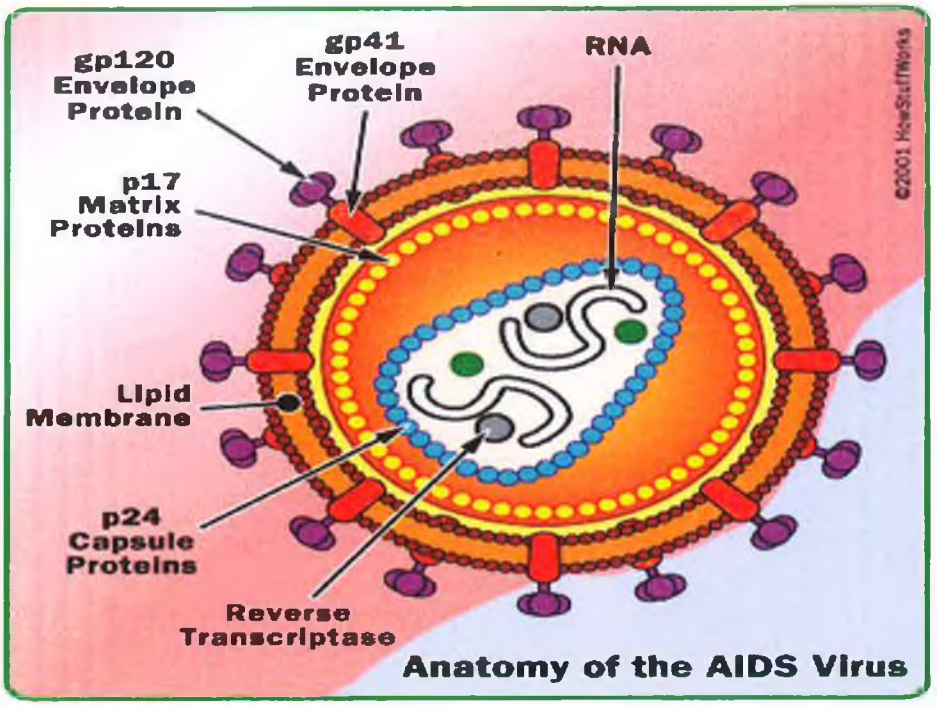

Figure 15: *Anatomy of the AIDS virus*[53]

- **Viral envelope** - This is the outer coat of the virus. It is composed of two layers of fatty molecules, called **lipids**. Embedded in the viral envelope are proteins from the host cell. There are also about 72 copies of **Env protein**, which protrudes from the envelope surface. Env consists of a cap made of three or four molecules called **glycoprotein** (gp) 120, and a stem consisting of three to four **gp41** molecules.
- **p17 protein** - The HIV matrix protein that lies between the envelope and core.

- **Viral core** - Inside the envelope is the core, which contains 2,000 copies of the viral protein, **p24**. These proteins surround two single strands of HIV RNA, each containing a copy of the virus's nine genes. Three of these genes: gag, pol and env - contain information needed to make structural proteins for new virions (a HIV virus particle) [53].

The entry of HIV into host cells is mediated by the viral envelope glycoproteins (gp), which are organised into oligomeric, probably trimeric spikes displayed on the surface of the virion. The viral envelope is synthesized as a 160-kilodalton (kD) (gp160) precursor glycoprotein, which is subsequently cleaved into 120-kD (gp120) and 41-kD (gp41) glycoproteins present on the virion particle. These envelope complexes are anchored in the viral membrane by the gp41 transmembrane envelope glycoprotein. The surface of the spike is composed primarily of the exterior envelope glycoprotein, gp120, associated by non-covalent interactions with each subunit of the trimeric gp41 glycoprotein complex. Comparison of the gp120 sequences of different primate immunodeficiency viruses identified five variable regions. The first four variable regions form surface-exposed loops that contain disulphide bonds at their bases. The conserved gp120 regions form discontinuous structures important for the interaction with the gp41 ectodomain and with the viral receptors on the target cell. Both conserved and variable gp120 regions are extensively glycosylated[55].

Entry of primate immunodeficiency viruses into the host cell involves the binding of the gp120 envelope glycoprotein to the CD4 glycoprotein, which serves as the primary receptor. The gp120 glycoprotein binds to the terminal amine of the four immunoglobin-like domains of CD4. The gp120 protein is held on the virion surface by a non-covalent interaction with gp41[56].

CD4 binding induces conformational changes in the gp120 glycoprotein, some of which involve the exposure and/or formation of a binding site for specific chemokine receptors. These chemokine receptors, mainly CCR5 and CXCR4 for HIV-1, serve as obligate second receptors for virus entry[57].

The gp120 third variable loop (V3) is the principal determinant of chemokine receptor specificity[58]. However, other more conserved gp120 structures that are exposed upon engagement of CD4 also seem to be involved in chemokine-receptor binding. This CD4 induced exposure is indicated by the enhanced binding of several gp120 antibodies, which, like V3-loop antibodies, efficiently block the binding of gp120-CD4 complexes to the chemokine receptor[58]. These are called CD4-induced (CD4i) antibodies. CD4 binding may trigger additional conformational changes in the envelope glycoproteins.

For example, binding of CD4 to the envelope glycoproteins of some HIV-1 isolates induces the release or 'shedding', of gp120 from the complex, although the relevance of this process to HIV entry is uncertain[55].

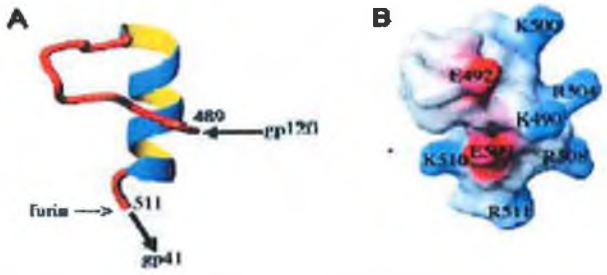

Figure 16: *(A) Ribbon diagram of the minimized mean structure of HIV gp120 C5 in 40% trifluoroethanol and (B) electrostatic map of the minimized mean structure of HIVg p120 C5.*

Because of the important role of the gp120 glycoprotein in receptor binding and interactions with neutralizing antibodies, information about the gp120 structure is important for understanding HIV infection and for the design of therapeutic and prophylactic strategies[55].

There is profuse evidence to suggest that CD4 binding induces a conformational change in gp120, but much of it derives from intact gp120 with variable loops in place of the oligomeric gp120-gp41 complex.

Analysis of the antigenic structure of gp120 shows that most of the envelope protein surface is hidden from humoral immune responses by glycosylation and oligomeric occlusion[59].

During virus entry, HIV surface proteins fuse the viral membrane with the target cell membrane. The gp120 protein is a vital participant in the control and initiation of fusion. It functions in positioning: locating a cell capable of prolific viral infection, anchoring the virus to the cell surface, and orienting the viral spike next to the target membrane. It also functions in timing: holding gp41 in a metastable conformation and triggering the coordinate release of the three N-terminal fusion peptides of the trimeric gp41.

HIV fusion can be inhibited by peptides that mimic the sequences of the N- and C-terminal helices by binding to the end N terminal heptad repeat triple helices, or to the C terminal regions of Env, thereby preventing six-helix bundle formation[60].

1.3.1 Viral Fusion Inhibitors

Binding of drugs can occur at two sites (figure 17). The first is the attachment site on the CD4 T-cell and the second is the fusion site on the gp120. In both cases the binding is brought on by electrostatic interactions.

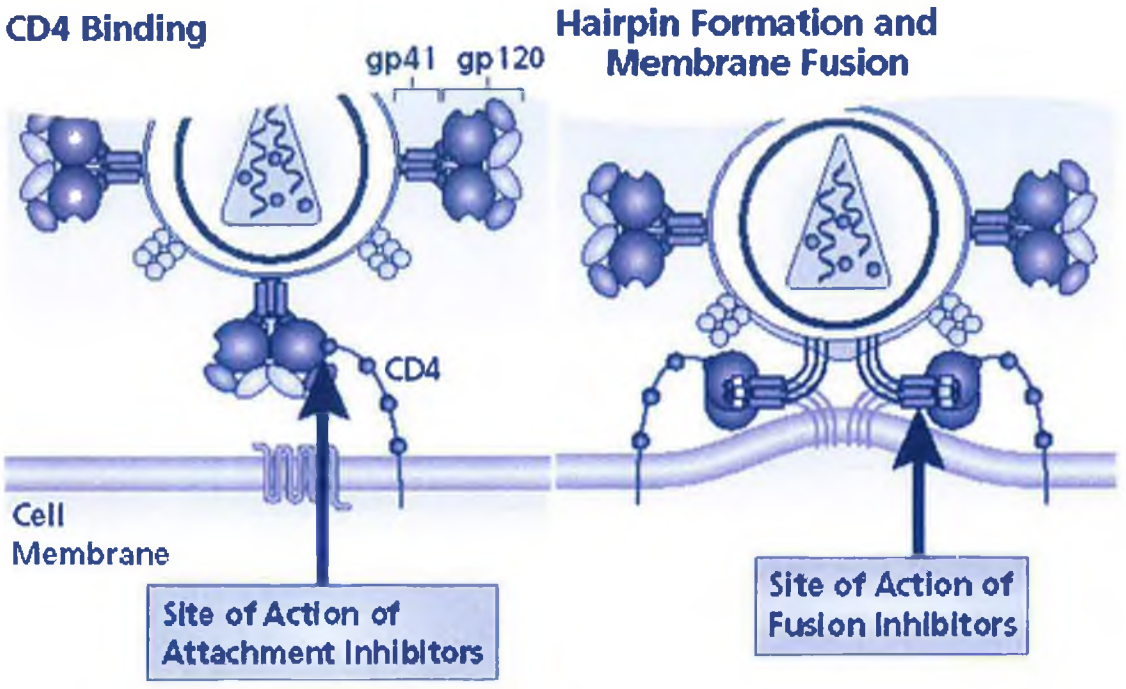

Figure 17: *a) CD4 Binding, b) Hairpin Formation and Membrane Fusion*[61].

In the first case of inhibition, drugs can block the interaction of CD4 receptors with the viral gp120. In the second case, they inhibit the conformational change (hairpin formation) that occurs with gp41 after gp120 binds to CD4.

It has been recently discovered that a cell surface enzyme called Protein Disulphide Isomerase (PDI), plays a vital role in HIV-1 cell entry. PDI attaches to CD4 close to

the gp120 binding site, which enables PDI to reduce the disulphide bonds of gp120, which leads to the conformational change in gp120 and gp41[62].

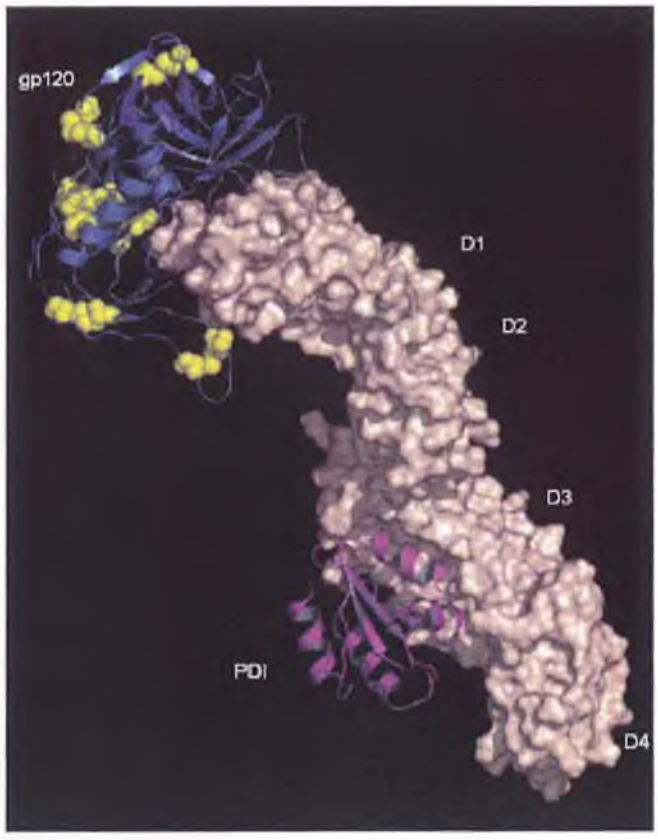

Figure 18: *Molecular Docking Analysis Model of PDI, CD4 and gp120 complex*[62]

Figure 18 shows a molecular docking analysis model of PDI, CD4 and gp120 complex[62]. The cysteine residues of gp120 (yellow), which contain the disulphide bonds, are in close proximity to PDI. There is a flexible molecular 'hinge' between the D2 and D3 regions of CD4, and it is believed that this hinge enables PDI to come into contact with gp120. It is also believed that inhibition of cell surface PDI prevents HIV-1 cell entry.

1.3.2 Current Commercially Available Drugs

Current therapies for the treatment of HIV-1 infection employ potent antiretroviral drugs that target two distinct retroviral functions: reverse transcription of the viral RNA genome and virion maturation. Despite the strength of these regimens, several complications exist that limit their efficacy. Current drug regimes are complex, involving a large pill burden, and are associated with major toxicity. These factors increase the potential for the development of resistance and virologic failure.
These issues highlight the need for the development of novel drugs targeting distinct processes in the viral lifecycle[63].

Virtually all the compounds that are currently used for the treatment of HIV infections, belong to one of the following classes:

1. nucleoside/nucleotide reverse transcriptase inhibitors- NRTIs (AZT, **55**, abacavir, **57** and didanosine, **56.**) – figure 19
2. non-nucleoside/nucleotide reverse transcriptase inhibitors- NNRTIs (nevirapine, **58** and efavirenz, **59**) – figure 19
3. protease inhibitors - PIs (saquinavir,**61,** indinavir, **60,** and lopinavir,**62**) – figure 19

In addition to the reverse transcriptase and protease reaction, various other events in the HIV replicative cycle can be considered as potential targets for chemotherapeutic intervention. The inhibition of viral entry or indeed binding to the host cells is a promising target for the development of new antiviral drugs.

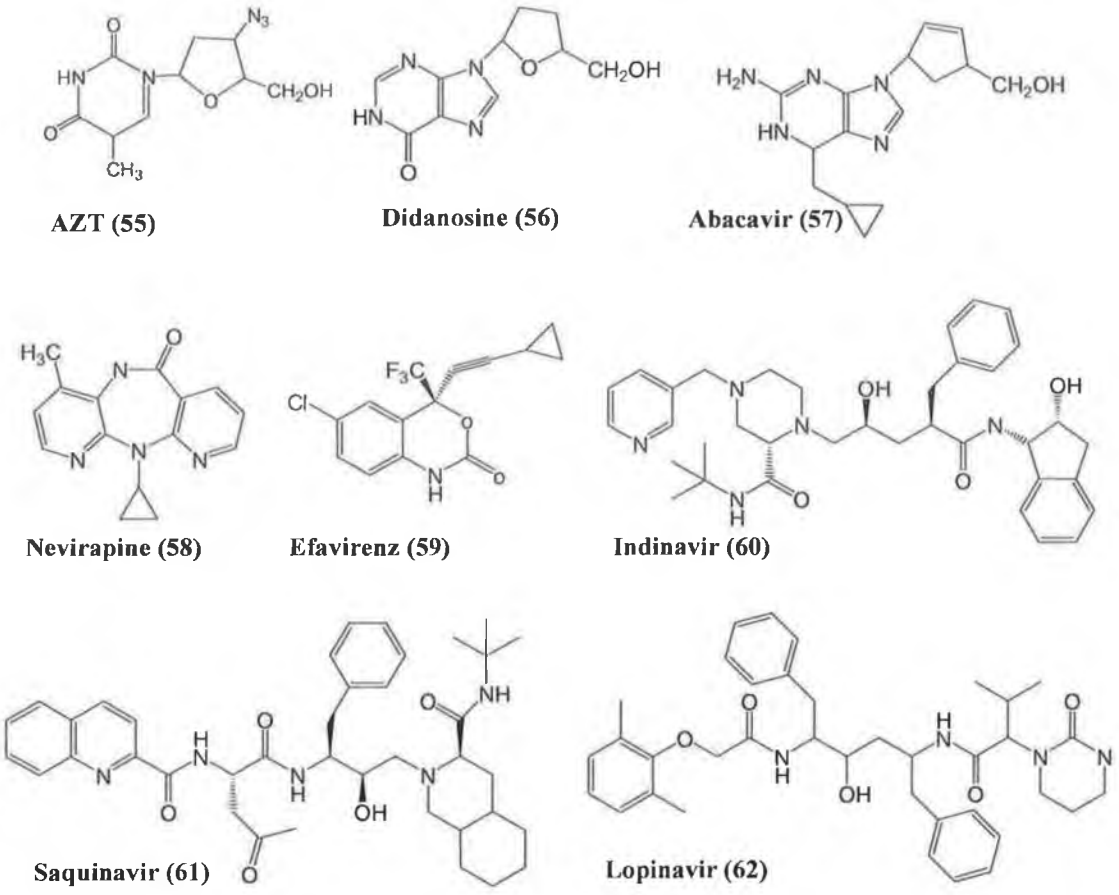

Figure 19: *Commercially available HIV therapeutics*

A great variety of polyanionic compounds have been found to be able to interfere with virus adsorption to the cell surface: i.e, polysulphates, polysulphonates, polycarboxylates, polyphosphates, polyphosphonates, polyoxometalates, etc. (Figure 20, D2S – poly sulphonate). This class of compounds also comprises the cosalane analogues (figure 21) containing the polycarboxylate pharmacophore. All these compounds exert their anti HIV activity by shielding off the positively charged sites in the V3 loop of the viral envelope glycoprotein (gp120), which is necessary for virus attachment to the cell surface heparin sulphate, a binding site, before a more specific binding occurs to the CD4 receptor[64].

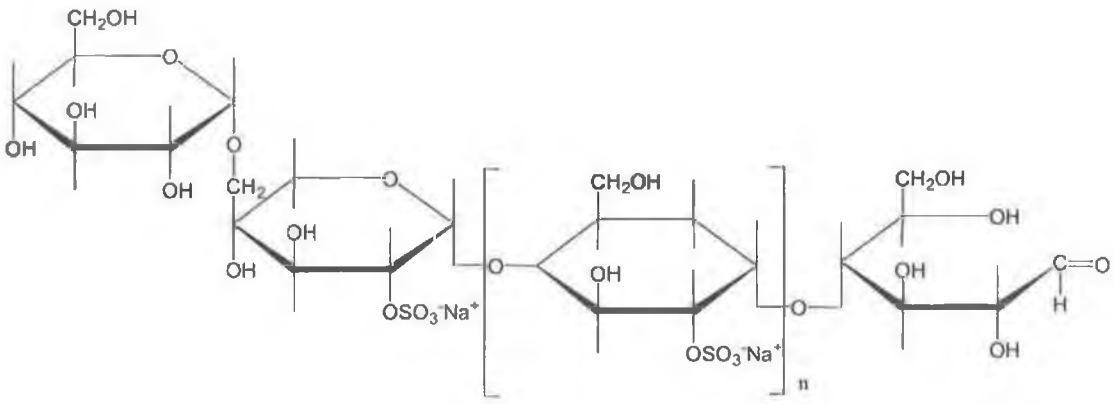

(63)

Figure 20: *Dextran-2-sulphate (D2S); n=30*

A number of studies have shown that sulphonated polysaccharides including dextran-2- sulphate (figure 20) and heparin inhibit HIV-1 *in vitro*. This is achieved by interfering with the interaction between the T-cell determinant CD4 and viral gp120[65].

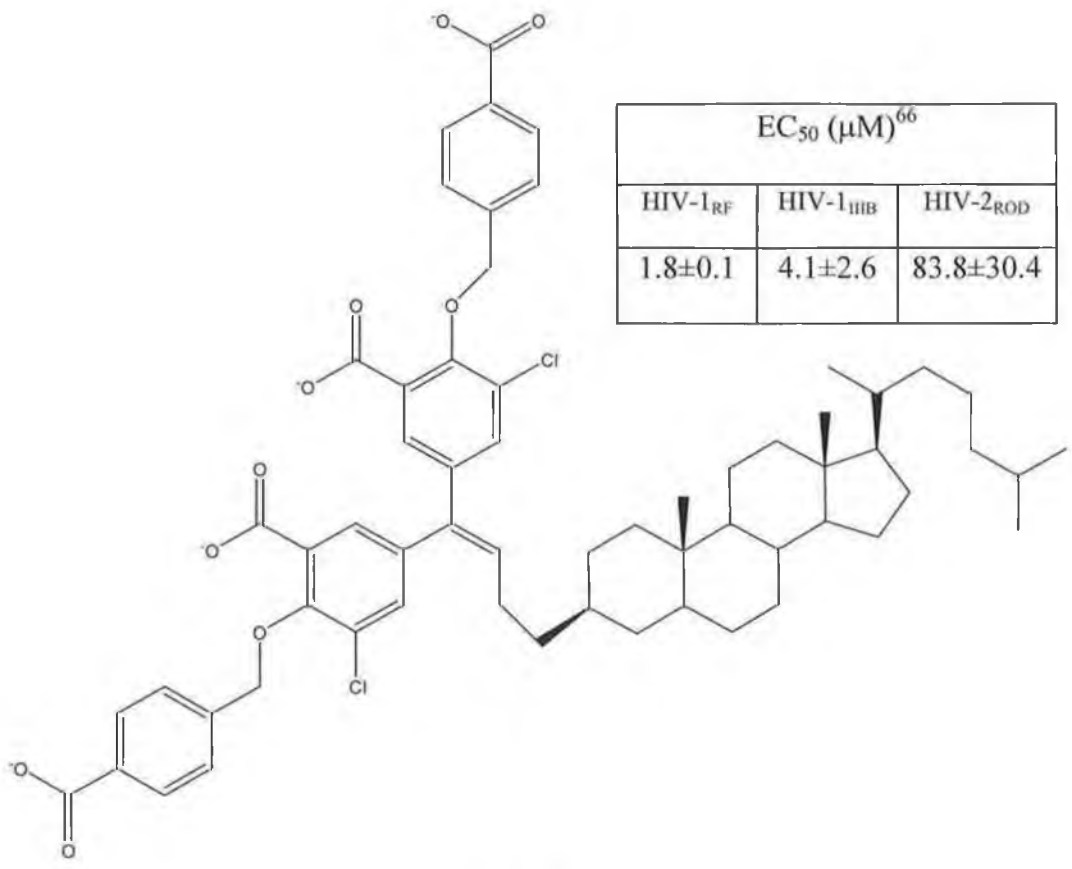

EC_{50} (μM)[66]		
$HIV\text{-}1_{RF}$	$HIV\text{-}1_{IIIB}$	$HIV\text{-}2_{ROD}$
1.8±0.1	4.1±2.6	83.8±30.4

(64)

Figure 21: *Cosalane analogue.*

Recent advances in the field of viral entry have led to the development of several novel antiviral agents that target separate steps in the viral entry process. Since these drugs are targeting the parts of the virus life cycle that occur outside the cell, they might be better than the traditional drugs which target events that take place inside the infected cell. This is because anti HIV drugs which need to be inside the infected cell to be active can be efficiently neutralized by some cells, using primitive innate self-defence mechanisms such as 'efflux pumps', which sense toxins and eject them outside of the cell.

D2S has microbiocidal applications (microbiocides kill microbes, such as bacteria, fungi or in this case viruses), its use in contraception devices such as condoms, is vast[67].

There is another recent commercially available drug called "Enfuvirtide®" (figure 22). The drug mimics gp41 as it consists of 36 amino acid residues. It works by inhibiting virus cell fusion through a coil-coil interaction with gp41.

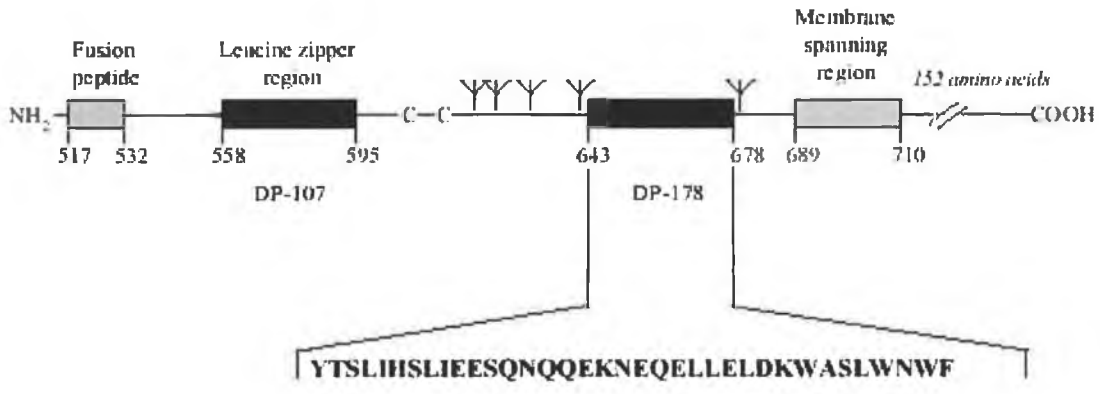

Figure 22: *Enfuvirtide® - commercially available drug*[67].

1.3.3 Macrocyclic Therapeutics

The development of a macrocyclic compound with potent and novel antiviral activity may provide a significant lead in the formulation of effective microbiocides, either as a stand-alone agent or in combination with other synergistic products. The structure of a new lead, **65** is shown in Figure 23; it is a macrocycle prepared from a pyrogallol-aldehyde condensation and subsequently alkylated and saponified to give the final potassium salt product. Work carried out recently by Dr. Nolan's group at Dublin City University has demonstrated that the original synthetic procedures used to prepare the target macrocycle (Figure 23) actually give a mixture of partially alkylated products.

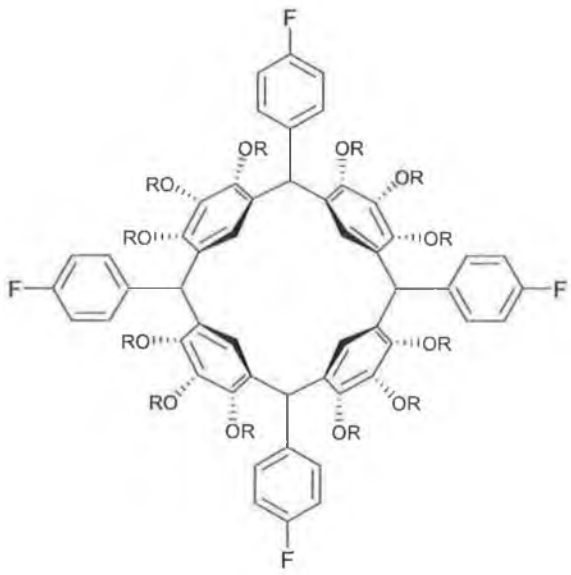

$R = CH_2CO_2K$, H

(65)

Figure 23: *Current lead pyrogall[4]arene.*

These mixtures have been biologically evaluated by both *in vitro* and *in vivo* methods[68]. *In vitro* studies have shown promising results with this initial mixture, and it is anticipated that with improved appropriate synthesis, this could be greatly improved.

We believe that these macrocyclic derivatives are excellent candidates as microbiocides, and although they exist as mixtures this may not be a significant problem for application since many of the microbiocides presently in phase III clinical trials (PRO2000, Dextran-2-sulphate, cellulose sulphate) are used as mixtures[68].

1.4 Thesis Proposal

The initial driving force behind our work was the interesting biodata from a pyrogallolarene moiety against HIV in clinical trials carried out in Uganda in the early nineties by Stephen Harris[69].

However many questions arose upon reproduction of this work by, DCU, TopChem laboratories® and AIDS Care Pharma here in Ireland.

1) Can the yields of macrocycle be improved?
2) What is the stereochemistry of these macrocycles?
3) Are the lead compounds partially or completely alkylated?
4) What form of these compounds, perform biologically: partial or completely alkylated?
5) What are the structural limitations for biological performance – mechanism of action?
6) Can effective HPLC methods be developed for the analytical detection of the macrocycles?
7) Can an improved lead be developed?

We wished to address all these problems in order to develop a better understanding of biological activity and also to optimise the synthetic methods used to prepare these compounds. Ultimately, we wished to develop a superior lead structure.

Chapter 2

Synthesis of Aryl and Alkyl Pyrogallol[4]arenes

2.1 Introduction:

The condensation of benzaldehyde, **66**, with pyrogallol, **50**, was first reported in the patent literature by Harris[69] in the early 1990's. This condensation saw equal molar quantities of aldehyde and pyrogallol condensed under acid conditions to form the tetraphenyl pyrogallol[4]arene, **67**, in a reproducible yield. The aim of this research was to investigate and optimise this condensation reaction.

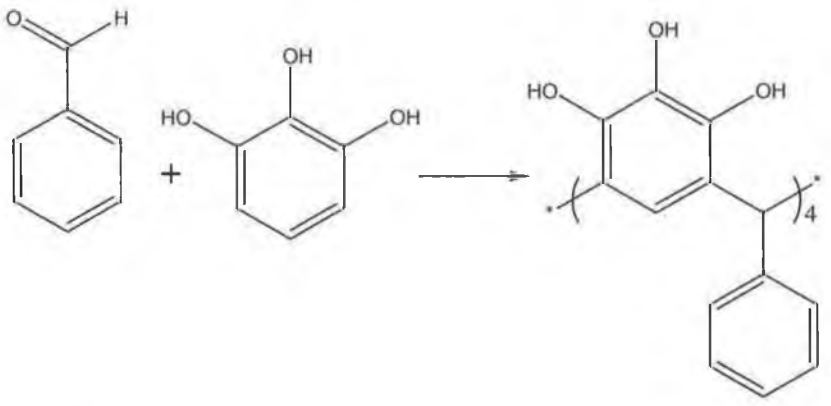

(66) **(50)** **(67)**

Scheme 19: *Preparation of tetra-4-fluorophenyl pyrogallol[4]arene*

We also were interested in comparing the condensation of various substituted aromatic aldehydes to that of the alkyl aldehydes. The condensation of acetaldehyde, **68**, with **50** was also investigated.

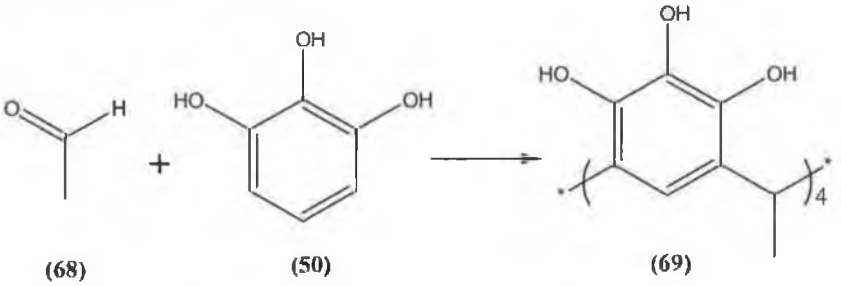

(68) **(50)** **(69)**

Scheme 20: *Preparation of tetramethyl pyrogallol[4]arene.*

2.2 Results and Discussion:

2.2.1 Tetramerisation of pyrogallol with 4-fluorobenzaldehyde.

The condensation of pyrogallol with 4-fluorobenzaldehyde under acidic conditions in ethanol at 78°C gives a reproducible yield of 35%. After only one hour reaction time a precipitate begins to form. When the reaction is complete (after five hours) a pink-purple product is then filtered and washed. Outlined in scheme 21 is a proposed mechanism for the condensation.

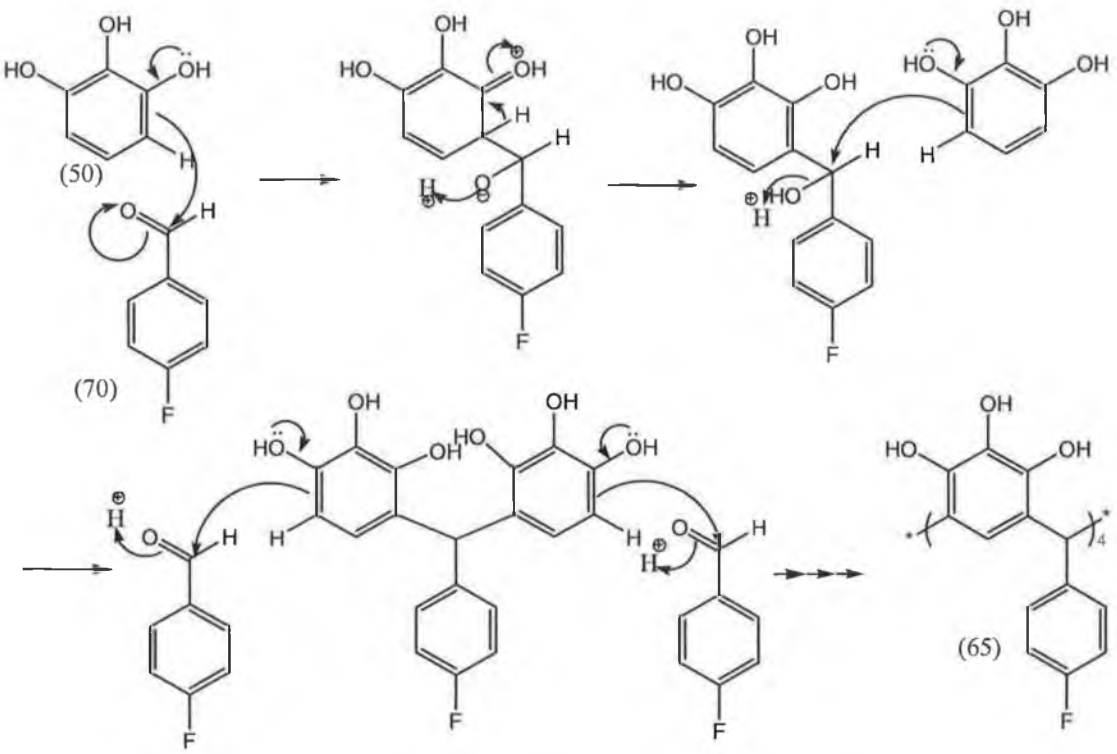

Scheme 21: *Mechanism of formation of pyrogallol[4]arenes*

The proposed mechanism involves a series of electrophilic substitutions, to yield a linear tetrameric species which cyclises to the thermodynamically stable tetramer. The arrangement of the various aromatic rings can vary and gives rise to a number of possible different conformations. There is of course the possibility of dimers being

formed, and two dimers coming together in different ways to form various isomers of pyrogallol[4]arene. (See chapter 4).

The ^{1}H-NMR data for this compound shows that the filtered residue is quite pure, however the reasonably low yield tells us that the soluble impurities and by-products are washed out in the filtrate. It is however unusual to achieve such high purity of a single product from a multi-component condensation. Many condensations of macrocycles (in particular classical calixarenes) give a complicated mixture of products. The proton splitting in the ^{1}H-NMR (figure 27) is at first confusing. For two years, until we managed to obtain a crystal structure we could not unambiguously assign the stereoisomer, but on reference to the crystal structure, the splitting is explained. We had assumed that we had the *rtct* cone conformation judging by the ^{1}H-NMR. This however was not the case, the crystal structure showed that in fact we had the chair *rctt* conformation

Two singlets at 4.8 ppm and 5.8 ppm each represent two pyrogallol aromatic protons. Two of these protons (from the crystal structure) are pointing between the 4-fluorophenyl rings of the pyrogallol[4]arene and are therefore shifted upfield by the anisotropic effect to 4.8ppm. The other two pyrogallol protons are not as greatly affected by these anisotropic effects due to their alignment and therefore appear at 5.8ppm.

All four protons on the methylene bridges are in the same chemical environment and therefore they appear as a singlet at 5.6ppm. The downfield shift is due to the three

aromatic substituents on the bridging carbons. These protons are equivalent to trityl protons.

The aromatic protons appear as a poorly resolved doublet of doublets at 6.5ppm and 6.6ppm, this is due to the presence of the fluorine atom on the ring. The hydroxyl protons appear as three distinct singlets at 7.5ppm, 7.6ppm, and 7.7ppm

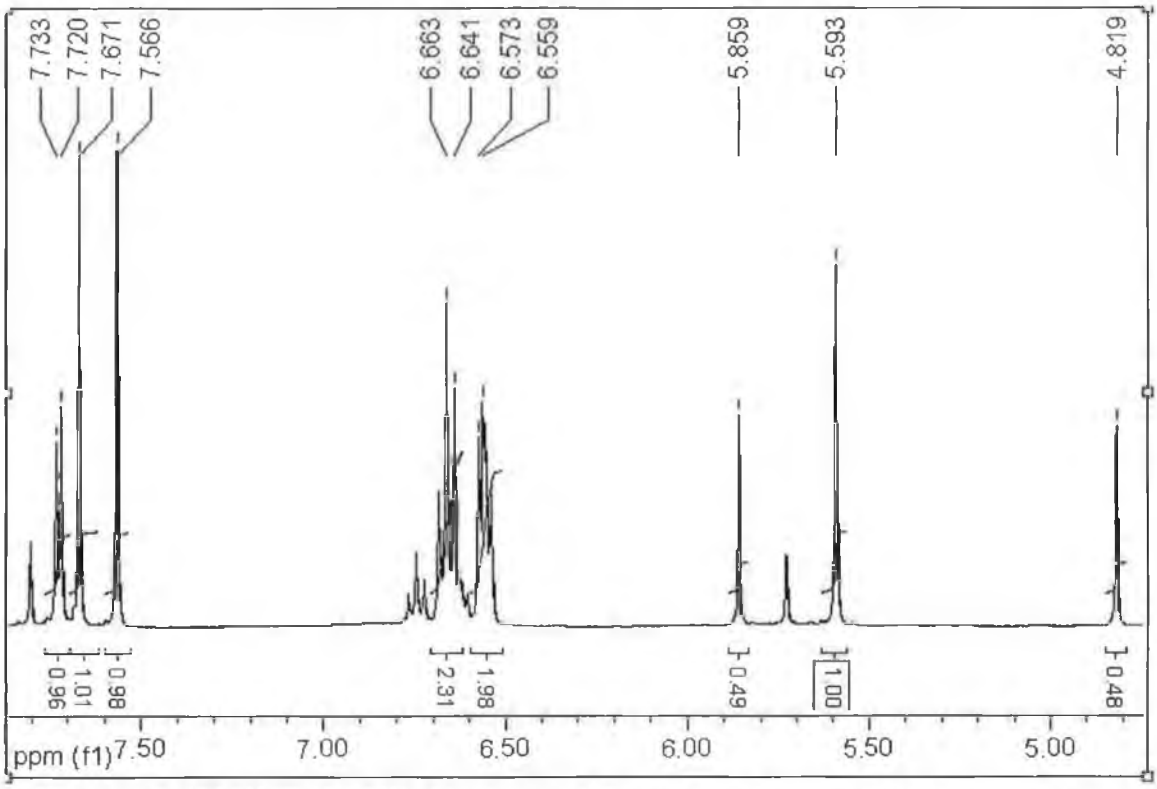

Figure 24: *^{1}H-NMR (DMSO-d_6) of tetra-4-fluorophenyl pyrogallol[4]arene – rctt chair conformation*

Mass spectrometry has also been used to confirm the structure of **65**, Electrospray Ionization – Mass Spectrometry (ESI-MS) has shown a single peak for the molecular ion M/Z: 951 (M+Na).

These compounds have poor solubility in most solvents. They have a low solubility in methanol, but are completely soluble in DMSO. They are not soluble in water, chloroform, ethyl acetate or hexane. Crystals of tetra-4-fluorophenyl pyrogallol[4]arene, **65,** were grown in DMSO and the X-ray structure is shown in figure 21. It would appear that the pyrogallolarene exists solely as a chair *rctt* isomer. The four 4-fluorophenyl rings project out at an angle of 88.5° from the plane of the bridging trityl carbons and are separated by 4.29Å from each other. The pyrogallol rings are at an angle of 87.62° from each other with two pyrogallol units lying in the plane. The protons of the pyrogallol subunits are shielded by the ring currents of the adjacent pyrogallol ring subunits. The structure obtained is very similar to the resorcinarenes prepared from aromatic aldehydes[70] except the ^{1}H-NMR spectra differ for the proton in the 5-position of the pyrogallol/resorcinol ring in the macrocycle.

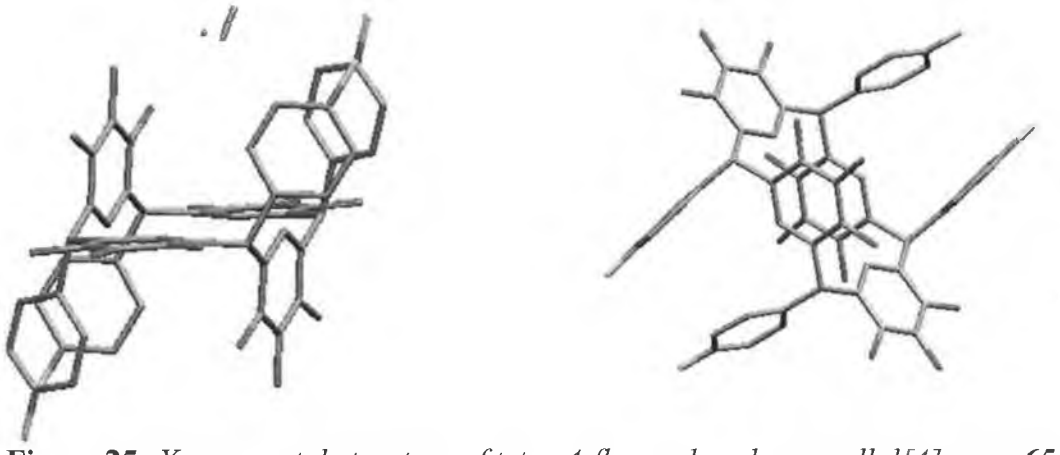

Figure 25: *X-ray crystal structure of tetra-4-fluorophenyl pyrogallol[4]arene,* ***65****. Two different views. (Structure drawn without Hydrogens for simplicity). See Appendix 1.*

All crystallography data can be found in Appendix 1. There are a few points to note from the crystallography data. The first one is the accuracy of the data. The accuracy is denoted by 2 different parameters F^2 and R1. F^2 is a "goodness of fit" parameter,

and should be as close to 1.000 as possible. Our crystal structure has an F^2 value of 1.030, which is very good. Secondly the R1 value gives a percentage of electron density present that is not accounted for by the crystal structure. Typically values less that 0.06 (6%) are acceptable. Our crystal structure has a R1 value of 0.0401 (4.01%), which is also a very good result, and denotes an accurate structure.

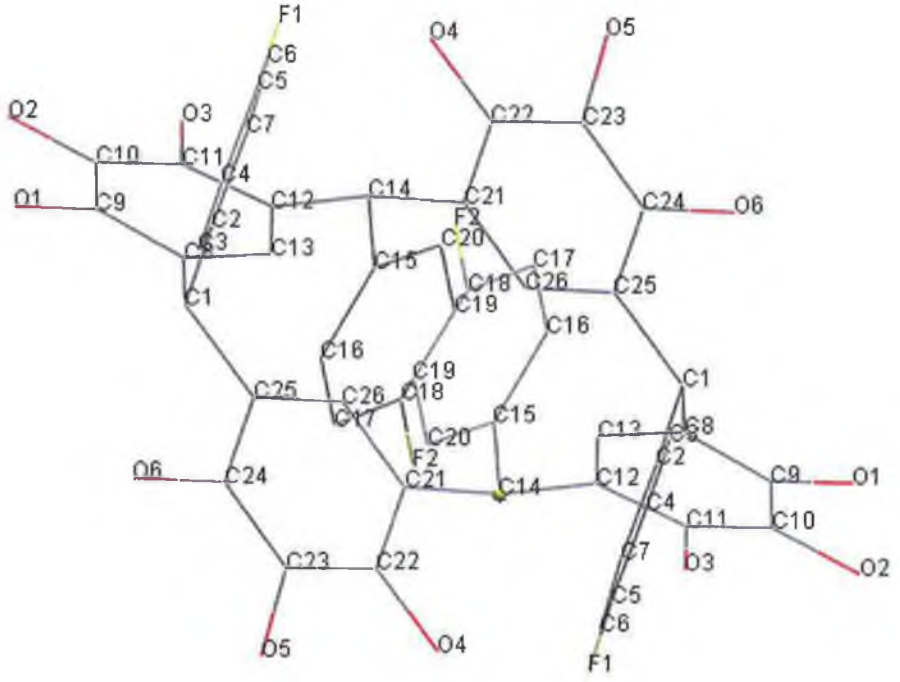

Figure 26: *X-ray crystal structure of tetra-4-fluorophenyl pyrogallol[4]arene,* ***65****.*

The second point to note is the crystal system. Our crystal adopts a triclinic system. There are seven crystal systems in total, they are cubic, tetragonal, orthogonal, hexagonal, trigonal, monoclinic and triclinic. Triclinic is the least symmetrical of the seven systems. None of the 3 unit cell parameters are equal and none of the sides are perpendicular to each other. This crystal system is the most novel of the seven. Figure 27 displays the crystal packing in a unit cell.

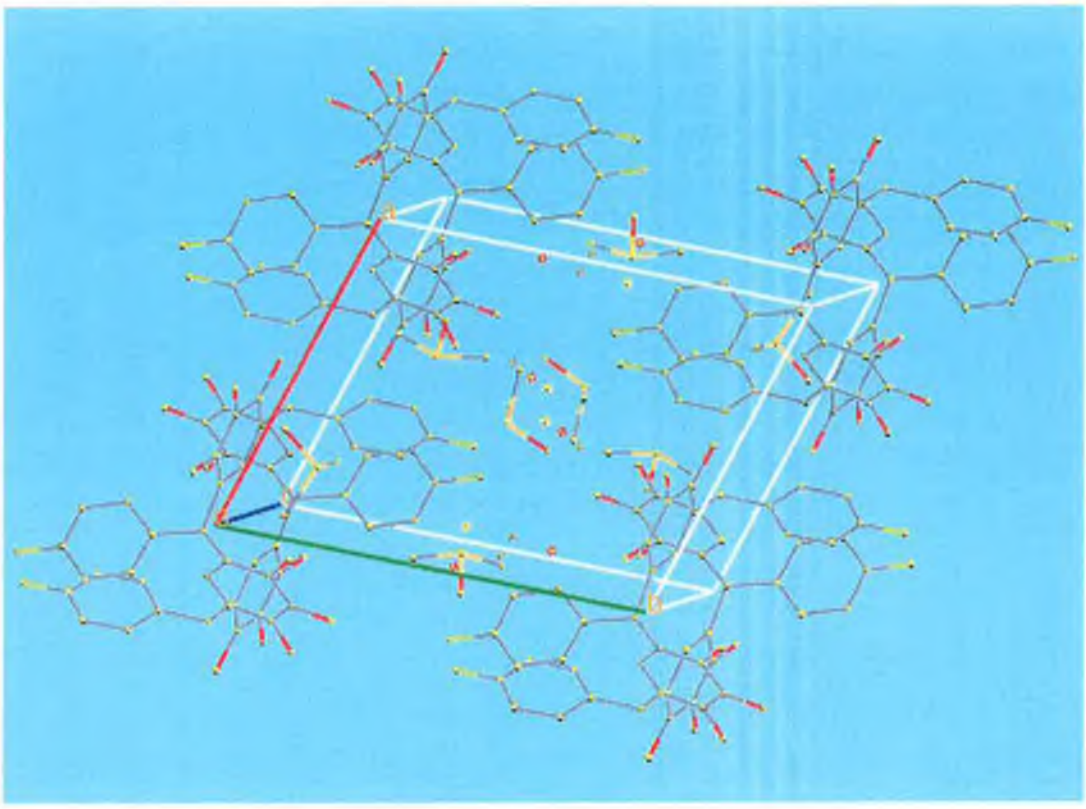

Figure 27: *Crystal packing of tetra-4-fluorophenyl pyrogallol[4]arene in a triclinic unit cell.*

The final point to note about the crystal structure is the temperature at which it was obtained. As expected, crystal structures are generally resolved at low temperatures. This is because at low temperatures there are less vibrations and therefore a clearer diffraction pattern. Our crystal structure is no exception, the structure was resolved at 100K (-173°C).

2.2.2 Yield Optimising Experiments

We were further interested in optimising the yields of **65**. The first parameter that was investigated was the effect of concentration of pyrogallol on the condensation. For this study we varied the concentration of starting materials in the reaction, to determine the effect on yield. The concentration of the starting materials was varied

from 0.250g/ml to 0.083g/ml for a 1g scale reaction. The yields of these reactions are shown in Table 2.

Experiment Number	Pyrogallol Concentration (g/ml)	Volume of Solvent (ml)	% Yield
2.1.1-1	0.250	2	0%
2.1.1-2	0.167	4	32%
2.1.1-3	0.14	5	37%
2.1.1-4	0.125	6	34%
2.1.1-5	0.100	8	8%
2.1.1-6	0.083	10	4%

Table 2: *Concentration study and yields*

No product was formed in the first reaction (only residual starting material), as the concentration was too high, reactions 2.1.1-2, 2.1.1-3 and 2.1.1-4 gave better yields, with the yield trailing off, as the concentration decreased. The optimum concentration was found to be 0.14g/ml (5mls of solvent) and this was used for future experiments. The dilution effect as seen in experiments 2.1.1-5 and 2.1.1-6 is quite common for macrocycle synthesis as dilution encourages oligomer formation.

We suspected that the reactivity of pyrogallol, **50,** would increase under base conditions due to the hydroxy groups being deprotonated. A series of experiments using five different bases were carried out using sodium hydroxide, pyridine, HOBT, DBU and triethylamine. On reaction with an aromatic aldehyde under base conditions a rapid formation of a green-black solid prevailed.

NMR and particle sizing measurements have shown this solid to be polymeric. There was no macrocyclic product formed. A possible explanation for this result involves the charge-charge repulsion between pyrogallol moieties, instead of cyclisation occurring we believe polymerisation of the pyrogallol occurs as shown in scheme 22b. It can be clearly seen that there is no "charge-charge repulsion" present in scheme 22b and polymerisation is free to occur. All reactions gave a similiar polymer product, we are unable to calculate a percentage yield as the molecular weight of the polymer (or mixture of polymers) is unknown.

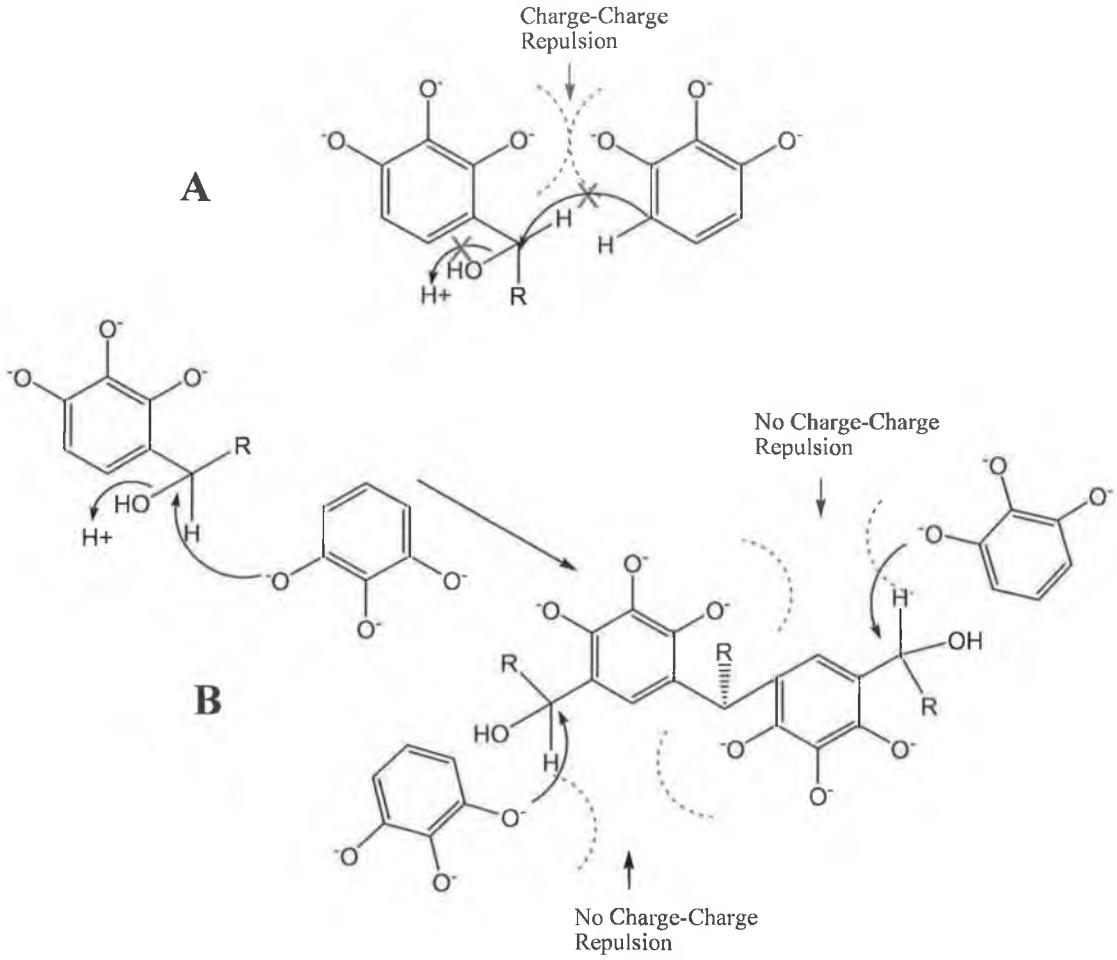

Scheme 22: *a) Charge-charge repulsion mechanism of deprotonated pyrogallol moieties, b) polymerisation mechanism of deprotonated pyrogallol moieties.*

2.2.3 Tetramerisation of Pyrogallol, 2, with Acetaldehyde, 27.

Experiment 2.3.1 was repeated using acetaldehyde in place of 4-fluorobenzaldehyde. The results of using an alkyl aldehyde instead of an aromatic aldehyde were interesting.

The ^{1}H-NMR initially looked more complicated than that of the tetra-4-fluorophenyl pyrogallol[4]arene, **68**, with a more complex splitting pattern. However on further analysis this was found to be the result of two distinct stereoisomers present. We developed a simple and efficient procedure to isolate each stereoisomer. As before with the tetra-4-fluorophenyl pyrogallol[4]arene column chromatography cannot be used owing to the highly polar nature of these compounds.

We first washed the precipitate with an ethanol/water solution (4:1). The filtrates from the washings were set aside. The collected precipitate was then recrystallised from hot ethanol. The collected reaction filtrates were then added to ice, causing a second precipitate to form. This precipitate was found to be a tetramer (M/Z: 608) and from ^{1}H-NMR it was discovered to be a different conformation to that of the precipitate isolated from the reaction mixture.

The first isolated product was found to be in the same conformation as that observed with the condensation with aromatic aldehydes – (*rctt* chair conformation). The latter product was seen to have a far simpler ^{1}H-NMR and for this reason it is believed to be the symmetrical *rccc* cone conformation. It would appear that the aromatic aldehydes give a distinctly different conformation than the alkyl aldehydes. The two products are illustrated in figure 28.

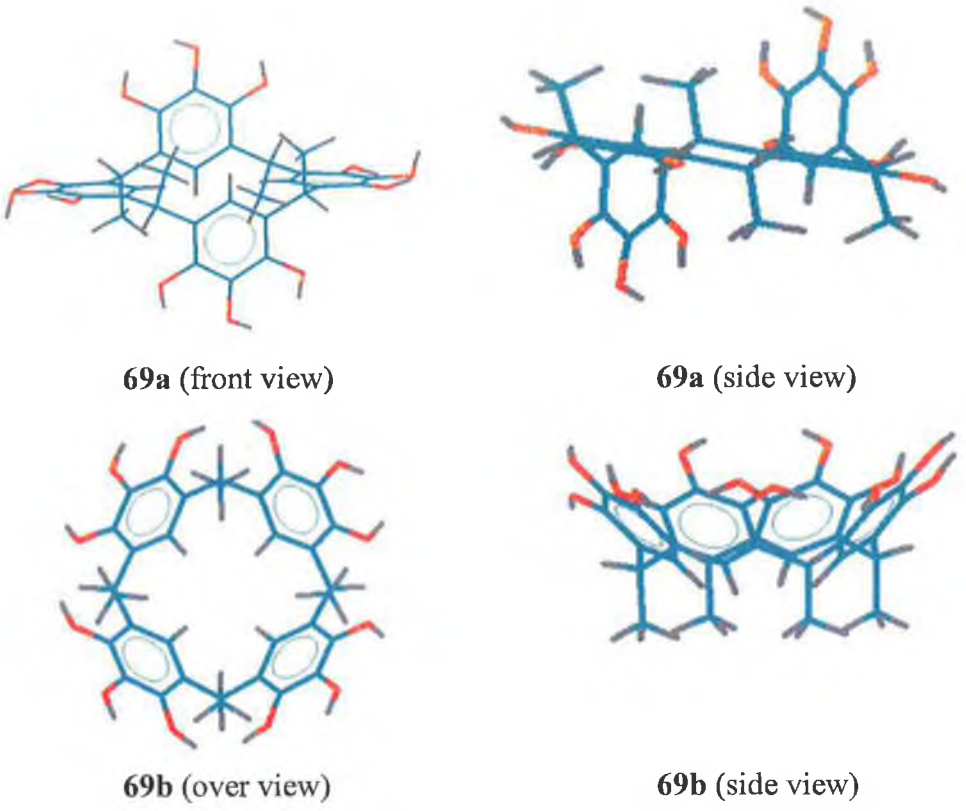

Figure 28: *Conformations of tetramethyl pyrogallol[4]arene* ***69a*** *rctt chair* ***69b*** *rccc cone*

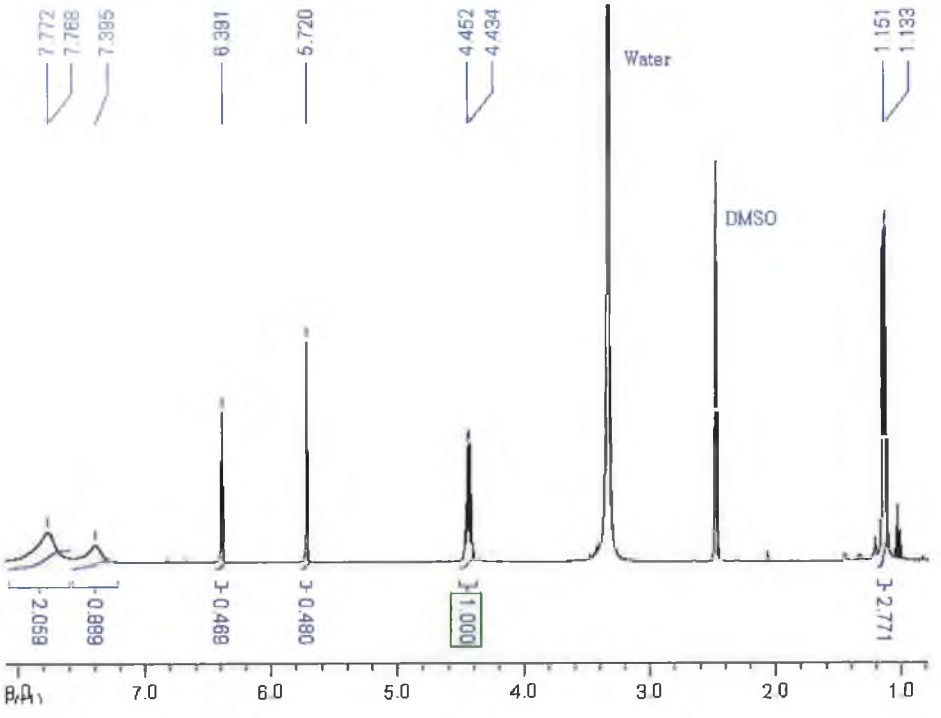

Figure 29: *^{1}H-NMR (DMSO-d_6) of tetramethyl pyrogallol[4]arene – rctt chair conformation,* ***69a.***

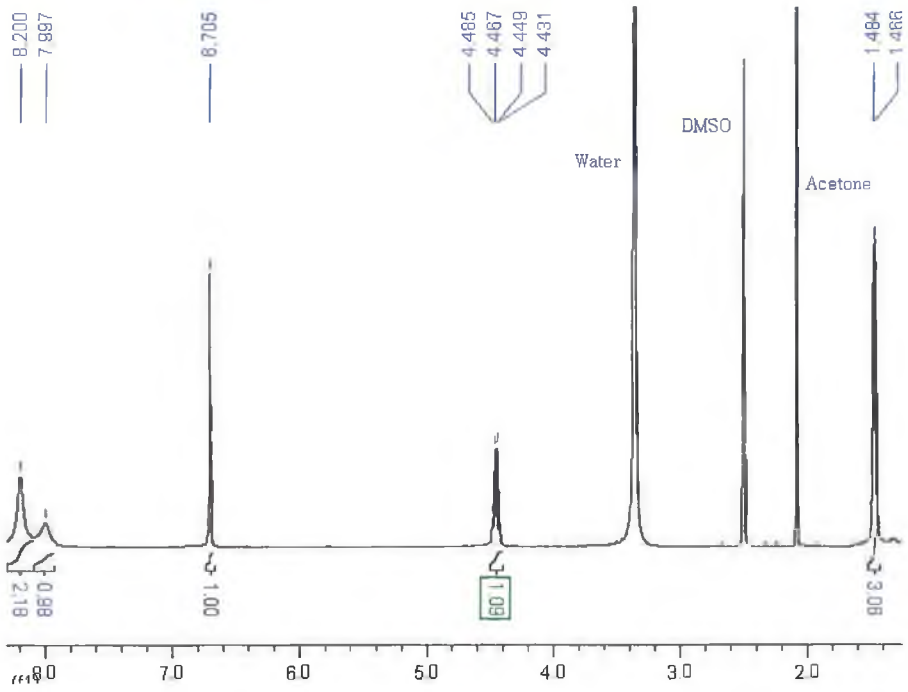

Figure 30: *^{1}H-NMR (DMSO-d_6) of tetramethyl pyrogallol[4]arene – rccc cone conformation,* ***69b.***

The combined yield for both conformations was 41% (*rctt* chair 34% and *rccc* cone was 7%), which is slightly higher but still comparative to that in experiment 2.1.

In both ^{1}H-NMR spectra above a doublet is observed for the methyl groups of the bridging carbons. For the *rccc* cone conformation they are found at 1.4ppm however in the *rctt* chair conformation they are shifted upfield to 1.1ppm, this is due to the methyl group pointing away from the annulus of the pyrogallolarene whereas in the case of the *rccc* cone conformation the methyl groups are in close proximity to the annulus and are shifted downfield.

In figure 31 we see a quartet at 4.4ppm, which corresponds to the bridging methylene protons. In the case of figure 30, a multiplet is observed for the bridging methylene protons, this is because the bridging protons in the *rctt* chair conformation (although

similar) are not in the exact same chemical environment. The multiplet is due to two overlapping quartets.

In the *rccc* cone conformation the aromatic protons for the pyrogallol ring are a singlet at 6.7ppm. In the case of the *rctt* chair conformation two distinct chemical environments exist for the four aromatic protons, as such there are two distinct singlets at 6.4ppm and 5.7ppm, each with an integration of 0.5. Again there is a significant shift upfield due to the anistropic effect from the pyrogallol[4]arene annulus.

Finally the hydroxy protons of the pyrogallol rings appear as two broad singlets between 7 and 8ppm. A smaller singlet corresponding to the centre hydroxy proton appears at 7.4ppm for the *rctt* chair conformation and at 8.0ppm for the *rccc* cone conformation. The outer two hydroxy protons are in the same chemical environment in both conformations and therefore appear as a broad singlet at 7.8ppm (in the *rctt* chair conformation) and 8.2ppm (*rccc* cone conformation). Here we see that the hydroxyl protons of the *rccc* cone conformation have been shifted downfield and this is due to the complex hydrogen bonding network in the upper rim of the pyrogallol[4]arene.

Alternative support for this argument comes from the difference in the OH bands in the IR spectra of the 2 conformations. The OH band of the *rccc* cone is far broarder than that of the corresponding band of the *rctt* chair conformation. This is due to the increased hydrogen bonding network within the *rccc* cone conformation.

2.2.4: Metal Templation Experiments

It was noted in the literature that various macrocycles are produced in higher yield when a specific metal chloride is added to the reaction[71]. This is due to a metal templation effect. The metal template effect can be used for cyclisation reactions as shown in scheme 23.

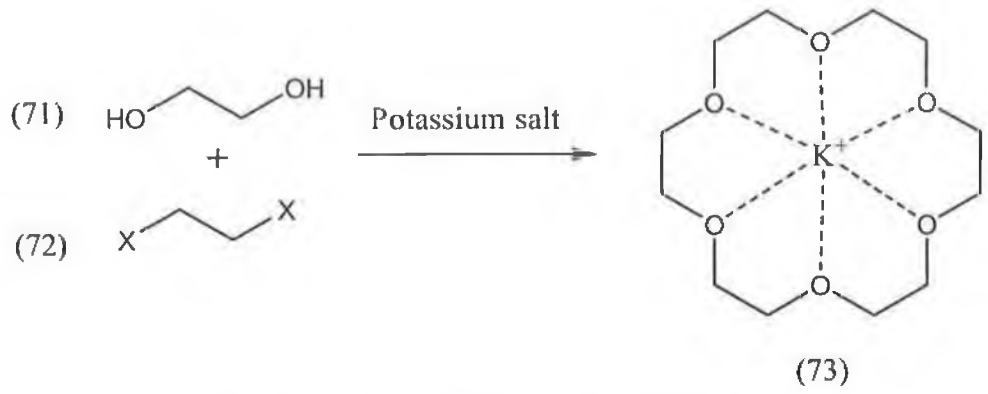

Scheme 23: *Metal templation mechanism of crown ethers*

Another example of a metal templation reaction is given in scheme 24, where the condensation of 2-aminobenzaldehyde, **74,** in the presence of anhydrous zinc(II) chloride gave a tetrameric species, **75.**

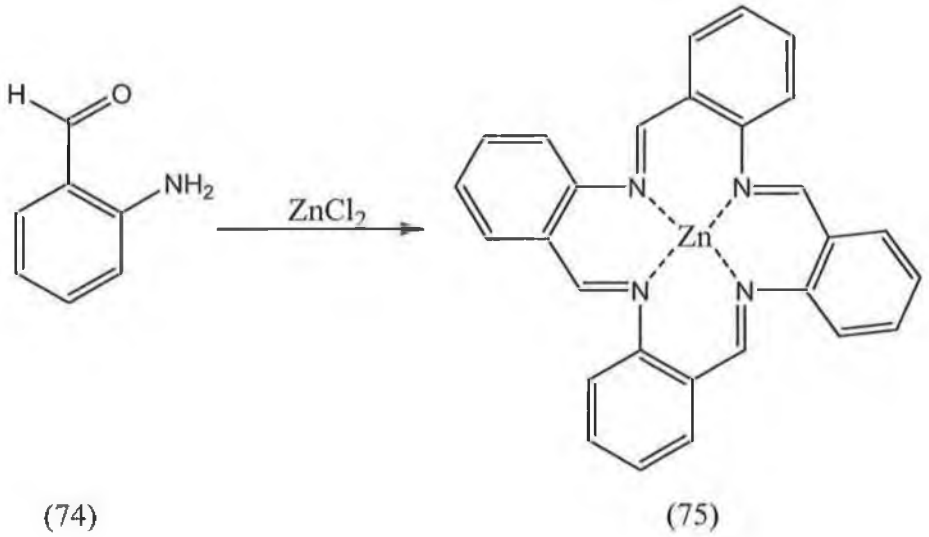

Scheme 24: *Metal templation assisted synthesis.*

We wanted to determine if metal templation could either enhance the yield of the tetramer or affect the stereochemical outcome of the reaction. A series of metal templation experiments was set up using different metal chlorides. We investigated the condensations of both 4-fluorobenzaldehyde, **70**, and acetaldehyde, **68**, with pyrogallol, **50**. These reactions involved adding an equivalent of a specific metal chloride to the reaction mixture. A total of eleven different salts were investigated. The results are shown in table 3.

Tetra-4-Fluorophenyl pyrogallol[4]arene, **70**			Tetramethyl pyrogallol[4]arene, **68**		
Expt No.	Salt	Yield (%)	Expt No.	Salt	Yield (%)
2.31-1	None	**35**	2.32-1	None	**34**
2.31-2	NaCl	**65**	2.32-2	NaCl	30
2.31-3	LiCl	51	2.32-3	LiCl	10
2.31-4	KBr	**70**	2.32-4	KBr	**49**
2.31-5	$CaCl_2$	39	2.32-5	$CaCl_2$	32
2.31-6	$MgCl_2$	50	2.32-6	$MgCl_2$	21
2.31-7	CsCl	61	2.32-7	CsCl	20
2.31-8	$BaCl_2$	No product	2.32-8	$ZnCl_2$	No product
2.31-9	$ZnCl_2$	**75**	2.32-9	CuCl	No product
2.31-10	CuCl	33	2.32-10	$NiCl_2$	No product
2.31-11	$CuCl_2$	No product	Yield Data refers only to the chair *rctt* Chair Tetramer, **5**		
2.31-12	$NiCl_2$	**81**			

Table 3: *Metal templation experiments and yields*

It can easily be seen from this table that certain metal ions enhanced the yield, increasing it over two-fold in some cases. For the condensation with 4-fluorobenzaldehyde; Sodium, Potassium, Zinc and Nickel ions favour the formation

of the tetramer, whereas for the tetramethylpyrogallol[4]arene, **65,** only potassium ion gives an enhancement.

It is possible that these enhancements are a result of a chelation effect, since only metals, of a specific size / charge ratios enhance the yield. However it is also a possibility that tetramerisation is enhanced due to the fact the pyrogallol is slightly deactivated by coordination to the metal. Deactivation of the pyrogallol moieties would inhibit the formation of polymers or long chain oligomers and perhaps encourage the formation of the tetramer. This could also be the reason that the addition of some salts to the reaction led to the formation of no product at all. Perhaps the pyrogallol was deactivated too much for a reaction to occur. (See chapter 4).

It is unlikely that we are seeing metal templation of the pyrogallol units (as in Figure 28a), as the *rctt* isomer is formed. However it could be the case that the intermediates are templated (as in figure 28b and 28c). However in the case of figure 28b, where two dimers are coming together, this should also lead to a substantial increase in the yield of the acetaldehyde condensation, which was not the case, suggesting that the process may be stepwise and not involve two dimers coming together.

We believe that the case described is figure 28d makes more sense of the results, that is, pyrogallol reactivity is lowered in the presence of a metal salt by chelation. The mechanism will be further discussed in chapter 4.

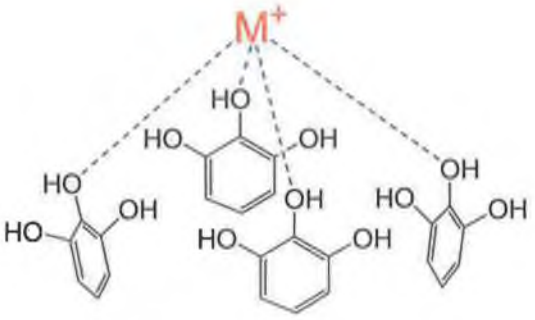

Figure 28a

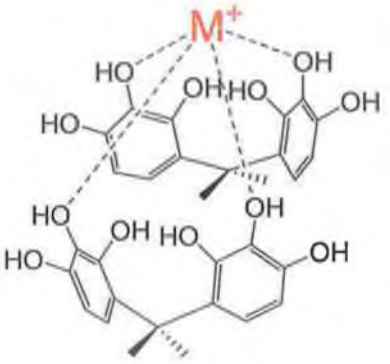

Figure 28b

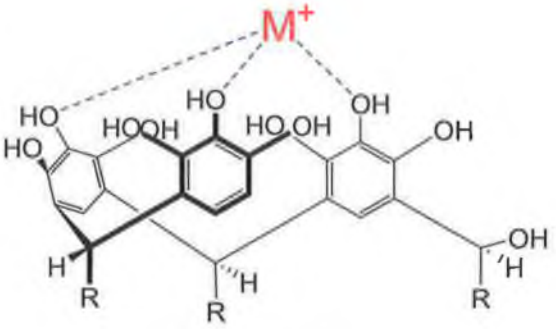

Figure 28c

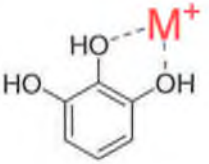

Figure 28d

Figure 31: *28a metal chelation to four pyrogallol units, 28b metal chelation to two approaching dimers, 28c metal chelation to a trimer intermediate and 28d metal chelation to an individual pyrogallol unit.*

2.3 Experimental:

2.3.1 Preparation of tetra-4-fluorophenyl pyrogallol[4]arene, 65.

38mmol (4.74g) of pyrogallol, **50**, and 38mmol (4.66g, 4.03ml) of 4-fluorobenzaldehyde, **70,** were placed into 67.5ml of HCl/ethanol (17.5/50). The reaction mixture was refluxed at 78°C – 80°C overnight, and the resulting insoluble tetramer was collected by filtration. The collected powder was exhaustively washed with a 80:20 mixture of ethanol:water to give 3.0mmol (2.76g, 32% yield) of tetramer **65.**

^{1}H-NMR- (400MHz) δ (DMSO-d_6) [ppm]

4.9ppm (2H, s, Ar-**H**), 5.9ppm (2H, s, Ar-**H**), 5.7ppm (4H, s, Ar-C**H-Ar**), 6.6ppm (8H, d, J=5.6Hz, Ar-**H**), 6.8ppm (8H, d, J=8.8Hz Ar-**H**), 7.7 (12H, broad multiplets, ArO**H**).

Mass Spec: M/Z: 951 (M+23)

Microanalysis: $C_{52}H_{36}O_{12}F_4.H_2O$; Calculated: %C = 65.96; %H = 4.05

Found: %C = 66.38; %H = 3.85

2.3.1.1: Concentration Study.

The standard conditions as described in **2.3.1** were used with 1g of Pyrogallol, **2**, and 0.85ml of 4-Flourobenzaldehyde, **70**.

A series of reactions was set up as outlined in Table 4.

Reaction Number	Pyrogallol	4-Fluoro benzaldehyde	HCl acid	Ethanol	% Yield
2.1.1-1	1.0g (8mmol)	0.85ml (8mmol)	2mls	2mls	n.p
2.1.1-2	1.0g (8mmol)	0.85ml (8mmol)	2mls	4mls	32%
2.1.1-3	1.0g (8mmol)	0.85ml (8mmol)	2ml	5ml	37%
2.1.1-4	1.0g (8mmol)	0.85ml (8mmol)	2mls	6mls	34%
2.1.1-5	1.0g (8mmol)	0.85ml (8mmol)	2mls	8mls	8%
2.1.1-6	1.0g (8mmol)	0.85ml (8mmol)	2mls	10mls	4%

Table 4: *Concentration Studies*

All Products were confirmed to be **65** by ^{1}H-NMR.

2.3.1.2: Tetramerisation under basic conditions

4mmol (0.5g) of pyrogallol, **50,** was treated with 4mmol (0.46g, 0.42ml) of 4-fluorobenzaldehyde in ethanol (50ml), under basic conditions (table 5). The reaction mixture was refluxed at 78°C – 80°C overnight, and the resulting (insoluble) tetramer was collected by filtration. The collected product was exhaustively washed with a 80:20 mixture of ethanol:water.

Pyrogallol	4-Fluoro benzaldehyde	Ethanol	Reagent	Reagent Amount	% Yield
4mmol (0.50g)	4mmol (0.42ml)	5ml	Hydrochloric Acid (37%)*	6mmol (0.6ml)	37%
4mmol (0.50g)	4mmol (0.42ml)	5ml	Sodium Hydroxide	6mmol (0.24g)	n.p
4mmol (0.50g)	4mmol (0.42ml)	5ml	Pyridine	6mmol (0.48ml)	n.p
4mmol (0.50g)	4mmol (0.42ml)	5ml	DBU	6mmol (0.87ml)	n.p
4mmol (0.50g)	4mmol (0.42ml)	5ml	HOBT	6mmol (0.82g)	n.p
4mmol (0.50g)	4mmol (0.42ml)	5ml	Triethylamine	6mmol (0.83ml)	n.p

Table 5*: Condensation under basic conditions*

*Control Reaction

* The product isolated from the control reaction was confirmed to be Tetramer **65** by ^{1}H-NMR.

2.3.2 Preparation of tetramethyl pyrogallol[4]arene, 69.

15.9mmol (2.00g) of pyrogallol, **50,** and 15.9mmol (0.70g, 0.90ml) of acetaldehyde, **68**, were placed into 27ml of ethanol:HCl (20:7) The reaction mixture was heated to 78°C – 80°C overnight, and the resulting insoluble tetramer was collected by filtration. The collected precipitate was washed with a 80:20 mixture of ethanol:water to give 1.25mmol (0.77g, 34%yield) of tetramer **69a**.

^{1}H-NMR- (400MHz) δ (DMSO-d_6) [ppm]

1.15ppm (12H, d, J= 7.2Hz CH-C**H**$_3$), 4.45ppm (4H, Multiplet, J=7.2Hz, Ar-C**H**-CH_3), 5.7ppm (2H, s, Ar**H**), 6.4ppm (2H, s, Ar**H**), 7.4ppm (4H, Broad Singlet, Ar**OH**). 7.8ppm (8H, Broad Singlet, Ar**OH**).

Mass Spec: M/Z: 631 (M+23)

Microanalysis: $C_{32}H_{32}O_{12}$; Calculated: %C = 63.13; %H = 5.30

Found: %C = 63.03; %H = 5.36

2.3.2.1 Isolation of **69b**:

The filtrate was poured onto ice to give a second precipitate. This precipitate was collected by suction filtration and was washed with cold water to give 0.26mmol (0.15, 7% yield) of tetramer **69b**.

^{1}H-NMR- (400MHz) δ (DMSO-d_6) [ppm]

1.48ppm (12H, d, J=7.2Hz CH-C**H**$_3$), 4.45ppm (4H, Quartet, J=7.2Hz, Ar-C**H**-CH_3), 6.7ppm (4H s, Ar**H**), 8.0ppm (4H Broad Singlet, Ar**OH**). 8.2ppm (8H Broad Singlet, Ar**OH**).

Mass Spec: M/Z: 631 (M+23)

Microanalysis: $C_{32}H_{32}O_{12}$; Calculated: %C = 63.13; %H = 5.30

Found: %C = 63.19; %H = 5.28

2.3.3.1 Metal-templation experiments: tetra-4-fluorophenylpyrogallol[4]arene

The reaction procedure used was the same as that used in the preparation of tetra-4-fluorophenyl pyrogallol[4]arene, **65,** in **2.3.1** above. (All reactions carried out for 36hrs) All reaction mixtures consisted of 8.0mmol (1.0g) of pyrogallol, 8.0mmol (0.99g, 0.86ml) of 4-fluorobenzaldehyde, **70,** 3.5mls of concentrated hydrochloric acid in 10ml of ethanol, with the exception that a metal salt chloride was added to the reaction mixture (see table 6).

EXPT NO.	SALT	QUANTITY OF SALT	%YIELD
2.31-1	None	N/A	35
2.31-2	NaCl	8mmol (0.47g)	65
2.31-3	LiCl	8mmol (0.34g)	51
2.31-4	KBr	8mmol (0.95g)	70
2.31-5	$CaCl_2$	8mmol (0.89g)	39
2.31-6	$MgCl_2$	8mmol (0.76g)	50
2.31-7	CsCl	8mmol (1.35g)	61
2.31-8	$BaCl_2$	8mmol (1.66g)	n.p
2.31-9	$ZnCl_2$	8mmol (1.09g)	75
2.31-10	CuCl	8mmol (0.79g)	33
2.31-11	$CuCl_2$	8mmol (1.08g)	n.p
2.31-12	$NiCl_2$*	8mmol (1.90g)	81

Table 6: *Metal templation experiments for tetra-4-fluorophenyl pyrogallol[4]arene.*
*$NiCl_2.6H_2O$ was used.

2.3.3.2 Metal-templation experiments: tetramethypyrogallol[4]arene.

The reaction procedure used was the same as that used in the preparation of **69**, in **2.3.2** above. (All reactions were carried out for 36hrs) All reaction mixtures consisted of 8.0mmol (1.0g) of pyrogallol, 8.0mmol (0.35g, 0.45ml) of acetaldehyde, 3.5mls of concentrated hydrochloric acid in 10ml of ethanol, with the exception that a metal salt chloride was added (see table 7).

EXPT NO.	SALT	QUANTITY OF SALT	%YIELD
2.32-1	None	N/A	34
2.32-2	NaCl	8mmol (0.47g)	30
2.32-3	LiCl	8mmol (0.34g)	10
2.32-4	KBr	8mmol (0.95g)	49
2.32-5	$CaCl_2$	8mmol (0.89g)	32
2.32-6	$MgCl_2$	8mmol (0.76g)	21
2.32-7	CsCl	8mmol (1.35g)	20
2.32-8	$ZnCl_2$	8mmol (1.09g)	n.p
2.32-9	CuCl	8mmol (0.79g)	n.p
2.32-10	$NiCl_2$*	8mmol (1.90g)	n.p

Table 7*: Metal templation experiments for tetramethyl pyrogallol[4]arene.*

*$NiCl_2.6H_2O$ was used.

Chapter 3

Synthesis of Pyrogallol[4]arenes II

3.1 Electronic Effects:

We were interested in determining the effect substituents in the benzaldehyde would have on both yield and stereochemical outcomes of the condensation reaction. 2-fluorobenzaldehyde, **79**, 3-fluorobenzaldehyde, **78**, 3,4-difluorobenzaldehyde, **81**, 3,5-difluorobenzaldehyde, **80** and pentafluorobenzaldehyde, **84**, were used to investigate the effect of the position of the fluorine on the ring. 4-chlorobenzaldehyde, **76** and 4-bromobenzaldehyde, **77** were used to complete the halo-benzaldehyde series. These were also compared to non-halogen systems using benzaldehyde, **67**, 4-ethoxybenzaldehyde, **85**, 4-nitrobenzaldehyde, **90** 4-hydroxybenzaldehyde, **88**, and *p*-tolualdehyde, **82**, which were subsequently compared to the trifluoro-*p*-tolualdehyde, **83**. (figure 32). All condensations were carried out in ethanol under acidic conditions (hydrochloric acid) for 5 hours.

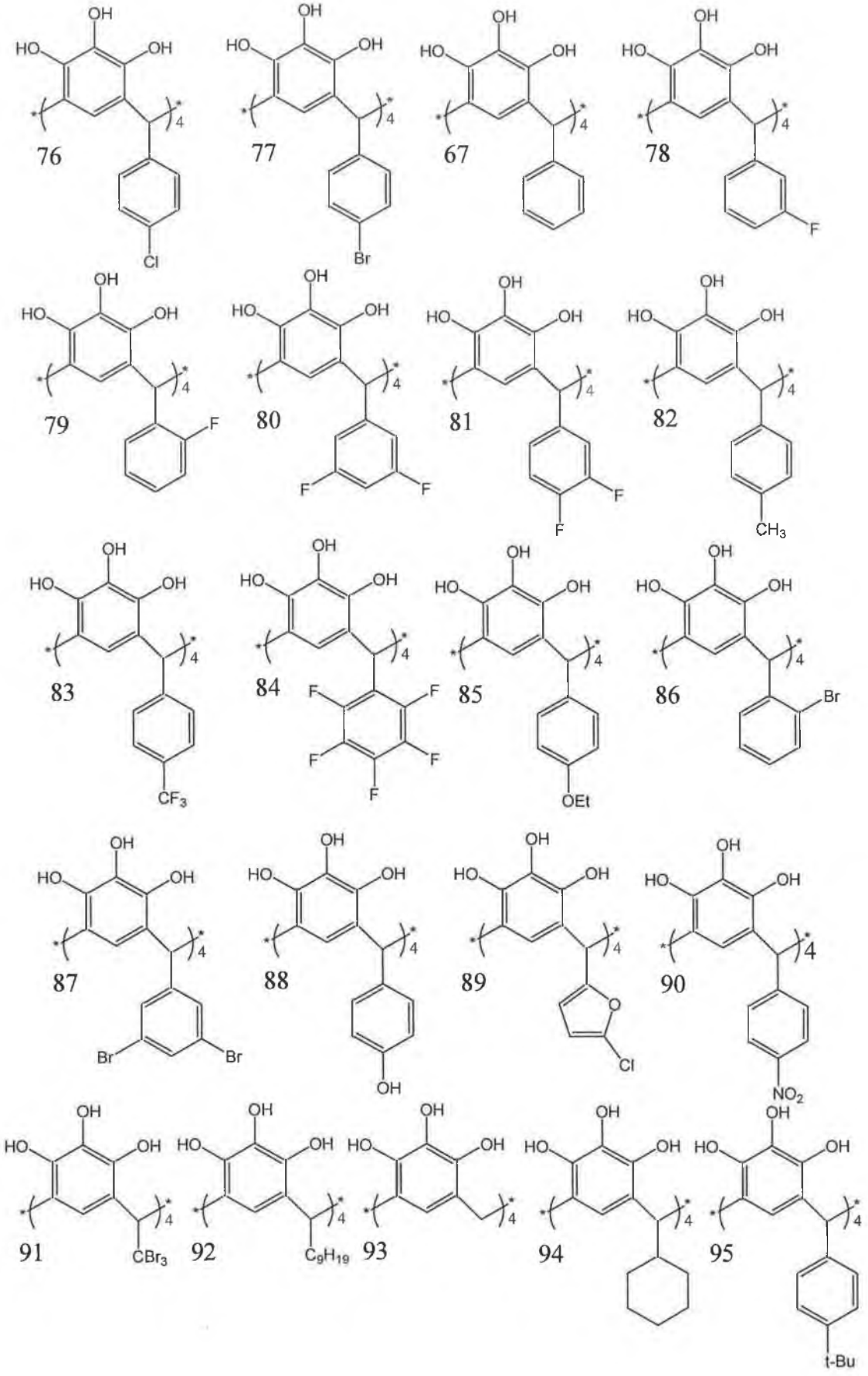

Figure 32: *Condensation products (67, 76-95).*

The yield results are tabulated in Table 8.

Tetramer No.	Aldehyde Used	%Yield – *rccc* Cone	% Yield – *rctt* Chair
76	4-Chlorobenzaldehyde	-	18
77	4-Bromobenzaldehyde	-	7
67	Benzaldehyde	-	15
78	3-Fluorobenzaldehyde	-	31
79	2-Fluorobenzaldehyde	-	46
80	3,5-Difluorobenzaldehyde	-	12
81	3,4-Difluorobenzaldehyde	-	16
82	*p*-Tolualdehyde	-	45
83	Trifluorotolualdehyde	-	26
84	Pentafluorobenzaldehyde	-	4
85	4-Ethoxybenzaldehyde	-	56
86	2-Bromobenzaldehyde	-	54
87	3,5-Dibromobenzaldehyde	-	47
88	4-Hydroxybenzaldehyde	-	58
89	2-Chlorofuraldehyde	No Product	No product
90	4-Nitrobenzaldehyde	-	8
91	Bromal	No Product	No Product
92	Decanal	55	-
93	Formaldehyde	No Product	No Product
94	Cyclohexanecarboxaldehyde	-	28
95	4-*t*-Butylbenzaldehyde	27	66
65	4-Fluorobenzaldehyde*	-	32
69	Acetaldehyde*	7	34

Table 8: *Yield Results*

*Experimental results for these condensations are in Chapter 2.

We will first discuss the results for **76, 77, 78, 82, 83, 85, 88, 90** and **65**, all of these tetramers are prepared from benzaldehydes possessing different substituents in the para and meta positions. A general trend can be observed: the stronger the electron withdrawing group in the benzaldehyde the lower the yield. This means that a positive inductive electronic effect (electron donating group) enhances the yield. We plotted yield against Hammett σ values to determine if a linear relationship exists. The results are shown in figure 33, a linear relationship does indeed exist with an R value of 0.93.

Cpd. No.	R-Group	%Yield	σ Value[72]
50	4-NO_2	8	0.78
36	4-Cl	18	0.23
37	4-Br	25	0.23
43	4-CF_3	26	0.54
38	3-F	31	0.34
30	4-F	32	0.06
42	4-CH_3	45	-0.17
45	4-OCH_2CH_3	56	-0.56
48	4-OH	58	-0.37

Table 9: *Trend of yield with σ values.*

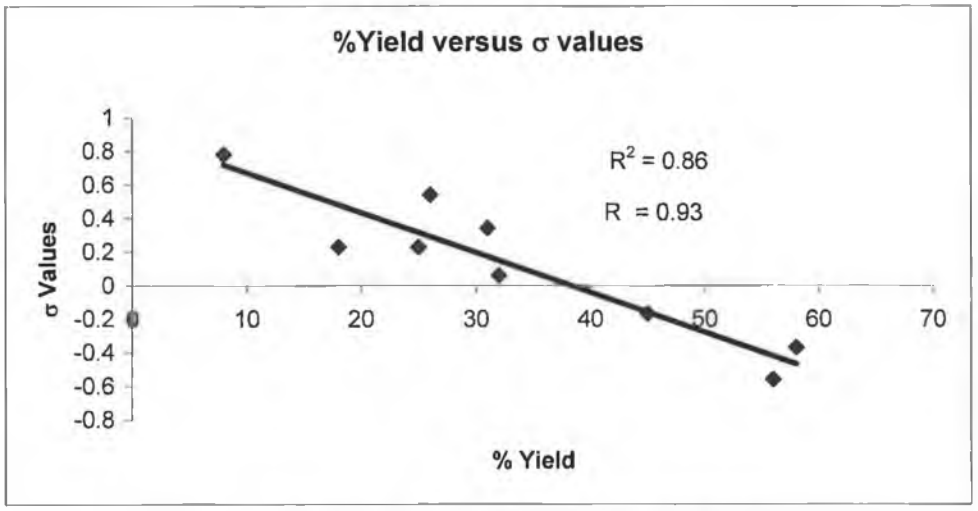

Figure 33: *Trend of yield with σ values*

This trend is obvious with the nitro groups being the strongest electron-withdrawing and as a result gave the lowest yield, only 8%, whereas aldehydes with strong electron donating groups, 4-ethoxybenzaldehyde and 4-hydroxybenzaldehyde, gave yields of 56-58%. It should be noted that all products gave the *rctt* chair stereoisomer based on the ^{1}H-NMR

3.2 Steric Factors:

We also wanted to consider steric effects on the outcome of these condensations, and we selected tetramers, **84, 86, 87, 92, 94, 95** and **69** (table 8), for this investigation.

For all the aromatic aldehyde derived tetramers prepared to this point the *rctt* chair conformer is the sole product. However, on using acelaldehyde (with an alkyl R group rather than aromatic) two conformations, the *rccc* cone conformation and *rctt* chair were isolated with the *rctt* chair being the major product.

A comparison was made using the longer chain alkyl aldehyde n-decanal. The resulting macrocycle, **92**, gave the *rccc* cone conformation as the sole product.

On its own the result for the decanal condensation is not surprising, as condensation of resorcinol with alkyl aldehydes gives the same result[73]. What is surprising is the formation of the *rctt* chair conformation on condensation with acetaldehyde. This conformation has been reported for resorcin[4]arenes[70] but only on condensation with aromatic aldehydes (4-hydroxbenzaldehyde) and even then it was a minor product.

The extra hydroxyl group on the benzene ring in pyrogallol (when compared to resorcinol) obviously adds to the reactivity of the phenyl ring to the extent that this conformation is thermodynamically favoured.

We then decided to condense cyclohexanecarboxaldehyde, **95**. We were interested in cyclohexane because like phenyl systems, it is a non aromatic six membered ring. Interestingly the cone conformation did not form but the *rctt* chair conformation formed in a reasonably low yield (≈25%) and also in low purity. Once again purification has proven difficult owing to the polar nature of these compounds. We believe that this result demonstrates that it is the six-membered ring (i.e. size) that dictates the stereochemical outcome of this reaction.

From here we attempted condensations with aromatic aldehydes that contained bulky groups on the phenyl ring, to give tetramers **84**, **86** and **87**. Condensation with 2-bromobenzaldehyde, gave **86** in high yield in the *rctt* chair conformation. This can be explained in terms of electronic factors, but it is quite surprising with regard to steric considerations, since one would have thought that a bromine group in the ortho-position would cause too much steric hindrance and condensation would not occur.

Based on the X-ray crystal structure of tetra-4-fluorophenyl pyrogallol[4]arene the three dimensional structure of tetramers **86** and **87** are shown in figure 34. For tetramer **86** we would assume the phenyl groups to be arranged so that the bromines are not in close proximity in order to relieve steric strain (as shown). As a result free rotation of the groups, should be inhibited, which should result in a poor yield. In the case of **87** the phenyl rings are completely locked in space, as a result of the size

(atomic radius Br = 1.2Å, compared with F = 0.7Å) of the pendant groups. The phenyl groups are not free to rotate therefore the reduction in yield of **87** in comparison to **86** is not surprising.

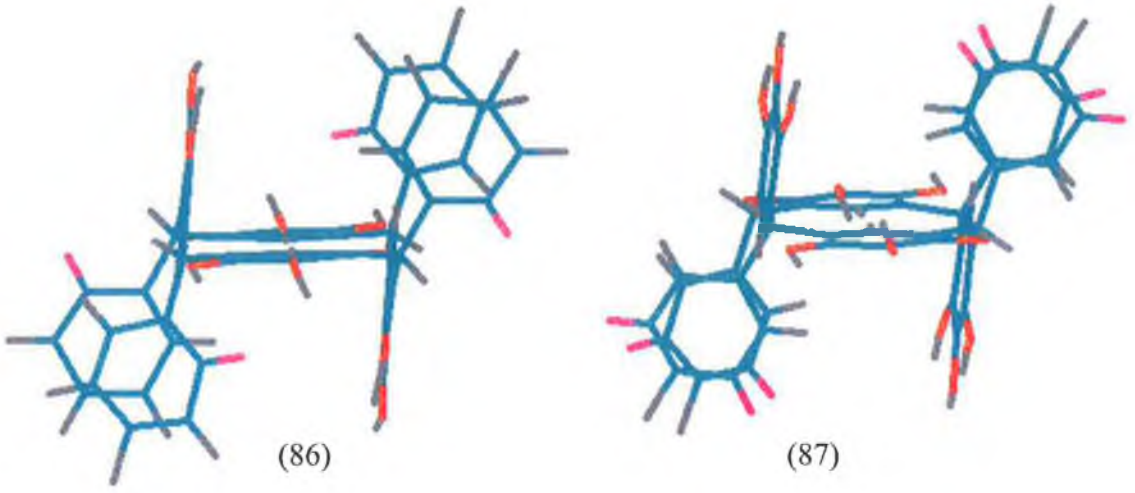

Figure 34: *a) Tetramer 46, tetra-2-bromophenyl pyrogallol[4]arene. b) Tetramer 47, tetra-3,5-dibromophenyl pyrogallol[4]arene. Both rctt chair stereoisomers.*

In the case of tetramer **84**, a low yield was obtained, we believe that the inductive effect on the ring was too great, (with five fluorine groups) and polymerisation occurred. This effect will be discussed in more detail later.

Following this we tried a condensation reaction with tetra-4-*t*-butylbenzaldehyde. We believed, based on the X-ray structure of **65**, that there would be far too much steric hindrance between the t-butyl groups on the neighbouring phenyl rings and either tetramerisation would be inhibited or the *rccc* cone conformation (or even the *rctc* cone conformation) would be the preferential conformation. This was not the case. An extraordinary high yield was recorded for this condensation. For the tetra-4-*t*-butylphenyl pyrogallol[4]arene, the *rccc* cone conformation was formed in 27% yield

(total yield for both conformations was 93%). This result was unexpected, it seems that the optimum isomer would be a *rtct* chair isomer, but this did not form at all. Electronically the *t*-Butyl group has a highly positive inductive effect on the ring and therefore would aid the condensation. However on looking at the crystal structure of the *rctt* chair conformation this would mean that two *t*-butyl groups are sterically close together in the product. This result tells us that although the tetramerisation is influenced by steric factors, electronic factors seem to play a more prominent role in the tetramerisation.

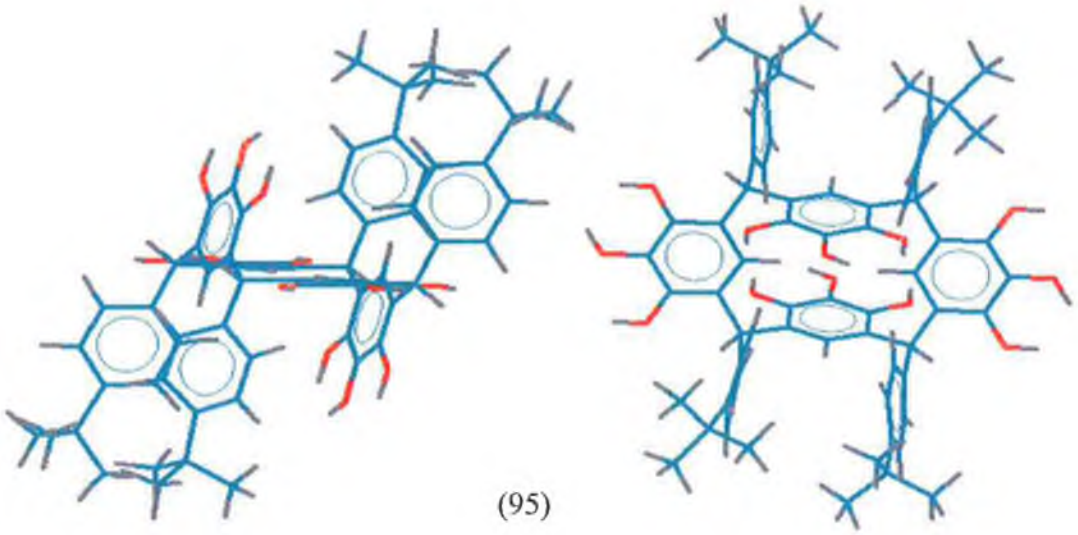

(95)

Figure 35: *3-D Schematic of rctt chair stereoisomer of tetra-4-t-butylphenyl pyrogallol[4]arene,* ***95***

3.3 Condensation with Non-benzyl Systems :

Bromal (CBr_3CHO) was condensed with pyrogallol, however instead of a tetramer being formed, a polymerisation reaction took place. We believe that this was due to the strong negative inductive effects of the three bromine atoms.

A furan ring was used in the place of benzene by using 2-chlorofuraldehyde. This heterocycle, although aromatic like benzene, has different electronic properties. 5-membered heteroaromatics have an increased reactivity when compared to benzene, as they are more π-electron rich (6π-electrons for 5 atoms)[74]. However according to this argument, the yield of the tetramer should have been enhanced. Perhaps the system is too reactive as polymerisation occurred once again.

Formaldehyde (HCHO) was condensed with the hope of investigating which conformation would be formed. However, again due to the enhanced reactivity (compared with acetaldehyde CH_3CHO), polymerisation occurred.

3.4 Gallic Acid Condensations:

After the library of pyrogallol[4]arenes was constructed, a series of condensations with gallic acid, in place of pyrogallol, was carried out with 4-fluorobenzaldehyde and acetaldehyde (scheme 24). A white insoluble solid was formed and due to its high insolubility it is believe to be a 3-D networked polymeric product. Microanalysis confirms that it is not the desired tetramer, as the carbon to hydrogen ratios are not the same as the theoretical values. It is believed that the formation of a 3-D network would be aided by the presence of the carboxylic acid group in the 5 position of pyrogallol.

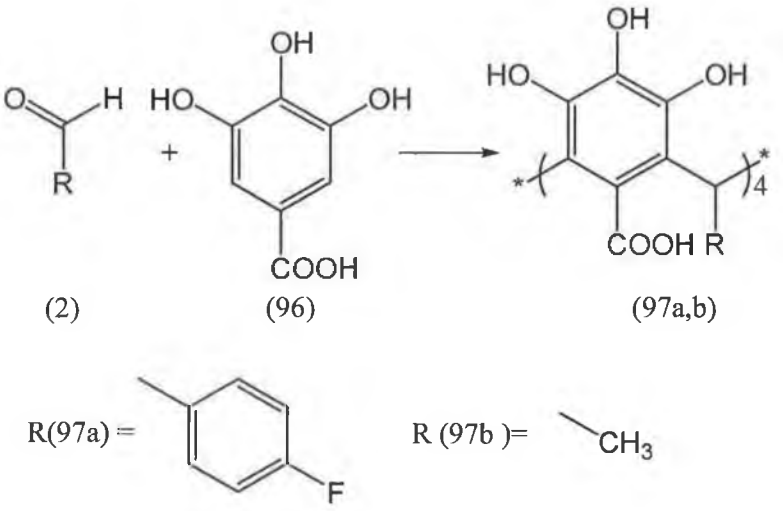

Scheme 25: *Condensation of gallic acid with 4-fluorobenzaldehyde and acetaldehyde.*

3.5 Experimental:

3.1 Preparation of tetra-4-chlorophenylpyrogallol[4]arene, 76.

3.9mmol (0.49g) of pyrogallol, **50**, was treated with 3.9mmol (0.55g) of 4-chlorobenzaldehyde in a HCl:ethanol (1.7ml:5ml) solution. The reaction mixture was refluxed at 78°C – 80°C overnight, and the resulting insoluble tetramer was collected by filtration. The precipitate was washed exhaustively with a 80:20 mixture of ethanol:water to give 0.17mmol (017g, 18% yield) of tetramer **76**.

^{1}H-NMR- (400MHz) (DMSO-d_6) δ [ppm]

4.9ppm (2H, s, Ar-**H**), 5.9ppm (2H, s, Ar-**H**), 5.6ppm (4H, s, Ar-C**H**-Ar), 6.6ppm (8H, d, J=7.2Hz Ar-**H**), 7.0ppm (8H, d, J=7.2Hz Ar-**H**), 7.7 (12H, broad multiplets, ArO**H**).

Mass Spec: m/z: 1018 (M+23)

Microanalysis: $C_{52}H_{36}O_{12}Cl_4 \cdot H_20$; Calculated: %C = 61.67; %H = 3.78

Found: %C = 61.67; %H = 3.64

3.2 Preparation of tetra-4-bromophenylpyrogallol[4]arene, 77.

The procedure described in 3.1 was followed using 7.53mmol (0.96g) of pyrogallol, **50**, 7.53mmol (1.39g) of 4-bromobenzaldehyde, to give 0.15mmol (0.18g, 7% yield) of tetramer **77.**

^{1}H-NMR- (400MHz) (DMSO-d_6) δ [ppm]

5.1ppm (2H, s, Ar-**H**), 5.9ppm (2H, s, Ar-**H**), 5.6ppm (4H, s, Ar-C**H**-Ar), 6.6ppm (8H, d, J=8.0Hz Ar-**H**), 7.1ppm (8H, d, J=8.0Hz Ar-**H**), 7.7 (12H, broad multiplets, ArO**H**).

Mass Spec: m/z: 1195 (M+23)

Microanalysis: $C_{52}H_{36}O_{12}Br_4 \cdot H_20$; Calculated: %C = 52.46; %H = 3.22

Found: %C = 52.28; %H = 3.00

3.3 Preparation of tetraphenylpyrogallol[4]arene, 67.

The procedure described in 3.1 was followed using 3.9mmol (0.49g) of pyrogallol, **50**, and 3.9mmol (0.41g) of benzaldehyde, to give 0.15mmol (0.13g, 15%yield) of tetramer **67** was collected.

^{1}H-NMR- (400MHz) (DMSO-d_6) δ [ppm]

5.2ppm (2H, s, Ar-**H**), 5.8ppm (2H, s, Ar-**H**), 5.7ppm (4H, s, Ar-C**H**-Ar), 6.6ppm (8H, d, J=7.6Hz Ar-**H**), 6.8ppm (8H, d, J= 7.6Hz Ar-**H** and 4H, multiplet, Ar-**H** overlapping), 7.6 (12H, broad multiplets, ArO**H**).

Mass Spec: m/z: 880 (M+23)

Microanalysis: $C_{52}H_{40}O_{12} \cdot H_20$; Calculated: %C = 71.39; %H = 4.84

Found: %C = 71.50; %H = 4.66

3.4 Preparation of tetra-3-fluorophenylpyrogallol[4]arene, 78.

The procedure described in 3.1 was followed using 8.0mmol (1.0g) of Pyrogallol, **50**, and 8.0mmol (0.99g, 0.85ml) of 3-fluorobenzaldehyde, to give 0.62mmol (0.57g, 31%yield) of tetramer **78**.

^{1}H-NMR- (400MHz) (DMSO-d_6) δ [ppm]

5.0ppm (2H, s, Ar-**H**), 6.0ppm (2H, s, Ar-**H**), 5.7ppm (4H, s, Ar-C**H**-Ar), 6.4ppm (4H, d, J=6.4Hz Ar-**H**), 6.45ppm (4H, d, J=6.4Hz Ar-**H**) 6.65ppm (4H, multiplet, Ar-**H**) 6.95ppm (4H, multiplet, J=6.8Hz Ar-**H**), 7.8 (12H, broad multiplet, ArO**H**).

Mass Spec: m/z: 951 (M+23)

Microanalysis: $C_{52}H_{36}O_{12}F_4 \cdot H_20$; Calculated: %C = 65.96; %H = 4.05

Found: %C = 66.36; %H = 3.93

3.5 Preparation of tetra-2-fluorophenylpyrogallol[4]arene, 79.

The procedure described in 3.1 was followed using 8.0mmol (1.0g) of Pyrogallol, **50**, and 8.0mmol (0.99g, 0.85ml) of 2-fluorobenzaldehyde, to give 0.92mmol (0.85g, 46% yield) of tetramer **79** was collected.

^{1}H-NMR- (400MHz) (DMSO-d_6) δ [ppm]

5.05ppm (2H, s, Ar-**H**), 6.0ppm (2H, s, Ar-**H**), 5.9ppm (4H, s, Ar-C**H**-Ar), 6.45ppm (4H, multiplet, Ar-**H**), 6.75ppm (8H, multiplet, Ar-**H**), 6.9ppm (4H, multiplet, Ar-**H**), 7.65-7.9 (12H, singlets, ArO**H**).

Mass Spec: m/z: 951 (M+23)

Microanalysis: $C_{52}H_{36}O_{12}F_4 H_20$; Calculated: %C = 65.96; %H = 4.05

Found: %C = 66.30; %H = 3.89

3.6 Preparation of tetra-3,5-fluorophenylpyrogallol[4]arene, 80.

The procedure described in 3.1 was followed using 8.0mmol (1.0g) of Pyrogallol and 8.0mmol (1.14g, 0.87ml) of 3,5-difluorobenzaldehyde, to give 0.24mmol (0.24g, 12% yield) of tetramer **80**.

^{1}H-NMR- (400MHz) (DMSO-d_6) δ [ppm]

4.85ppm (2H, s, Ar-**H**), 5.9ppm (2H, s, Ar-**H**), 5.75ppm (4H, s, Ar-C**H**-Ar), 6.25ppm (8H, multiplet, Ar-**H**), 6.70ppm (4H, multiplet, Ar-**H**), 7.9ppm (12H, broad multiplet, ArO**H**).

Mass Spec: m/z: 1023 (M+23)

Microanalysis: $C_{52}H_{32}O_{12}F_8 H_20$; Calculated: %C = 61.42; %H = 3.17

Found: %C = 61.62; %H = 3.31

3.7 Preparation of tetra-3,4-difluorophenylpyrogallol[4]arene, 81.

The procedure described in 3.1 was followed using 12.0mmol (1.5g) of Pyrogallol, **50**, and 12.0mmol (1.71g, 1.33ml) of 3,4-difluorobenzaldehyde, to give 0.47mmol (0.47g, 16% yield) of tetramer **81**.

^{1}H-NMR- (400MHz) (DMSO-d_6) δ [ppm]

4.70ppm (2H, s, Ar-**H**), 5.85ppm (2H, s, Ar-**H**), 5.65ppm (4H, s, Ar-C**H**-Ar), 6.40ppm (4H, multiplet, Ar-**H**), 6.50ppm (4H, multiplet, Ar-**H**), 6.95ppm (4H, multiplet, Ar-**H**), 7.7-8.0 (12H, singlets, ArO**H**).

Mass Spec: m/z: 1023 (M+23)

Microanalysis: $C_{52}H_{32}O_{12}F_8 \cdot H_20$; Calculated: %C = 61.42; %H = 3.17

Found: %C = 61.73; %H = 3.47

3.8 Preparation of tetra-*4*-methylphenylpyrogallol[4]arene, 82.

The procedure described in 3.1 was followed using 8.0mmol (1.0g) of pyrogallol, **50**, and 8.0mmol (0.96g, 0.94ml) of *p*-tolualdehyde, to give 0.43mmol (0.83g, 45% yield) of tetramer **82**.

^{1}H-NMR- (400MHz) (DMSO-d_6) δ [ppm]

5.10ppm (2H, s, Ar-**H**), 5.85ppm (2H, s, Ar-**H**), 5.60ppm (4H, s, Ar-C**H**-Ar), 6.53ppm (8H, d, J=7.6Hz Ar-**H**), 6.67ppm (8H, multiplet, Ar-**H**), 7.5 (12H, broad multiplet, ArO**H**).

Mass Spec: m/z: 935 (M+23)

Microanalysis: $C_{55}H_{48}O_{12} \cdot H_20$; Calculated: %C = 71.88; %H = 5.48

Found: %C = 72.32; %H = 5.21

3.9 Preparation of tetra-4-trifluoromethylphenylpyrogallol[4]arene, 83.

The procedure described in 3.1 was followed using 8.0mmol (1.0g) of pyrogallol, **50**, and 8.0mmol (1.39g, 1.09ml) of *p*-trifluorotolualdehyde, to give1.24mmol (0.59g, 26% yield) of tetramer **83**.

^{1}H-NMR- (400MHz) (DMSO-d_6) δ [ppm]

5.05ppm (2H, s, Ar-**H**), 5.95ppm (2H, s, Ar-**H**), 5.75ppm (4H, s, Ar-C**H**-Ar), 6.85ppm (8H, d, J=7.6Hz Ar-**H**), 7.35ppm (8H, d, J=7.6Hz Ar-**H**), 7.9 (12H, broad multiplet, ArO**H**).

Mass Spec: m/z: 1128 (M+23)

Microanalysis: $C_{56}H_{36}O_{12}F_{12}\cdot H_20$; Calculated: %C = 58.65; %H = 3.34

Found: %C = 58.56; %H = 3.23

3.10 Preparation of tetra-(pentafluoro)-phenylpyrogallol[4]arene, 84.

The procedure described in 3.1 was followed using 8.0mmol (1.0g) of pyrogallol, **50**, and 8.0mmol (1.57g, 0.99ml) of pentafluorobenzaldehyde, to give 0.08mmol (0.10g, 4% yield) of tetramer **84**.

^{1}H-NMR- (400MHz) (DMSO-d_6) δ [ppm]

5.15ppm (2H, s, Ar-**H**), 5.80ppm (2H, s, Ar-**H**), 5.45ppm (4H, s, Ar-C**H**-Ar), 7.3-7.9 (12H, broad multiplet, ArO**H**).

Mass Spec: m/z: 1249 (M+23)

Microanalysis: $C_{52}H_{20}O_{12}F_{20}\cdot H_20$; Calculated: %C = 50.58; %H = 1.80

Found: %C = 50.37; %H = 1.65

3.11 Preparation of tetra-4-ethoxyphenylpyrogallol[4]arene, 85.

The procedure described in 3.1 was followed using 15.9mmol (2.0g) of pyrogallol, **50**, and 15.9mmol (2.39g, 3.0ml) of 4-ethoxybenzaldehyde. After washing, the product was still found to be quite impure and recrystalisation from an 80:20 mixture of Ethanol:Water was carried out. 2.22mmol (2.29g, 56% yield) of tetramer **85.**

^{1}H-NMR- (400MHz) (DMSO-d_6) δ [ppm]

1.1 ppm (12H, broad singlet, Ar-O-$CH_2C\mathbf{H}_3$), 3.7ppm (8H, broad singlet, Ar-O-$C\mathbf{H}_2CH_3$), 5.05ppm (2H, s, Ar-**H**), 5.75ppm (2H, s, Ar-**H**), 5.35ppm (4H, s, Ar-C**H**-Ar), 6.35ppm (16H, broad singlet, Ar-**H**), 7.2-7.9 (12H, broad multiplet, ArO**H**).

Mass Spec: m/z: 1056 (M+23)

3.12 Preparation of tetra-2-bromophenylpyrogallol[4]arene, 86.

The procedure described in 3.1 was followed using 16.0mmol (2.0g) of pyrogallol, **50**, was treated with 16.0mmol (2.92g, 1.84ml) of 2-bromobenzaldehyde, to give2.16mmol (2.53g, 54% yield) of tetramer **86**.

^{1}H-NMR- (400MHz) (DMSO-d_6) δ [ppm]

5.05ppm (2H, s, Ar-**H**), 6.0ppm (2H, s, Ar-**H**), 5.9ppm (4H, s, Ar-C**H**-Ar), 6.45ppm (4H, d, J=7.2Hz Ar-**H**), 6.75ppm (8H, d, J=7.2Hz Ar-**H**), 6.9ppm (4H, Multiplet, Ar-**H**), 7.65-7.9ppm (12H, singlets, ArO**H**).

Mass Spec: m/z: 1195 (M+23)

Microanalysis: $C_{52}H_{36}O_{12}Br_4 \cdot H_20$; Calculated: %C = 52.46; %H = 3.22

Found: %C = 52.02; %H = 2.94

3.13 Preparation of tetra-3,5-dibromophenylpyrogallol[4]arene, 87.

The procedure described in 3.1 was followed using 16.0mmol (2.0g) of pyrogallol, **50**, and 16.0mmol (4.20g) of 3,5-dibromobenzaldehyde, to give1.89mmol (2.80g, 47%yield) of tetramer **87**.

^{1}H-NMR- (400MHz) (DMSO-d_6) δ [ppm]

4.85ppm (2H, s, Ar-**H**), 6.05ppm (2H, s, Ar-**H**), 5.80ppm (4H, s, Ar-C**H**-Ar), 6.8ppm (8H, s, Ar-**H**), 7.35ppm (4H, s, Ar-CH-Ar), 7.8ppm (4H, s, ArO**H**), 8.1ppm (8H, s, ArO**H**)

Mass Spec: m/z: 1511 (M+23)

Microanalysis: $C_{52}H_{32}O_{12}Br_8$; Calculated: %C = 41.97; %H = 2.17

Found: %C = 41.88; %H = 2.14

3.14 Preparation of tetra-4-hydroxyphenylpyrogallol[4]arene, 88.

The procedure described in 3.1 was followed using 16.0mmol (2.0g) of pyrogallol, **50**, and 16.0mmol (1.94g) of 4-hydroxybenzaldehyde, to give2.29mmol (2.10g, 58%yield) of tetramer **88**.

^{1}H-NMR- (400MHz) (DMSO-d_6) δ [ppm]

5.52ppm (2H, s, Ar-**H**), 5.95ppm (2H, s, Ar-**H**), 5.58ppm (4H, s, Ar-C**H**-Ar), 6.35ppm (8H, d, J=9.2Hz Ar-**H**), 6.45ppm (8H, d, J=9.2Hz Ar-**H**), 7.3-7.9ppm (12H, broad multiplet, ArO**H**), 8.7ppm (4H, broad singlet, ArO**H**)

Mass Spec: m/z: 944 (M+23)

Microanalysis: $C_{52}H_{40}O_{16}H_20$; Calculated: %C = 66.52; %H = 4.51

Found: %C = 65.91; %H = 4.32

3.15 Attempted preparation of tetra-5-chlorofuranpyrogallol[4]arene, 89.

8.0mmol (1.0g) of pyrogallol, **50,** was treated with 8.0mmol (1.04g) of 5-chloro-2-furaldehyde under concentrated acid conditions (HCl, 2ml) in ethanol (5ml). The reaction mixture was refluxed at 78°C – 80°C overnight, and the resulting (insoluble) black solid was collected by filtration. The collected precipitate was washed exhaustively with a 80:20 mixture of ethanol:water. After washing the product was still found to be quite impure and recrystallisation from an 80:20 mixture of ethanol:water was carried out. On analysis this product was found not to be tetramer **89**, but a mixture of oligomers and polymers.

3.16 Preparation of tetra-4-nitrophenylpyrogallol[4]arene, 90.

The procedure described in 3.1 was followed using 16.0mmol (2.0g) of pyrogallol, **50**, and 16.0mmol (4.20g) of 4-nitrobenzaldehyde, to give 0.32mmol (0.33g, 8%yield) of tetramer **90** was collected.

^{1}H-NMR- (400MHz) (DMSO-d_6) δ [ppm]

4.6ppm (2H, s, Ar-**H**), 5.9ppm (2H, s, Ar-**H**), 5.75ppm (4H, s, Ar-C**H**-Ar), 6.85ppm (8H, d, J=7.6Hz Ar-**H**), 7.75ppm (8H, d, J=7.6Hz Ar-**H**), 7.9-8.1ppm (12H, broad multiplet, ArO**H**).

Mass Spec: m/z: 1060 (M+23)

Microanalysis: $C_{52}H_{36}O_{20}N_4 \cdot H_20$; Calculated: %C = 65.96; %H = 5.31

Found: %C = 60.07; %H = 3.29; %N= 5.10

3.17 Attempted preparation of tetra-(tribromo)-methylpyrogallol[4]arene, 91.

15.9mmol (2.0g) of pyrogallol, **50**, was treated with 15.9mmol (4.47g, 1.68ml) of bromal under concentrated acid conditions (HCl, 3.7ml) in ethanol (10ml). The reaction mixture was refluxed at 78°C – 80°C overnight, and the resulting (insoluble) black solid was collected by filtration. The collected precipitate was washed exhaustively with a 80:20 mixture of ethanol:water. After washing the product was still found to be quite impure and recrystalisation from an 80:20 mixture of ethanol:water was carried out. On analysis this product was found not to be tetramer **91**, but a mixture of oligomers and polymers.

3.18 Preparation of tetradecylpyrogallol[4]arene, 92.

The procedure described in 3.1 was followed using 15.9mmol (2.0g) of pyrogallol, **50**, and 15.9mmol (2.48g, 3.0ml) of n-decanal. 2.20mmol (2.32g, 55%yield) of tetramer **92** was collected.

^{1}H-NMR- (400MHz) (DMSO-d_6) δ [ppm]

1.25ppm (19H, broad singlet, -C**H**$_2$-C**H**$_3$), 4.15ppm (4H, quartet, Ar-C**H**-CH$_2$), 6.80ppm (4H, multiplet, Ar-**H**), 8.15 (4H, s, ArO**H**) 8.65 (8H, s, ArO**H**).

Mass Spec: m/z: 1080 (M+23)

Microanalysis: $C_{64}H_{96}O_{12} \cdot H_2O$; Calculated: %C = 71.48; %H = 9.18

Found: %C = 71.57; %H = 9.00

3.19 Attempted preparation of pyrogallol[4]arene, 93.

The procedure described in 3.1 was followed using 16.0mmol (2.0g) of pyrogallol, **50**, and 16.0mmol (4.20g) of 3,5-dibromobenzaldehyde. The reaction mixture was refluxed at 78°C – 80°C overnight, and the resulting (insoluble) black solid was collected by filtration. The collected precipitate was washed exhaustively with a 80:20 mixture of ethanol:water. After washing the product was still found to be quite impure and recrystallisation from an 80:20 mixture of ethanol:water was carried out. On analysis this product was found not to be tetramer **93**, but a mixture of oligomers and polymers.

3.20 Preparation of tetra-4-cyclohexylpyrogallol[4]arene, 94.

The procedure described in 3.1 was followed using 6.36mmol (0.80g) of pyrogallol, **50**, and 6.36mmol (0.77ml) of cyclohexane carboxaldehyde, to give 0.44mmol (0.39g, 28% yield) of tetramer **94**.

Mass Spec: m/z: 903 (M+23)

Microanalysis: $C_{52}H_{64}O_{12}\cdot H_2O$; Calculated: %C = 69.47; %H = 7.40

Found: %C = 70.67; %H = 7.20

3.21 Preparation of tetra-4-*t*-butylphenylpyrogallol[4]arene, 95.

The procedure described in 3.1 was followed using 15.9mmol (2.0g) of pyrogallol, **50**, and 15.9mmol (2.58g, 2.66ml) of 4-*t*-butylbenzaldehyde, to give2.63mmol (2.84g, 66% yield) of tetramer **95** (*rctt* Chair).

^{1}H-NMR- (400MHz) (DMSO-d6) δ [ppm]

1.05 ppm (36H , broad singlet, C(C**H**$_3$)$_3$), 5.6ppm (4H, s, Ar-C**H**-Ar), 5.8ppm (2H, s, Ar-**H**), 6.1ppm (2H, s, Ar-**H**), 6.6ppm (8H, d, j=8.0Hz Ar-**H**), 6.9ppm (8H, d, J=8.0Hz Ar-**H**), 7.5ppm (8H, d, J=11.2Hz ArO**H**), 7.6ppm (2H, s, ArO**H**), 7.9ppm (2H, s, ArO**H**).

Mass Spec: m/z: 1104 (M+23)

Microanalysis: $C_{68}H_{72}O_{12}$ H_2O; Calculated: %C = 74.29; %H = 6.78

Found: %C = 74.59; %H = 6.64

Combined washings and filtrates were then treated with ice and 1.08mmol (1.16g, 27% yield) of tetramer **95a** (*rccc* cone) was collected.

^{1}H-NMR- (400MHz) (DMSO-d6) δ [ppm]

1.29 ppm (36H , broad singlet, C(C**H**$_3$)$_3$), 5.7ppm (4H, s, Ar-C**H**-Ar), 6.4ppm (4H, s, Ar-**H**), 6.8ppm (8H, d, J=8.4Hz Ar-**H**), 7.1ppm (8H, d, J=8.4Hz Ar-**H**), 7.6ppm (8H, s, ArO**H**), 7.8ppm (4H, s, ArO**H**).

Mass Spec: m/z: 1104 (M+23)

Microanalysis: $C_{68}H_{72}O_{12}$; Calculated: %C = 74.29; %H = 6.78

Found: %C = 74.49; %H = 6.72

3.22 Condensation of Gallic Acid, 58 with 4-fluorobenzaldehyde.

58.8mmol (10.0g) of gallic acid, **58**, and 58mmol (7.11g, 6.15ml) of 4-fluorobenzaldehyde were placed into 81ml of HCl/ethanol (21/60). The reaction mixture was refluxed at 78°C – 80°C overnight. The reaction yielded trace amount of an insoluble white solid, which could not be characterised.

3.23 Condensation of Gallic Acid, 58 with acetaldehyde.

58.8mmol (10.0g) of gallic acid, **58**, and 58.8mmol (2.60g, 3.30ml) of acetaldehyde were placed into 81ml of HCl/ethanol (21/60). The reaction mixture was refluxed at 78°C – 80°C overnight. The reaction yielded 0.3g of an insoluble white solid, which could not be characterised.

Chapter 4

Condensation Mechanism

The optimisation work carried out in the previous chapters raises some interesting questions concerning the mechanism of reaction and the conformational outcome:

1) We have observed a strong electronic effect with respect to the various substitutents of the benzaldehydes used.
2) The benzaldehydes yield different stereoisomers relative to the alkyl aldehydes. Furthermore, within the alkyl aldehyde series it would appear that acetaldehyde is unique in that it yields two different stereoisomers.
3) A 'metal effect' is observed in the reactions with 4-fluorobenzaldehyde.
4) Steric repulsion can be used with benzaldehydes to give a change in stereochemical outcome of the macrocycles.

The electronic effects indicate that the less reactive the aldehyde the higher the yield of product, indicating that competing reactions such as polymerisation are lowered.

The stereochemical outcome for these reactions seems to be independent of electronic factors for the benzaldehyde series, all derivatives (barring the t-butyl derivatives) yielded the *rctt* chair conformations. We believe that the driving force for the stereochemical outcome for these reactions result from steric effects. This is perhaps best demonstrated from the result of the condensation of cyclohexanecarboxaldehyde which yielded the *rctt* stereoisomer. Although it is an alkyl aldehyde, it's size and shape sterically mimics the size and shape of a phenyl ring, and this dictates the stereochemical outcome.

Outlined in scheme 25 is a proposed mechanism for the condensation of pyrogallol, **50**, with substituted aldehydes. A few things should be pointed out concerning the intermediates formed, first of all intermediate A, **98**, is chiral and should be produced as a racemate under the conditions used. Intermediates C, **100**, and D, **101**, are diastereomers. From simple molecular modelling (stick and ball models) we have found that only certain diastereomers will yield a macrocycle and these are identified in scheme 25. The macrocycles yielded from these intermediates are the *rctt* chair stereoisomers. The reason for this is that the other diastereomers are sterically repulsed upon approach to each other.

However, it should be noted that carbocation intermediates may be generated during the reaction (scheme 25) if this is the case then the enantiomeric effect of intermediate A, **98**, may be eliminated since racemisation will occur upon formation of the carbocation.

To explain the observed metal effect on yield we must look at a series of possible explanations. The first involves a metal templation effect, as mentioned in Chapter 2; this is observed with other macrocycle systems. Outlined in figure 36 are a series of possible templation interactions that can occur between metal salt and the hydroxy groups of pyrogallol. Each situation shown should lead to the *rccc* cone stereoisomer, however for the benzylaldehydes we still observe the *rctt* stereoisomer, and interestingly the acetaldehyde condensation does not show a change in stereoisomer ratio. We believe, based on these results that we can eliminate this particular templation effect as an explanation for yield enhancement.

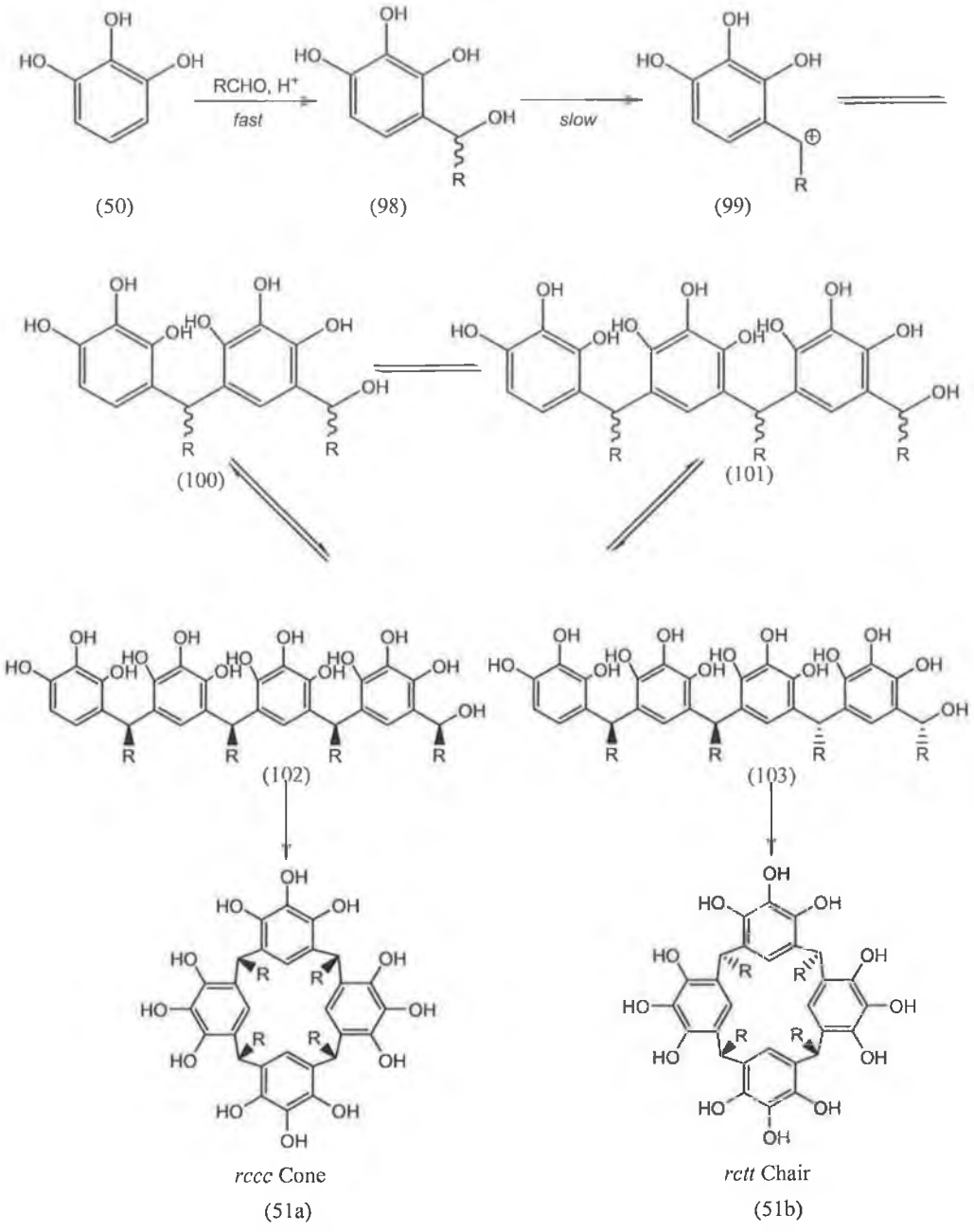

Scheme 26: *Condensation mechanism.*

A second templation could also occur between two dimeric intermediates B, **100**, as outlined in figure 36. However, if this was to occur then we should see an observable increase in yield of not only the benzaldehyde products but also of the acetaldehyde condensation reaction. Since an increase is not observed in the latter case we believe that this alternative templation is occurring.

We believe that cyclotetramerisation is enhanced in the presence of metal salts as a consequence of chelation between pyrogallol, **50**, and the metal salt as shown in figure 36. If such chelation occurs, then pyrogallol should be slightly deactivated toward electrophilic attack, since electron density within the pyrogallol ring would be lowered as a result of chelation. The substituent studies of the benzaldehydes also support this idea, that is, the less reactive substrates generate the highest yields. We believe that deactivation of the pyrogallol moieties would inhibit the formation of polymers or long chain oligomers (competing reactions) and perhaps encourage the formation of the tetramer. This could also be the reason that the addition of some salts to the reaction led to the formation of no product at all. Perhaps the coordination of pyrogallol caused a strong deactivation preventing reaction from occurring.

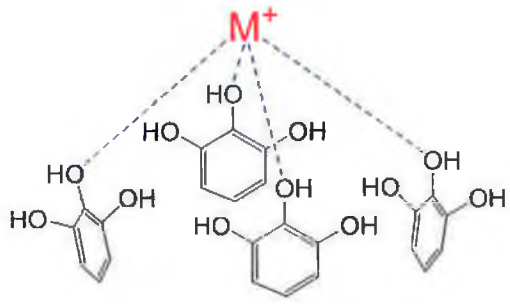

Figure 36a

Figure 36b

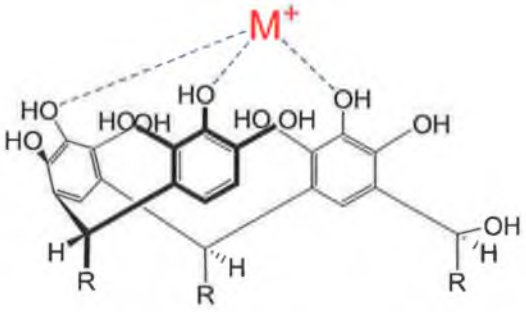

Figure 36c

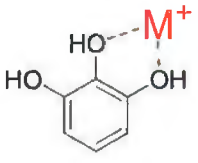

Figure 36d

Figure 36: *36a metal chelation to four pyrogallol units, 36b metal chelation to two approaching dimers, 36c metal chelation to a trimer intermediate and 36d metal chelation to an individual pyrogallol unit.*

Chapter 5

Derivatisation of Pyrogallol[4]arenes

5.1 Results and Discussion

5.1.1 Alkylation 1: Toward a completely alkylated pyrogallol[4]arene:

The first attempt at alkylating pyrogallol[4]arenes, **51**, was reported in the patent literature by Harris in 1995[69]. Although Harris claimed to have produced the fully alkylated species, we believe he may not have had. On analysis, and duplication of his synthetic methods, we found that a mixture of partially alkylated products was formed. To this end we endeavoured to solve this problem and develop methods to prepare fully alkylated pyrogallol[4]arenes.

We started our investigation with a variety of *rctt* chair pyrogallol[4]arenes, described in the previous chapter. The first alkylation reaction we considered involved using ethylbromoacetate, in acetone under basic conditions at 60°C (scheme 27).

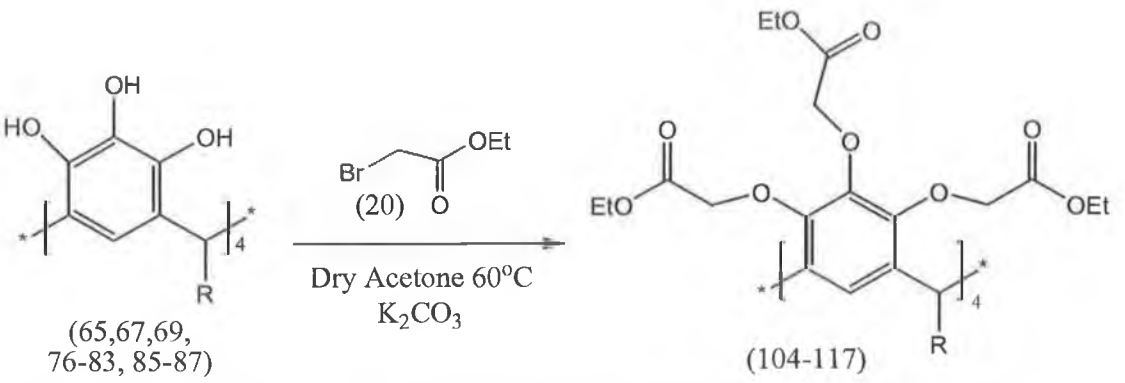

104	R_1	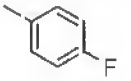	105	R_2	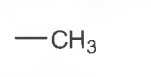
106	R_3	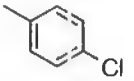	107	R_4	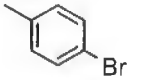
108	R_5		109	R_6	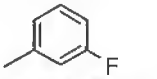
110	R_7	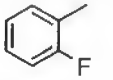	111	R_8	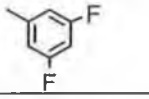
112	R_9	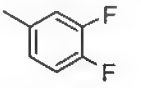	113	R_{10}	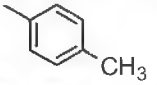
114	R_{11}	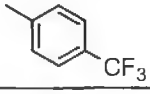	115	R_{12}	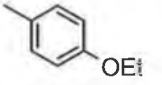
116	R_{13}	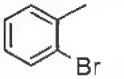	117	R_{14}	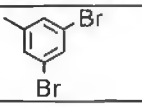

Scheme 27: *Alkylation of pyrgallol[4]arene to corresponding dodeca acetate ester.*

If left to react for one or two days, we found that only partially alkylated products were prepared. We found that this reaction had to be driven to completion. To achieve this goal extra equivalents of ethylbromoacetate and potassium carbonate were added each day over a five-day period. After the 5 days, all solvents were removed and the crude ester was precipitated with dilute acid, after filtration the crude ester was recrystallised from hot methanol. The main impurities were found to be bromine salt by-products. We attempted to purify these reaction mixtures by silica gel column chromatography however; we found this to be 'impossible' since we would only obtain less than 5% of the compound loaded onto the column. We believe this is due

to the highly polar nature of the compounds. We even found that solvents such as methanol would not improve the recovery of these compounds (when using ethyl actetate, or chloroform only trace amounts of compound could be eluted from the column). Therefore purification had to be carried out by repeated recrystallisations. Unfortunately even with repeated recrystallisation, absolute purity (determined by ^{1}H-NMR and microanalysis) was not achieved and therefore complete characterisation was not possible at this stage, although all products were identified by mass spectrometry confirming the presence of a single dodeca substituted product.

The yields for the alkylation reactions are outlined in table 10. These results are quite interesting, the esters prepared from tetramers possessing substituents *ortho* to the bridging carbon **110** and **116,** (figure 37) give rise to lower yields on alkylation. On examining our crystal structure (Chapter 2) we can see why this would be so. In tetramers with phenyl rings that contain *ortho*-substituents, alkylation to the neighbouring pyrogallol hydroxy group would be inhibited for steric reasons. This is more so the case for larger substituents, than smaller substituents as seen on comparison of **116** (6% yield) to **110** (24% yield). All other esters give respectable yields except for **117** which possesses two bromine groups *meta* to the bridging carbons. Again we believe size of the substituents may be playing an important role since **111** gives a respectable yield.

%Yield Results	
Number of R-Group	**Dodeca-acetate Ester**
1. 4-fluorophenyl	35%
2. methyl	80%
3. 4-chlorophenyl	88%
4. 4-bromophenyl	72%
5. phenyl	29%
6. 3-fluorophenyl	81%
7. 2-fluorophenyl	24%
8. 3,5-difluorophenyl	57%
9. 3,4-difluorophenyl	28%
10. 4-methylphenyl	62%
11.(trifluoro)-4-methylphenyl	57%
12. 4-ethoxyphenyl	54%
13. 2-bromophenyl	6%
14. 3,5-dibromophenyl	17%

Table 10: *Yield results from esterification reaction.*

We also attempted to completely alkylate the cone *rccc* isomer of the pyrogallol[4]arene prepared from acetaldehyde, **69**. We found that even under forced reaction conditions and extended reaction times that only a mixture of partially alkylated products could be prepared. We believe that this is largely due to two effects: 1) steric hindrance in the upper rim of the pyrogallol[4]arene and 2) the upper rim of a cone *rccc* pyrogallol[4]arene also possesses a large and very strong hydrogen bonding network between the twelve hydroxy groups (The difficulty in deprotonating

resorcinarenes is discussed in chapter 1). In order to alkylate the upper rim, we must overcome this highly stable hydrogen bonding network. This same difficulty also occurs with calix[4]arenes in the alkylation of the lower rim hydroxy groups[75].

The recrystallised chair *rctt* dodeca-acetate ester derivatives were then hydrolysed into the corresponding dodeca acetate potassium salts, (scheme 28). This reaction was found to be straightforward and usually reached completion in two hours.

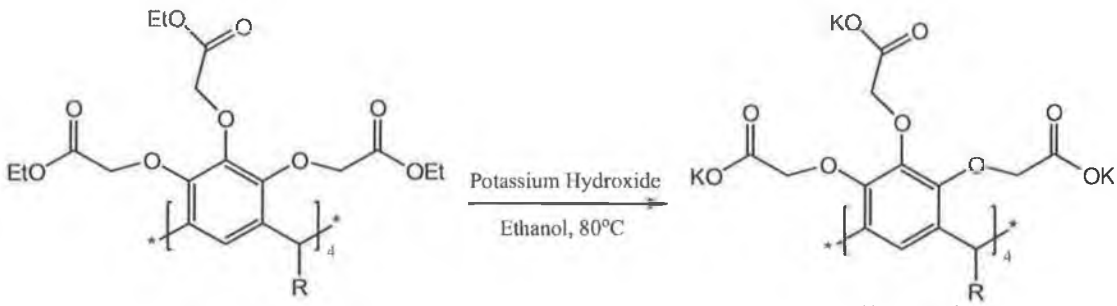

(104-117) (118-131)

Scheme 28: *Base catalysed hydrolysis of dodeca-acetate pyrogallol[4]arene to the corresponding dodeca-potassium acetate salt.*

Yield values for this reaction are shown in table 11 and are generally quite high. The dodeca-acetate salt is water-soluble.

We found that the most efficient way to purify the resulting salts is by a simple reprecipitation, from hydrochloric acid, to form the corresponding dodeca-acetate acid, (scheme 29) which is insoluble in water. The salt is regenerated in high purity by a further precipitation of the acid by treatment with potassium hydroxide in ethanol (the salt is insoluble in ethanol).

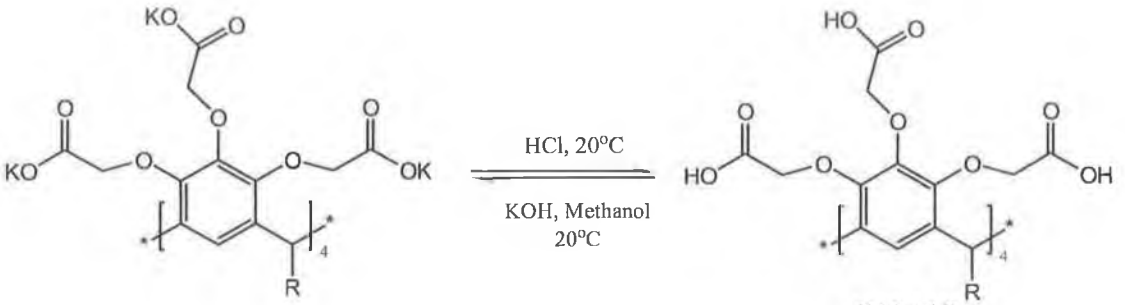

(118-131) (132-145)

Scheme 29: *Acid catalysed precipitation of dodeca-acetate acid from corresponding dodeca-potassium acetate salt, and the reformation of the dodeca salt by base catalysed precipitation.*

Number of R-Group	Dodeca-acetate Potassium Salt	Dodeca-acetate Acid
1. 4-fluorophenyl	95	72
2. methyl	95	80
3. 4-chlorophenyl	77	93
4. 4-bromophenyl	79	85
5. phenyl	91	63
6. 3-fluorophenyl	73	95
7. 2-fluorophenyl	80	84
8. 3,5-difluorophenyl	76	95
9. 3,4-difluorophenyl	76	95
10. 4-methylphenyl	75	96
11.(trifluoro)-4-methylphenyl	74	83
12. 4-ethoxyphenyl	63	81
13. 2-bromophenyl	94	93
14. 3,5-dibromophenyl	95	80

Table 11: *Yield Results for all salt and acid formation reactions.*

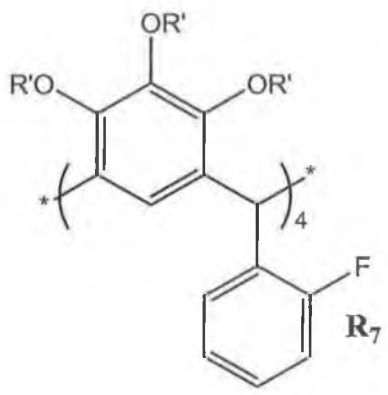

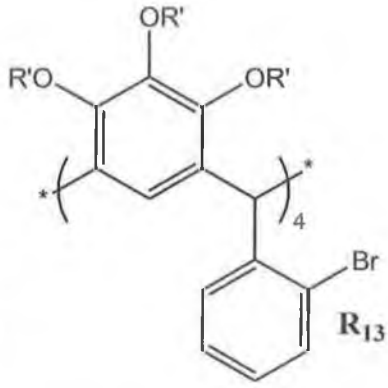

110. Ester: R' = CH_2COOEt 116. Ester: R' = CH_2COOEt
124. Salt: R' = CH_2COOK 130. Salt: R' = CH_2COOK
138. Acid: R' = CH_2COOH 144. Acid: R' = CH_2COOH

Figure 37: *Alkylated pyrogallol[4]arenes with ortho-substituted aryl groups.*

The dodeca-acetate acids (scheme 28) are formed in high purity and are fully characterised by ^1H NMR (figure 38), microanalysis and ESI mass spectrometry. We also grew crystals of the dodeca ester derivatives for X-ray crystallography, but they were of insufficient size for X-ray diffraction studies to be carried out.

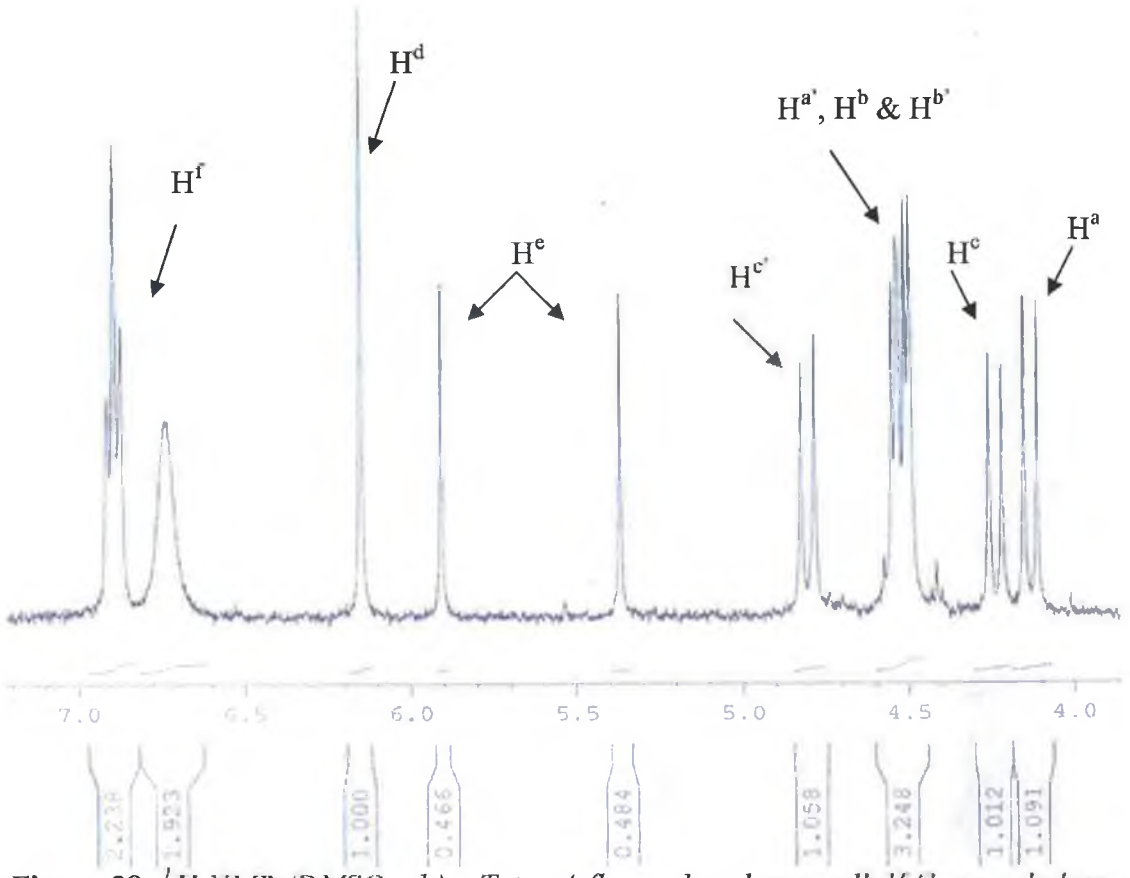

Figure 38: *^{1}H-NMR (DMSO - d_6) – Tetra-4-fluorophenyl pyrogallol[4]arene dodeca-acetate acid derivative.*

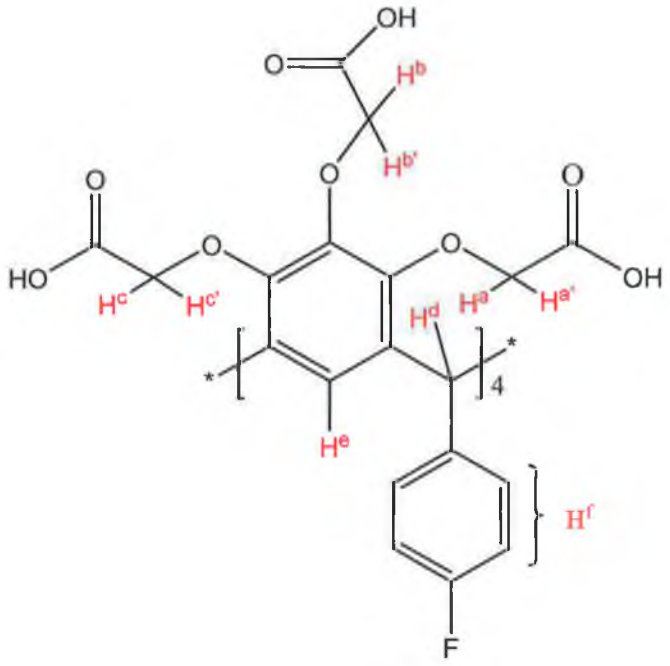

(132)

Figure 39: *Tetra-4-fluorophenyl pyrogallol[4]arene dodeca-acetate acid derivative, 132. (Equivalent protons labelled for ^{1}H-NMR interpretation)*

The ^{1}H-NMR of tetra-4-fluorophenyl pyrogallol[4]arene dodeca-acetate acid derivative, **132**, is shown in figure 38. There are six different acetate protons (H^a, $H^{a'}$, H^b, $H^{b'}$, H^c and $H^{c'}$). H^a and H^c appear as 2 distinct doublets at 4.12ppm and 4.25ppm. These two protons are pointing away from the centre of the ring and therefore appear more upfield than the other acetate protons. H^b and $H^{b'}$ each appear as singlets which are overlapping with a doublet derived from either $H^{a'}$ or $H^{c'}$. This multiplet appears at 4.5ppm. $H^{a'}$ and $H^{c'}$ appear as 2 doublets, one of which is overlapping with the two singlets from H^b and $H^{b'}$ at 4.5ppm and the other singlet appears at 4.8ppm. The protons on the methylene bridges of the pyrogallol[4]arene (H^d) are seen as a singlet at 6.2ppm. The aromatic pyrogallol protons (H^e) are split into two distinct singlets owing to the *rctt*-chair isomer (chapter 2). These are observed at 5.4ppm and 5.9ppm respectively. The doublet of doublets (H^f) is poorly resolved due to the presence of a fluorine atom on the ring and is seen at 6.6ppm and 6.9ppm. The carboxylic acid protons are not observed owing to some D_2O in DMSO-d_6.

5.1.2 Alkylation 2: Toward a Single Partially Alkylated Pyrogallol[4]arene

As mentioned previously, partially alkylated derivatives have shown biological activity, however, it is not possible to purify these complicated reaction mixtures into their single components thus identification as to which alkylated species possesses the 'best' biological activity is not possible.

With this in mind we came up with an alternative synthetic strategy to prepare a pure tetra-substitued pyrogallol[4]arene as outlined in scheme 30. We first attempted to stoichiometrically alkylate one of the three hydroxyl groups of pyrogallol, then this

derivative would then be condensed with an aldehyde to yield the target tetramer. (scheme 30)

The hydrogen on the central hydroxy group (Carbon 2) of pyrogallol is the most acidic hydroxyl proton and therefore should be displaced more readily than the other two. We had hoped that we could stoichiometrically control the alkylation to give the monoalkylated pyrogallol.

The first step in this reaction was successful, after intense purification, via column chromatography and recrystallisation, the desired product was isolated and characterised. **146** was then condensed with 4-fluorobenzaldehyde, **70**, however only a black precipitate was recovered, no target tetramer, **147**, was found.
It has been seen with calix[4]arenes[75,76], that when a calix[4]arene with acetate groups on it, undergoes a reaction in harsh acidic conditions, the acetate groups can be cleaved off of the calix[4]arene. We believe this to be the case here also. Under hydrochloric acid conditions the acetate group is being cleaved as shown in scheme 30. This synthetic plan was abandoned.

Attempt 1

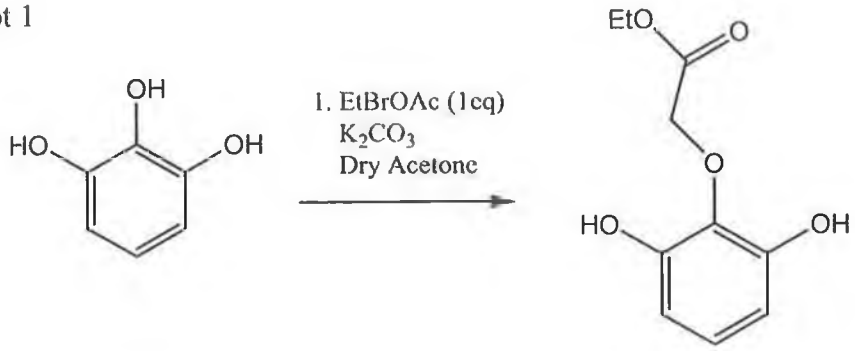

(50) (146)

Attempt 2

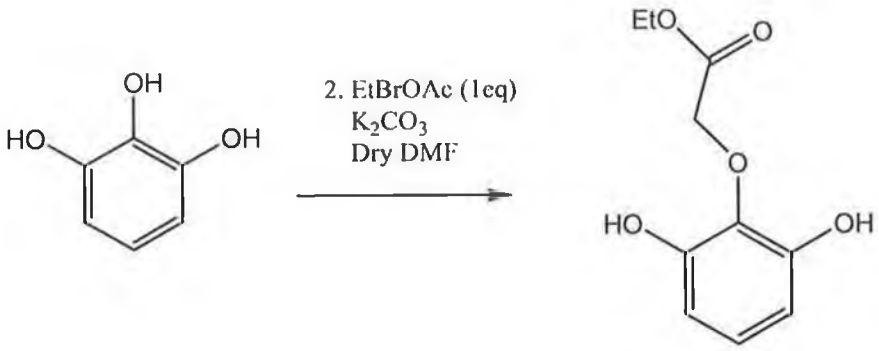

(50) (146)

Attempted Condensation

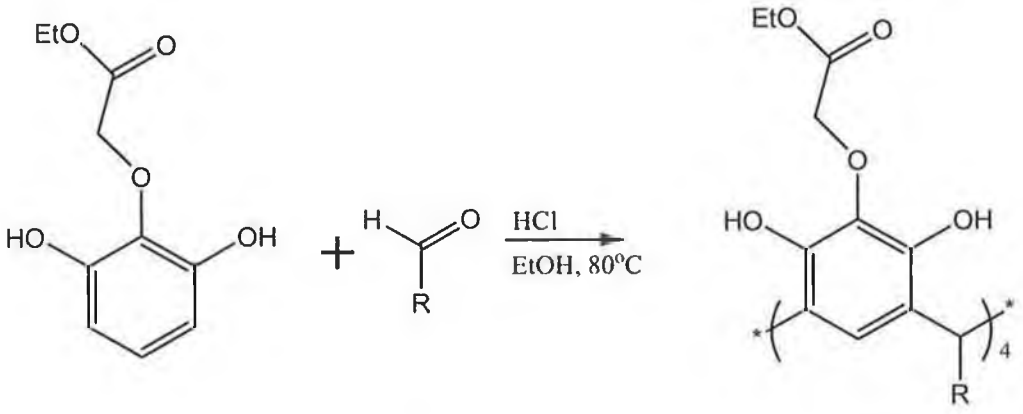

(146) (2) (147)

Scheme 30: *Attempt at partial alkylation.*

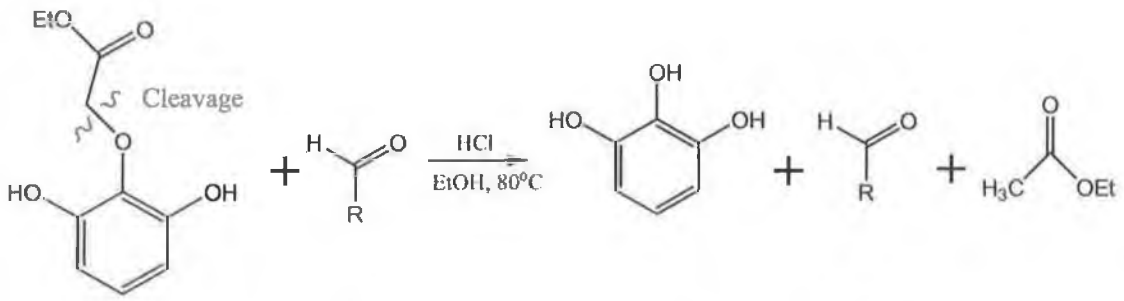

(146) (2) (50) (2)

Scheme 31: *Acid Catalysed cleavage and regeneration of starting material.*

5.1.3 Alkylation 3: Toward Partially Alkylated Pyrogallol[4]arenes using Stoichiometric Control.

As mentioned previously the hydroxy group on the two position of the pyrogallol is more acidic, and would undergo alkylation more readily than the other two. This is still the case in the pyrogallol[4]arene tetramer. In order to synthesise partially alkylated derivatives, we attempted a series of stoichiometrically-controlled alkylations as shown in scheme 32.

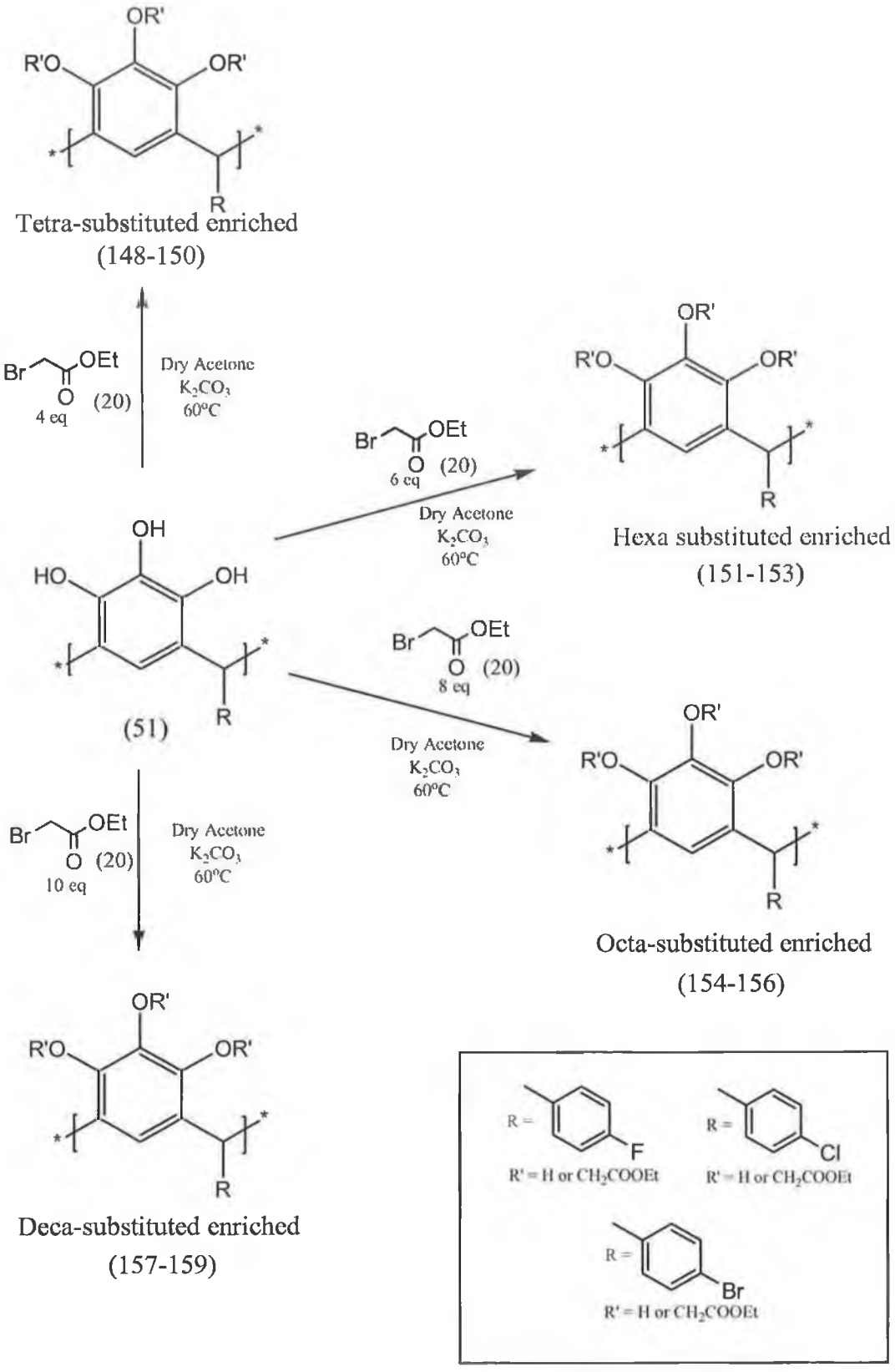

Scheme 32: *Partial alkylation attempt 2.*

We realised that this procedure would not yield a single pure compound, however we endeavoured to make an enriched sample of a particular partially substituted derivative. For example reaction 2 (using six equivalents) would yield a mixture of predominately hexa-alkylated pyrogallol[4]arene (along with some tetra-alkylated to octa-alkylated).

The first two attempts of this reaction, using 4 and 6 equivalents of ethylbromoacetate, yielded no product, and the third attempt (8 equivalents) gave a low yield, <5%. Using 10 equivalents of ethylbromoacetate gave a mixture of partially and completely alkylated pyrogallol[4]arenes, in substantial yield. It would appear that the alkylation reaction has a minimum stoichiometric threshold, anything under 10 equivalents yields little or no alkylation product.

The partially alkylated esters were converted to the corresponding potassium salts and acids as outlined in schemes 28 and 29. ^{1}H-NMR and ESI mass spectrometry were used to characterise the acid derivatives, the ^{1}H-NMR spectra were poorly resolved owing to a mixture of compounds. Mass Spectra gave a bell curve of molecular ion peaks centralising about 200-300 a.m.u.'s below the mass of the completely alkylated products.

These partially alkylated salt derivatives were also evaluated as Gp120 inhibitors (chapter 7).

5.1.4 Alkylation 4: Alkylations using Various other Alkylating Agents

As part of our SAR study, we were interested in observing:

1) The effect of a longer carbon chain carboxy substituent on biological activity
2) The effect of a neutral substituent
3) The effect of replacing the carboxylate with a sulfonate group.

We decided to prepare a series of new alkylated derivatives of the tetra-4-fluorophenyl pyrogallol[4]arene, **65.**

Ethylbromopropionate:

For the first case we decided to introduce ethlybromopropionate since it contains an extra methylene spacer (scheme 33).

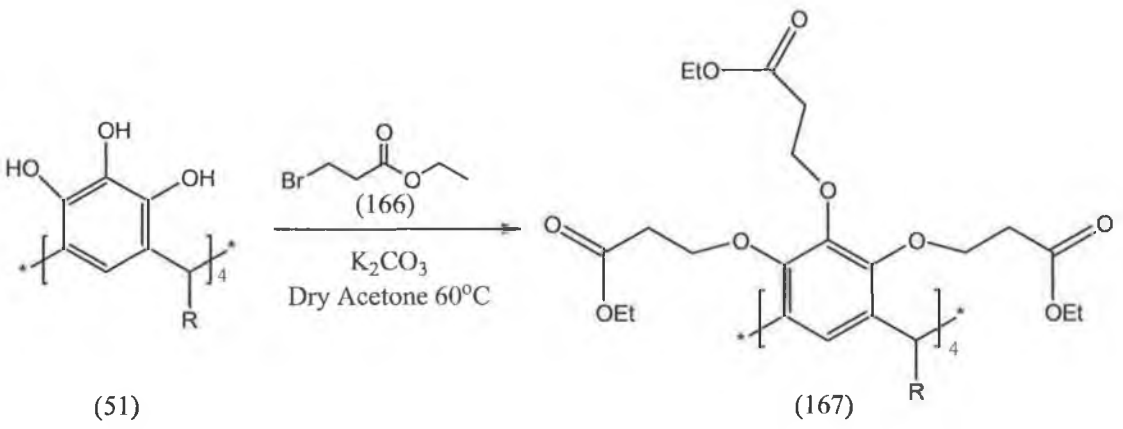

Scheme 33: *Alkylation of pyrgallol[4]arene using ethylbromopropionate.*

We employed the same reaction conditions developed for the preparation of the acetate derivatives. This reaction resulted in a fine yellow powder, and on recrystallisation from hot methanol very little product was present. The impurities removed were found to be a mixture of water-soluble inorganic bromine salts. It was not possible to characterise or continue the reaction as the amount of product obtained was so little and it was also very impure. It is thought that this system would be too

sterically hindered for alkylation to occur, but more than likely it is because ethylbromopropionate is a poorer electrophile than ethylbromoacetate, and therefore less reactive.

1-Bromopropane:

The next alkylating agent that was used was 1-bromopropane, this attempt proceeded as in scheme 34, again using the tetra-4-fluorophenyl pyrogallol[4]arene, **65,** and also the tetramethyl pyrogallol[4]arene, **69**.

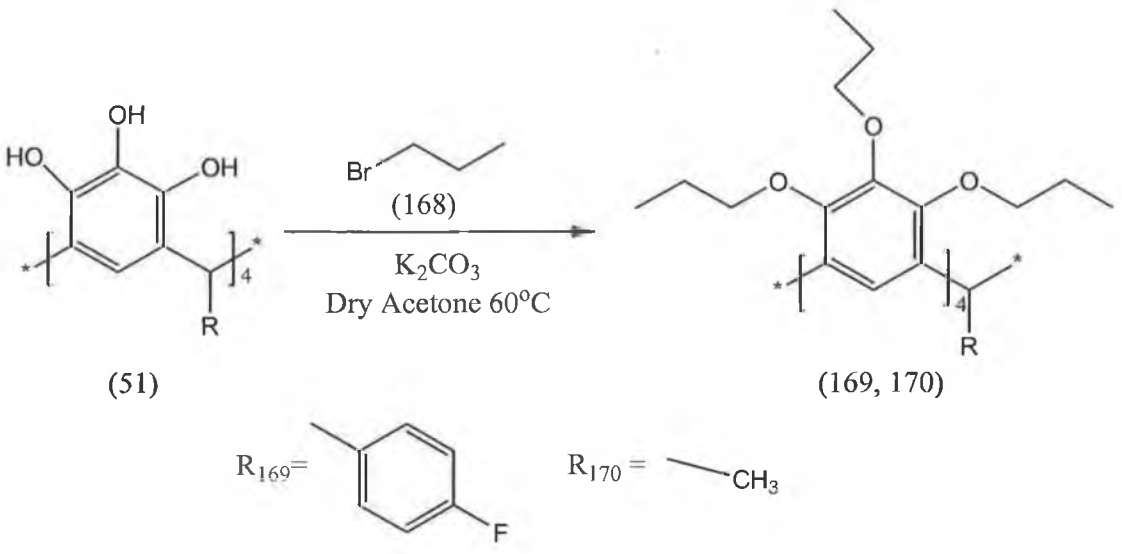

Scheme 34: *Alkylation of pyrogallol[4]arene using 1-bromopropane.*

Once again this reaction was unsuccessful, as only inorganic bromine salts were produced. This reaction is reported in the literature for calix[4]arenes[77,78]. In the first reference Budka *et al.* uses propyl iodide with caesium carbonate in acetone (41%). However he reports that this reaction only gives an alkylated product of the 1,3-alternate conformation of the calixarene. In the other reference Dudic *et al.* reports the alkylation in 76% yield (conformation not specified) using propyl iodide and sodium hydride in anhydrous DMF. These are very severe conditions, and there are only four

alkylation sites. In the case of pyrogallol[4]arenes there are 12 alkylation sites. It is clear from this that propyliodide is too weak an electrophile for this alkylation.

2-Chloroethyl Sulphonate Sodium Salt:

The final alkylating agent used was 2-chloroethyl sulphonate sodium salt, again using the tetra-4-fluorophenyl pyrogallol[4]arene, **65,** via scheme 35. We were interested in pursuing this class of compound for biological reasons. It is known that polyanions can act as GP120 inhibitors[66], furthermore the charge on sulphonates are independent of pH unlike carboxylates. To this end we endeavoured to form a range of dodecasulphonate derivatives.

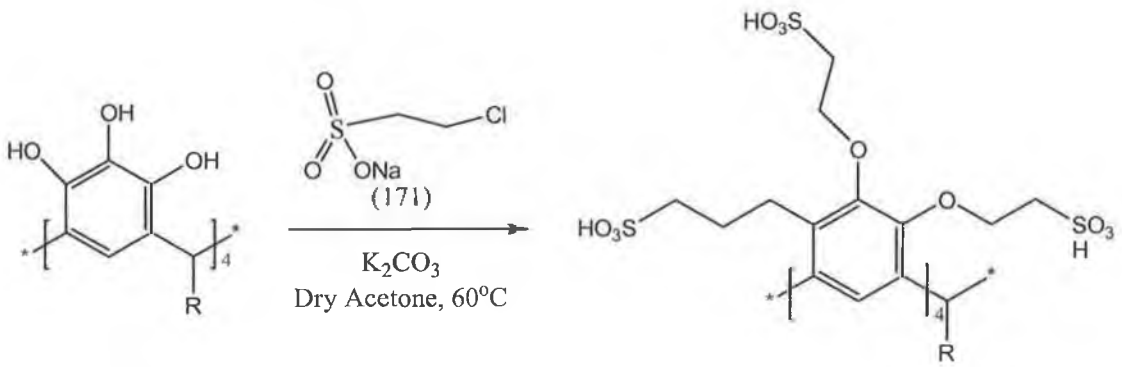

(65) (172)

Scheme 35: *Alkylation of pyrogallol[4]arene using 2-chloroethylsulphonate sodium salt.*

Once again this reaction was unsuccessful, the yellow-orange product that was produced was found to be inorganic halogen salts. Again this is due to the electrophile being too weak to undergo alkylation.

5.2 Experimental:

5.1.1 General procedure: alkylation of tetra-4-fluorophenyl pyrogallol[4]arene, 30, with ethylbromoacetate

4.32mmol (4.00g) of tetramer **65**, (scheme 26) were reacted with 69.12mmol (11.54g, 7.66ml) of ethylbromoacetate and potassium carbonate (108mmol, 14.90g) in 240ml of dry acetone. The reaction was carried out at 60°C for 5 days. The reaction was driven to completion by the addition of 0.2 equivalents of ethylbromoacetate and potassium carbonate each day. On cooling to room temperature all volatiles were removed under reduced pressure. The residue was treated with 5ml of dilute HCl and then filtered to yield a fine yellow powder. The crude ester was purified by recrystallisation from hot methanol, to give 1.51mmol (2.96g, 35% yield), of dodeca-ethylacetate pyrogallol[4]arene tetramer **104**

5.1.2 Base hydrolysis of dodeca-acetate ester 104

0.10mmol (0.19g) of dodeca-acetate ester **104** was treated with 5.0mmol (0.28g) of potassium hydroxide under reflux in ethanol at 80°C for overnight. On filtration 0.10mmol (0.19g 95% yield) of dodeca-acetate potassium salt **118** was recovered.

5.1.3 Acid hydrolysis of dodeca-acetate potassium salt 118

0.09mmol (0.19g) of the dodeca-acetate potassium salt **118** was dissolved in distilled water. Concentrated hydrochloric acid was added drop-wise, until a white precipitate

formed. The reaction mixture was allowed to stand overnight whereupon the dodeca-acetate acid, **132,** was isolated by centrifugation and washed with distilled water, to give 0.07mmol (0.11g, 72% yield) of dodeca-acetate acid **132**.

^{1}H-NMR- (400MHz) (DMSO-d_6) δ [ppm]

4.1 ppm (4H, d, J=7.2Hz, Ar-O-C**H**$_2$-COOH), 4.3 ppm (4H, d, J=7.2Hz, Ar-O-C**H**$_2$-COOH), 4.5 ppm (12H, multiplet, Ar-O-C**H**$_2$-COOH), 4.8 ppm (4H, d, J=7.2Hz, Ar-O-C**H**$_2$-COOH), 5.4ppm (2H, s, Ar-**H**), 5.9ppm (2H, s, Ar-**H**), 6.2ppm (4H, s, Ar-C**H**-Ar), 6.7ppm (8H, broad singlet, Ar-**H**), 6.9ppm (8H, multiplet, Ar-**H**).

Mass Spec: m/z: 1647 (M+Na), 1663 (M+K)

5.2.1 Alkylation of tetramethyl pyrogallol[4]arene, 69, (*rctt* – Chair) with ethylbromoacetate

The general procedure as described in 5.1.1 was followed using 0.82mmol (0.50g) of tetramer **69**, (scheme 26), 13.16mmol (2.20g, 1.46ml) of ethylbromoacetate, and 20.6mmol (2.84g) of potassium carbonate, in 30ml of dry acetone, to give 0.66mmol (0.6g, 80% yield) of dodeca-ethylacetate pyrogallol[4]arene tetramer **105.**

5.2.2 Base hydrolysis of dodeca-acetate ester 105

The procedure as described in 5.1.2 was followed using 0.33mmol (0.3g) of dodeca-acetate ester **105** and 9.9mmol (0.56g) of potassium hydroxide, to give 0.31mmol (0.32g 95% yield) of dodeca-acetate potassium salt **119**.

5.2.3 Acid hydrolysis of dodeca-acetate potassium salt 119

The general procedure as described in 5.1.3 was followed using 0.26mmol (0.15g) of dodeca-acetate potassium salt **119**, to give 0.21mmol (0.12g, 80% yield) of dodeca-acetate acid **133**.

^{1}H-NMR- (400MHz) (DMSO-d_6) δ [ppm]

1.3 ppm (12H, s, -C**H**$_3$), 4.3 ppm (4H, s, Ar-C**H**-CH$_3$), 4.5 ppm (8H, d, J=8.4Hz, Ar-O-C**H**$_2$-COOH), 4.7 ppm (16H, multiplet, Ar-O-C**H**$_2$-COOH), 5.5ppm (2H, s, Ar-**H**), 6.9ppm (2H, s, Ar-**H**),

Mass Spec: m/z: 1327 (M+Na), 1343 (M+K)

5.3.1 Alkylation of tetra-4-chlorophenyl pyrogallol[4]arene, 76, with ethylbromo acetate

The general procedure as described in 5.1.1 was followed using 0.30mmol (0.30g) of tetramer **76**, (scheme 26) **,** 4.83mmol (0.80g, 0.53ml) of ethylbromoacetate, and 7.55mmol (1.04g) of potassium carbonate, in 5ml of dry acetone, to give 0.26mmol (0.54g, 88% yield) of dodeca-ethylacetate pyrogallol[4]arene, tetramer **106**.

5.3.2 Base hydrolysis of dodeca-acetate ester 106

The procedure as described in 5.1.2 was followed using 0.15mmol (0.30g) of dodeca-acetate ester **106** and 3.03mmol (0.17g) of potassium hydroxide. 0.12mmol (0.25g 77% yield) of dodeca-acetate potassium salt **120**.

5.3.3 Acid hydrolysis of dodeca-acetate potassium salt 120

The general procedure as described in 5.1.3 was followed using 0.14mmol (0.30g) of dodeca-acetate potassium salt **120**, to give 0.13mmol (0.22g, 93% yield) of dodeca-acetate acid **134**.

^{1}H-NMR- (400MHz) (DMSO- d_6) δ [ppm]

4.0 ppm (8H, d, J=8.4Hz, Ar-O-C**H**$_2$-COOH), 4.4 ppm (12H, multiplet, Ar-O-C**H**$_2$-COOH), 4.7 ppm (4H, d, J=8.4Hz, Ar-O-C**H**$_2$-COOH), 5.3ppm (2H, s, Ar-**H**), 5.8ppm (2H, s, Ar-**H**), 6.0ppm (4H, s, Ar-C**H**-Ar), 6.6ppm (8H, broad singlet, Ar-**H**), 7.0ppm (8H, d, J=9.2Hz, Ar-**H**).

Mass Spec: m/z: 1729 (M+Na)

5.4.1 Alkylation of tetra-4-bromophenyl pyrogallol[4]arene, 77, with ethylbromo acetate

The procedure as described in 5.1.1 was followed using 0.26mmol (0.30g) of tetramer **77**, (scheme 26) , 4.10mmol (0.68g, 0.45ml) of ethylbromoacetate, and 6.40mmol (0.88g) of potassium carbonate, in 5ml of dry acetone, to give 0.18mmol (0.40g, 72% yield) of dodeca-ethylacetate pyrogallol[4]arene, tetramer **107**.

5.4.2 Base hydrolysis of dodeca-acetate ester 107

The general procedure as described in 5.1.2 was followed using 0.14mmol (0.30g) of dodeca-acetate ester **107** and 3.03mmol (0.17g) of potassium hydroxide, to give 0.11mmol (0.24g 79% yield) of dodeca-acetate potassium salt **121**.

5.4.3 Acid hydrolysis of dodeca-acetate potassium salt 121

The procedure as described in 5.1.3 was followed using 0.13mmol (0.30g) of dodeca-acetate potassium salt **121**, to give 0.11mmol (0.21g, 85% yield) of dodeca-acetate acid **135**.

^{1}H-NMR- (400MHz) (DMSO-d_6) δ [ppm]

4.1 ppm (8H, overlapping doublets, J=7.2Hz, Ar-O-C**H**$_2$-COOH), 4.4 ppm (12H, multiplet, Ar-O-C**H**$_2$-COOH), 4.7 ppm (4H, d, J=7.6Hz, Ar-O-C**H**$_2$-COOH), 5.5ppm (2H, s, Ar-**H**), 5.9ppm (2H, s, Ar-**H**), 6.1ppm (4H, s, Ar-C**H**-Ar), 6.6ppm (8H, broad singlet, Ar-**H**), 7.2ppm (8H, d, J=8.4Hz, Ar-**H**).

Mass Spec: m/z: 1887 (M+ Na)

5.5.1 Alkylation of tetraphenyl pyrogallol[4]arene, 67, with ethylbromoacetate

The general procedure as described in 5.1.1 was followed using 0.70mmol (0.60g) of tetramer **67**, (scheme 26) , 11.1mmol (1.84g, 1.22ml) of ethylbromoacetate, and 17.35mmol (2.40g) of potassium carbonate, in 25ml of dry acetone, to give 0.20mmol (0.38g, 29% yield) of dodeca-ethylacetate pyrogallol[4]arene, tetramer **108**.

5.5.2 Base hydrolysis of dodeca-acetate ester 108

The procedure as described in 5.1.2 was followed using 0.159mmol (0.30g) of dodeca-acetate ester **108** and 2.39mmol (0.13g) of potassium hydroxide, to give 0.14mmol (0.29g, 91% yield) of dodeca-acetate potassium salt **122**.

5.5.3 Acid hydrolysis of dodeca-acetate potassium salt 122

The procedure as described in 5.1.3 was followed using 0.06mmol (0.12g) of dodeca-acetate potassium salt **122**, to give 0.038mmol (0.07g, 63% yield) of dodeca-acetate acid **136**.

Mass Spec: m/z: 1575 (M+ Na)

5.6.1 Alkylation of tetra-3-fluorophenyl pyrogallol[4]arene, 78, with ethylbromo acetate

The procedure as described in 5.1.1 was followed using 0.32mmol (0.30g) of tetramer **78**, (scheme 26) . 5.12mmol (0.86g, 0.57ml) of ethylbromoacetate, and 8.0mmol (1.1g) of potassium carbonate, in 5ml of dry acetone, to give 0.26mmol (0.51g, 81% yield) of dodeca-ethylacetate pyrogallol[4]arene, tetramer **109**.

5.6.2 Base hydrolysis of dodeca-acetate ester 109

The procedure as described in 5.1.2 was followed using 0.15mmol (0.30g) of dodeca-acetate ester **109** and 3.03mmol (0.17g) of potassium hydroxide, to give 0.11mmol (0.28g 73% yield) of dodeca-acetate potassium salt **123**.

5.6.3 Acid hydrolysis of dodeca-acetate potassium salt 123

The procedure as described in 5.1.3 was followed using 0.06mmol (0.12g) of dodeca-acetate potassium salt **123**, to give 0.06mmol (0.10g, 95% yield) of dodeca-acetate acid **137**.

^{1}H-NMR- (400MHz) (DMSO- d_6) δ [ppm]

4.0 ppm (8H, overlapping doublets, J=7.6Hz, Ar-O-C**H**$_2$-COOH), 4.5 ppm (12H, multiplet, Ar-O-C**H**$_2$-COOH), 4.8 ppm (4H, d, J=8.4Hz, Ar-O-C**H**$_2$-COOH), 5.4ppm (2H, s, Ar-**H**), 5.9ppm (2H, s, Ar-**H**), 6.1ppm (4H, s, Ar-C**H**-Ar), 6.5ppm (8H, broad singlet, Ar-**H**), 6.9ppm (4H, triplet, J=6.8Hz, Ar-**H**), 7.1ppm (4H, quartet, J=6.4Hz, Ar-**H**).

Mass Spec: m/z: 1647 (M+ Na)

5.7.1 Alkylation of tetra-2-fluorophenyl pyrogallol[4]arene, 79, with ethylbromo acetate

The procedure as described in 5.1.1 was followed using 0.32mmol (0.30g) of tetramer **79**, (scheme 26) , 5.12mmol (0.86g, 0.57ml) of ethylbromoacetate, and 8.0mmol (1.1g) of potassium carbonate, in 5ml of dry acetone, to give 0.08mmol (0.15g, 24% yield) of dodeca-ethylacetate pyrogallol[4]arene, tetramer **110**.

5.7.2 Base hydrolysis of dodeca-acetate ester 110

The procedure as described in 5.1.2 was followed using 0.04mmol (0.08g) of dodeca-acetate ester **110** and 1.07mmol (0.06g) of potassium hydroxide, to give 0.03mmol (0.06g 80% yield) of dodeca-acetate potassium salt **124**.

5.7.3 Acid hydrolysis of dodeca-acetate potassium salt 124

The procedure as described in 5.1.3 was followed using 0.025mmol (0.050g) of dodeca-acetate potassium salt **124**, to give 0.021mmol (0.034g, 84% yield) of dodeca-acetate acid **138**.

^{1}H-NMR- (400MHz) (DMSO- d_6) δ [ppm]

3.8 ppm (4H, d, J=6.8Hz, Ar-O-C**H**$_2$-COOH), 4.2 ppm (4H, d, J=6.8Hz, Ar-O-C**H**$_2$-COOH), 4.5 ppm (12H, multiplet, Ar-O-C**H**$_2$-COOH), 4.7 ppm (4H, d, J=6.8Hz, Ar-O-C**H**$_2$-COOH), 5.5ppm (2H, s, Ar-**H**), 6.2ppm (2H, s, Ar-**H**), 6.4ppm (4H, s, Ar-C**H**-Ar), 6.9ppm (8H, broad multiplet, Ar-**H**), 7.1ppm (8H, broad singlet, Ar-**H**).

Mass Spec: m/z: 1663 (M+K)

5.8.1 Alkylation of tetra-3,5-difluorophenyl pyrogallol[4]arene, 80, with ethylbromoacetate

The procedure as described in 5.1.1 was followed using 0.30mmol (0.30g) of tetramer **80**, (scheme 26) , 4.80mmol (0.80g, 0.53ml) of ethylbromoacetate, and 7.5mmol (1.04g) of potassium carbonate, in 5ml of dry acetone, to give 0.17mmol (0.35g, 57% yield) of dodeca-ethylacetate pyrogallol[4]arene, tetramer **111**.

5.8.2 Base dydrolysis of dodeca-acetate ester 111

The procedure as described in 5.1.2 was followed using 0.10mmol (0.20g) of dodeca-acetate ester **111** and 2.15mmol (0.12g) of potassium hydroxide, to give 0.076mmol (0.16g 76% yield) of dodeca-acetate potassium salt **125**.

5.8.3 Acid hydrolysis of dodeca-acetate potassium salt 125

The procedure as described in 5.1.3 was followed using 0.056mmol (0.12g) of dodeca-acetate potassium salt **125**, to give 0.053mmol (0.09g, 95% yield) of dodeca-acetate acid **139**.

^{1}H-NMR- (400MHz) (DMSO- d_6) δ [ppm]

4.0 ppm (4H, d, J=8.0Hz, Ar-O-C**H**$_2$-COOH), 4.1 ppm (4H, d, J=8.0Hz, Ar-O-C**H**$_2$-COOH), 4.4 ppm (12H, multiplet, Ar-O-C**H**$_2$-COOH), 4.7 ppm (4H, d, J=8.4Hz, Ar-O-C**H**$_2$-COOH), 5.2ppm (2H, s, Ar-**H**), 5.8ppm (2H, s, Ar-**H**), 6.1ppm (4H, s, Ar-C**H**-Ar), 6.2ppm (8H, broad singlet, Ar-**H**), 6.8ppm (4H, triplet, J=6.8Hz, Ar-**H**).

Mass Spec: m/z: 1735 (M+K)

5.9.1 Alkylation of tetra-3,4-difluorophenyl pyrogallol[4]arene, 81, with ethylbromoacetate

The procedure as described in 5.1.1 was followed using 0.30mmol (0.30g) of tetramer **81**, (scheme 26) , 4.80mmol (0.80g, 0.53ml) of ethylbromoacetate, and 7.5mmol (1.04g) of potassium carbonate, in 5ml of dry acetone, to give 0.083mmol (0.17g, 28% yield) of dodeca-ethylacetate pyrogallol[4]arene, tetramer **112**.

5.9.2 Base hydrolysis of dodeca-acetate ester 112

The procedure as described in 5.1.2 was followed using 0.05mmol (0.10g) of dodeca-acetate ester **112** and 1.21mmol (0.07g) of potassium hydroxide, to give 0.038mmol (0.08g 76% yield) of dodeca-acetate potassium salt **126**.

5.9.3 Acid hydrolysis of dodeca-acetate potassium salt 126

The procedure as described in 5.1.3 was followed using 0.028mmol (0.06g) of dodeca-acetate potassium salt **126**, to give 0.027mmol (0.045g, 95% yield) of dodeca-acetate acid **104**.

^{1}H-NMR- (400MHz) (DMSO- d_6) δ [ppm]

4.1 ppm (8H, overlapping doublets, J=8.0Hz, Ar-O-C**H**$_2$-COOH), 4.3 ppm (4H, s, Ar-O-C**H**$_2$-COOH), 4.4ppm (8H, multiplet, Ar-O-C**H**$_2$-COOH), 4.7 ppm (4H, d, J=8.4Hz, Ar-O-C**H**$_2$-COOH), 5.1ppm (2H, s, Ar-**H**), 5.7ppm (2H, s, Ar-**H**), 6.1ppm (4H, s, Ar-C**H**-Ar), 6.3ppm (4H, broad singlet, Ar-**H**), 6.6ppm (4H, broad singlet, Ar-**H**), 7.0ppm (4H, quartet, J=6.4Hz, Ar-**H**).

Mass Spec: m/z: 1719 (M+ Na)

5.10.1 Alkylation of tetra-4-methylphenyl pyrogallol[4]arene, 82, with ethylbromoacetate

The procedure as described in 5.1.1 was followed using 0.33mmol (0.30g) of tetramer **82**, (scheme 26) , 5.28mmol (0.88g, 0.59ml) of ethylbromoacetate, and 8.25mmol (1.14g) of potassium carbonate, in 5ml of dry acetone, to give 0.21mmol (0.40g, 62% yield) of dodeca-ethylacetate pyrogallol[4]arene, tetramer **113**.

5.10.2 Base hydrolysis of dodeca-acetate ester 113

The procedure as described in 5.1.2 was followed using 0.16mmol (0.30g) of dodeca-acetate ester **113** and 3.03mmol (0.17g) of potassium hydroxide, to give 0.12mmol (0.24g 75% yield) of dodeca-acetate potassium salt **127**.

5.10.3 Acid hydrolysis of dodeca-acetate potassium salt 127

The procedure as described in 5.1.3 was followed using 0.06mmol (0.12g) of dodeca-acetate potassium salt **127**, to give 0.055mmol (0.09g, 96% yield) of dodeca-acetate acid **141**.

^{1}H-NMR- (400MHz) (DMSO- d_6) δ [ppm]

2.1ppm (12H, s, Ar-C**H**$_3$), 3.9 ppm (8H, overlapping doublets, J=7.2Hz, Ar-O-C**H**$_2$-COOH), 4.4 ppm (12H, multiplet, Ar-O-C**H**$_2$-COOH), 4.6 ppm (4H, d, J=7.2Hz, Ar-O-C**H**$_2$-COOH), 5.6ppm (2H, s, Ar-**H**), 5.8ppm (2H, s, Ar-**H**), 5.9ppm (4H, s, Ar-C**H**-Ar), 6.5ppm (8H, broad singlet, Ar-**H**), 6.8ppm (8H, d, J=6.4Hz, Ar-**H**).

Mass Spec: m/z: 1631 (M+ Na)

5.11.1 Alkylation of tetra-(trifluoro)-4-methylphenyl pyrogallol[4]arene, 83, with ethylbromoacetate

The procedure as described in 5.1.1 was followed using 0.27mmol (0.30g) of tetramer **83**, (scheme 26) , 4.32mmol (0.72g, 0.48ml) of ethylbromoacetate, and 6.75mmol (0.93g) of potassium carbonate, in 5ml of dry acetone, to give 0.15mmol (0.33g, 57% yield) of dodeca-ethylacetate pyrogallol[4]arene, tetramer **114**.

5.11.2 Base hydrolysis of dodeca-acetate ester 114

The procedure as described in 5.1.2 was followed using 0.16mmol (0.30g) of dodeca-acetate ester **114** and 3.03mmol (0.17g) of potassium hydroxide, to give 0.12mmol (0.27g 74% yield) of dodeca-acetate potassium salt **128**.

5.11.3 Acid hydrolysis of dodeca-acetate potassium salt 128

The procedure as described in 5.1.3 was followed using 0.053mmol (0.12g) of dodeca-acetate potassium salt **128**, to give 0.044mmol (0.08g, 83% yield) of dodeca-acetate acid **142**.

^{1}H-NMR- (400MHz) (DMSO- d_6) δ [ppm]

4.0 ppm (4H, d, J=7.6Hz, Ar-O-C**H**$_2$-COOH), 4.2 ppm (4H, d, J=7.6Hz, Ar-O-C**H**$_2$-COOH), 4.4 ppm (12H, multiplet, Ar-O-C**H**$_2$-COOH), 4.8 ppm (4H, d, J=7.6Hz, Ar-O-C**H**$_2$-COOH), 5.5ppm (2H, s, Ar-**H**), 5.9ppm (2H, s, Ar-**H**), 6.2ppm (4H, s, Ar-C**H**-Ar), 6.9ppm (8H, broad singlet, Ar-**H**), 7.4ppm (8H, d, J=6.4Hz, Ar-**H**).

Mass Spec: m/z: 1847 (M+ Na)

5.12.1 Alkylation of tetra-4-ethoxyphenyl pyrogallol[4]arene, 85, with ethylbromo acetate

The procedure as described in 5.1.1 was followed using 0.29mmol (0.30g) of tetramer **85**, (scheme 26) , 4.65mmol (0.77g, 0.51ml) of ethylbromoacetate, and 7.27mmol (1.00g) of potassium carbonate, in 5ml of dry acetone, to give 0.16mmol (0.36g, 54% yield) of dodeca-ethylacetate pyrogallol[4]arene, tetramer **115**.

5.12.2 Base hydrolysis of dodeca-acetate ester 115

The procedure as described in 5.1.2 was followed using 0.15mmol (0.30g) of dodeca-acetate ester **115** and 3.03mmol (0.17g) of potassium hydroxide, to give 0.095mmol (0.23g, 63% yield) of dodeca-acetate potassium salt **129**.

5.12.3 Acid hydrolysis of dodeca-acetate potassium salt 129

The procedure as described in 5.1.3 was followed using 0.05mmol (0.12g) of dodeca-acetate potassium salt **129**, to give 0.041mmol (0.8g, 81% yield) of dodeca-acetate acid **143**.

^{1}H-NMR- (400MHz) (DMSO- d_6) δ [ppm]

1.3ppm (12H, triplet, J=6.4ppm, -OCH_2CH_3), 3.9ppm (16H overlapping multiplets-8H multiplet, -OCH_2CH_3, 8H, multiplet, Ar-O-CH_2-COOH), 4.5ppm (12H, multiplet, Ar-O-CH_2-COOH), 4.7 ppm (4H, d, J=7.6Hz, Ar-O-CH_2-COOH), 5.8ppm (2H, s, Ar-**H**), 5.9ppm (2H, s, Ar-**H**), 6.0ppm (4H, s, Ar-C**H**-Ar), 6.6ppm (16H, broad multiplet, Ar-**H**).

Mass Spec: m/z: 1751 (M+ Na)

5.13.1 Alkylation of tetra-2-bromophenyl pyrogallol[4]arene, 86, with ethylbromoacetate

The procedure as described in 5.1.1 was followed using 1.71mmol (2.00g) of tetramer **86**, (scheme 26) **,** 27.36mmol (4.57g, 3.03ml) of ethylbromoacetate, and 42.75mmol (5.90g) of potassium carbonate, in 60ml of dry acetone, to give 0.10mmol (0.22g, 6% yield) of dodeca-ethylacetate pyrogallol[4]arene, tetramer **116**.

5.13.2 Base hydrolysis of dodeca-acetate ester 116

The procedure as described in 5.1.2 was followed using 0.078mmol (0.18g) of dodeca-acetate ester **116** and 1.51mmol (0.09g) of potassium hydroxide, to give 0.073mmol (0.17g 94% yield) of dodeca-acetate potassium salt **130**.

5.13.3 Acid hydrolysis of dodeca-acetate potassium salt 130

The procedure as described in 5.1.3 was followed using 0.052mmol (0.12g) of dodeca-acetate potassium salt **130**, to give 0.048mmol (0.09g, 93% yield) of dodeca-acetate acid **144**.

^{1}H-NMR- (400MHz) (DMSO- d_6) δ [ppm]

4.1 ppm (8H, overlapping doublets, J=7.2Hz, Ar-O-C**H**$_2$-COOH), 4.5 ppm (16H, multiplet, Ar-O-C**H**$_2$-COOH), 5.0ppm (2H, s, Ar-**H**), 5.8ppm (2H, s, Ar-**H**), 6.1ppm (4H, s, Ar-C**H**-Ar), 6.3ppm (4H, broad doublet, J=6.4Hz, Ar-**H**), 6.9ppm (8H, multiplet, Ar-**H**), 7.3ppm (4H, d, J=7.2Hz, Ar-**H**). 12.9ppm (12H, broad singlet, -OCH$_2$COO**H**)

Mass Spec: m/z: 1887 (M+ Na)

5.14.1 Alkylation of tetra-3,5-dibromophenyl pyrogallol[4]arene, 87, with ethylbromoacetate

The procedure as described in 5.1.1 was followed using 0.68mmol (1.00g) of tetramer **87**, (scheme 26) , 10.81mmol (1.81g, 1.20ml) of ethylbromoacetate, and 16.89mmol (2.33g) of potassium carbonate, in 30ml of dry acetone, to give 0.116mmol (0.29g, 17% yield) of dodeca-ethylacetate pyrogallol[4]arene, tetramer **117**.

5.14.2 Base hydrolysis of dodeca-acetate ester 117

The procedure as described in 5.1.2 was followed using 0.10mmol (0.25g) of dodeca-acetate ester **117** and 2.00mmol (0.11g) of potassium hydroxide, to give 0.095mmol (0.25g 95% yield) of dodeca-acetate potassium salt **131**.

5.14.3 Acid hydrolysis of dodeca-acetate potassium salt 131

The procedure as described in 5.1.3 was followed using 0.046mmol (0.12g) of dodeca-acetate potassium salt **131**, to give 0.037mmol (0.08g, 80% yield) of dodeca-acetate acid **145**.

^{1}H-NMR- (400MHz) (DMSO- d_6) δ [ppm]

4.0 ppm (4H, d, J=8.8Hz, Ar-O-C**H**$_2$-COOH), 4.2 ppm (4H, d, J=8.4Hz, Ar-O-C**H**$_2$-COOH), 4.5 ppm (12H, multiplet, Ar-O-C**H**$_2$-COOH), 4.9 ppm (4H, d, J=8.8Hz, Ar-O-C**H**$_2$-COOH), 5.3ppm (2H, s, Ar-**H**), 5.9ppm (2H, s, Ar-**H**), 6.2ppm (4H, s, Ar-C**H**-Ar), 7.5ppm (12H, broad singlet, Ar-**H**).

Mass Spec: m/z: 2203 (M+ Na)

5.15.1 Partial alkylation of tetra-4-fluorophenyl pyrogallol[4]arene, 65, with ethylbromoacetate

The procedure as described in 5.1.1 was followed using 0.43mmol (0.40g) of tetramer **65**, (scheme 26) , 4.30mmol (0.72g, 0.48ml) of ethylbromoacetate, and 6.90mmol (0.95g) of potassium carbonate, in 7ml of dry acetone, to give 0.12g of n-ethylacetate pyrogallol[4]arene, tetramer **157**. Yield values are not possible to calculate, as exact molecular masses are unknown.

5.15.2 Base hydrolysis of n-acetate ester 157

The procedure as described in 5.1.2 was followed using 0.10g of dodeca-acetate ester **157** and 1.25mmol (0.07g) of potassium hydroxide, to give 0.09g of dodeca-acetate potassium salt **160**. Yield values are not possible to calculate, as exact molecular masses are unknown.

5.15.3 Acid hydrolysis of n-acetate potassium salt 160

The procedure as described in 5.1.3 was followed using 0.06g of dodeca-acetate potassium salt **160**, to give 0.06g of dodeca-acetate acid **163**. Yield values are not possible to calculate, as exact molecular masses are unknown.

^{1}H-NMR- (400MHz) (DMSO- d_6) δ [ppm]*

3.9 ppm (6H, broad multiplet, Ar-O-C**H**$_2$-COOH), 4.3 ppm (6H, broad multiplet, Ar-O-C**H**$_2$-COOH), 4.6 ppm (2H, broad multiplet, Ar-O-C**H**$_2$-COOH), 5.2ppm (2H, multiplet, Ar-**H**), 5.7ppm (2H, multiplet, Ar-**H**), 5.9ppm (4H, multiplet, Ar-C**H**-Ar), 6.6ppm (8H, broad singlet, Ar-**H**), 6.7ppm (8H, broad multiplet, Ar-**H**).

Mass Spec: m/z: Bell curve of peak observed between 1400 and 1700

* ^{1}H-NMR Splitting is poor owing to there being a mixture of similar compounds present.

5.16.1 Partial alkylation of tetra-4-chlorophenyl pyrogallol[4]arene, 76, with ethylbromoacetate

The procedure as described in 5.1.1 was followed using 0.40mmol (0.40g) of tetramer **76**, (scheme 26) , 4.00mmol (0.67g, 0.44ml) of ethylbromoacetate, and 6.40mmol (0.88g) of potassium carbonate, in 7ml of dry acetone, to give 0.29g of n-ethylacetate pyrogallol[4]arene, tetramer **158**. Yield values are not possible to calculate, as exact molecular masses are unknown.

5.16.2 Base hydrolysis of n-acetate ester 158

The procedure as described in 5.1.2 was followed using 0.20g of dodeca-acetate ester **158** and 2.50mmol (0.14g) of potassium hydroxide, to give 0.19g of dodeca-acetate potassium salt **161**. Yield values are not possible to calculate, as exact molecular masses are unknown.

5.16.3 Acid hydrolysis of n-acetate potassium salt 161

The procedure as described in 5.1.3 was followed using 0.10g of dodeca-acetate potassium salt **161**, to give 0.09g of dodeca-acetate acid **164**. Yield values are not possible to calculate, as exact molecular masses are unknown.

^{1}H-NMR- (400MHz) (DMSO- d_6) δ [ppm]*

4.4ppm (16H, broad multiplet, Ar-O-C**H**$_2$-COOH), 4.6ppm (4H, broad multiplet, Ar-O-C**H**$_2$-COOH), 5.4ppm (2H, s, Ar-**H**), 5.8ppm (2H, s, Ar-**H**), 6.1ppm (4H, broad singlet, Ar-C**H**-Ar), 6.7ppm (8H, broad singlet, Ar-**H**), 7.1ppm (8H, broad doublet, Ar-**H**).

Mass Spec: m/z: Bell curve of peak observed between 1550 and 1800

* ^{1}H-NMR Splitting is poor owing to there being a mixture of similar compounds present.

5.17.1 Partial alkylation of tetra-4-bromophenyl pyrogallol[4]arene, 77, with ethylbromoacetate

The procedure as described in 5.1.1 was followed using 0.34mmol (0.40g) of tetramer **77**, (scheme 26) , 3.40mmol (0.57g, 0.38ml) of ethylbromoacetate, and 5.50mmol (0.75g) of potassium carbonate, in 7ml of dry acetone, to give 0.16g of n-ethylacetate pyrogallol[4]arene, tetramer **159**. Yield values are not possible to calculate, as exact molecular masses are unknown.

5.17.2 Base hydrolysis of n-acetate ester 159

The procedure as described in 5.1.2 was followed using 0.10g of dodeca-acetate ester **159** and 1.25mmol (0.07g) of potassium hydroxide, to give 0.08g of dodeca-acetate potassium salt **162**. Yield values are not possible to calculate, as exact molecular masses are unknown.

5.17.3 Acid hydrolysis of n-acetate potassium salt 162

The procedure as described in 5.1.3 was followed using 0.05g of dodeca-acetate potassium salt **162**, to give 0.05g of dodeca-acetate acid **165**. Yield values are not possible to calculate, as exact molecular masses are unknown.

^{1}H-NMR- (400MHz) (DMSO- d_6) δ [ppm]*

4.4ppm (12H, broad multiplet, Ar-O-C**H**$_2$-COOH), 4.7ppm (4H, broad multiplet, Ar-O-C**H**$_2$-COOH), 5.5ppm (2H, multiplet, Ar-**H**), 5.9ppm (2H, multiplet, Ar-**H**), 6.0ppm (4H, broad singlet, Ar-C**H**-Ar), 6.6ppm (8H, broad singlet, Ar-**H**), 7.2ppm (8H, broad singlet, Ar-**H**).

Mass Spec: m/z: Broad bell curve of peak observed between 1300 and 2000

* ^{1}H-NMR Splitting is poor owing to there being a mixture of similar compounds present.

5.18.1 Alkylation of tetra-4-fluorophenyl pyrogallol[4]arene, 65, with ethylbromo propionate

The procedure as described in 5.1.1 was followed using 1.08mmol (1.00g) of tetramer **65**, (scheme 26), 16.23mmol (2.94g, 2.08ml) of ethylbromopropionate, and 22.68mmol (3.13g) of potassium carbonate, in 30ml of dry acetone. After

recrystallisation <0.01mmol of tetramer **167** was retrieved and the hydrolysis reactions were not carried out.

5.19.1 Alkylation of tetra-4-fluorophenyl pyrogallol[4]arene, 65, with 1-bromopropane.

0.22mmol (0.20g) of tetramer **65**, (scheme 26) was reacted with 3.45mmol (0.42g, 0.31ml) of 1-bromopropane under base conditions of potassium carbonate (5.39mmol, 0.74g) in 12ml of dry acetone. The reaction was carried out at 60°C for 2 days. On cooling to room temperature all volatiles were removed under reduced pressure. The residue was treated with 5ml of dilute HCl and then filtered to yield 0.25g of a sticky yellow paste. Based on the ^{1}H-NMR spectrum of this paste, it was assumed to be residual inorganic bromine salts.

5.20.1 Alkylation of tetramethyl pyrogallol[4]arene, 69, with 1-bromopropane.

The reaction as in 5.19.1 was followed using 0.33mmol (0.20g) of tetramer **69**, (scheme 26), 5.26mmol (0.65g, 0.42ml) of 1-bromopropane and 8.22mmol (1.13g) of potassium carbonate in 12ml of dry acetone. Again the reaction yielded 0.29g of a sticky yellow paste. Based on the ^{1}H-NMR spectrum of this paste, it was assumed to be residual inorganic bromine salts.

5.21.1 Alkylation of tetra-4-fluorophenyl pyrogallol[4]arene, 65, with 2-chloro ethyl sulphonate sodium salt.

0.54mmol (0.50g) of tetramer **65**, (scheme 26) was reacted with 8.64mmol (1.59g) of 2-chloro ethyl sulphonate sodium salt under base conditions of potassium carbonate (13.50mmol, 1.86g) in 30ml of dry acetone. The reaction was carried out at 60°C for 6

days. The reaction was driven to completion by the addition of 0.2 equivalents of 2-chloro ethyl sulphonate sodium salt and potassium carbonate each day. On cooling to room temperature all volatiles were removed under reduced pressure. The residue was treated with 15ml of dilute HCl and then filtered to yield a yellow-orange product. This product was then recrystallised from hot methanol, however no product was recovered from the recrystallisation. On evaporation of the methanol, the yellow-orange product was recovered, and again NMR implied that the product was residual inorganic salt.

Chapter 6

Polymer Synthesis

An attempt was made to prepare on a large scale tetramer **65**. The reaction was carried out on a 100g scale. We noticed immediately that an exotherm occurred upon addition of all reagents at room temperature. We brought the exotherm under control by cooling the reaction mixture in an icebath. Once the temperature normalised the reaction mixture was brought back to 80°C and allowed to stir for five hours.

The product of this reaction was purified using the same procedures described for the tetramer however the product remained highly discoloured and the yield of product was calculated at 40% (based on tetramer formation). We proceeded to brominate (scheme 36) this recovered product using bromine in glacial acetic acid at room temperature. Upon addition of bromine the reaction mixture turned from red to a dark purple. It should be noted that we had previously attempted bromination of the tetramer isolated (see scheme 37) from small scale reactions, and we observed that bromination did not occur. However, in this case a reaction did occur. The product was worked up by simple washing with water. We proceeded to alkylate using ethylbromoacetate, this reaction was carried out for 24 hours and the isolated product was immediately saponified with sodium hydroxide.

The crude product was purified using acid/base precipitations, however we also noticed that a percentage of this product (in the acid form) was insoluble in methanol. After a series of precipitations from methanol we isolated an orange red product. Mass specrometery by both ESI and MALDI techniques did not give any identifiable peaks. However, the ^{1}H NMR of this product clearly demonstrates that this product is not a macrocycle, but a polymer by-product. Based on integrations we believe that this polymer is 50% alkylated.

These results demonstrate that polymerisation is indeed in competition with cyclisation. But of perhaps greater significance is that the isolated product from this work is at least one order of magnitude higher in bioactivity relative to the best alkylated macrocycles

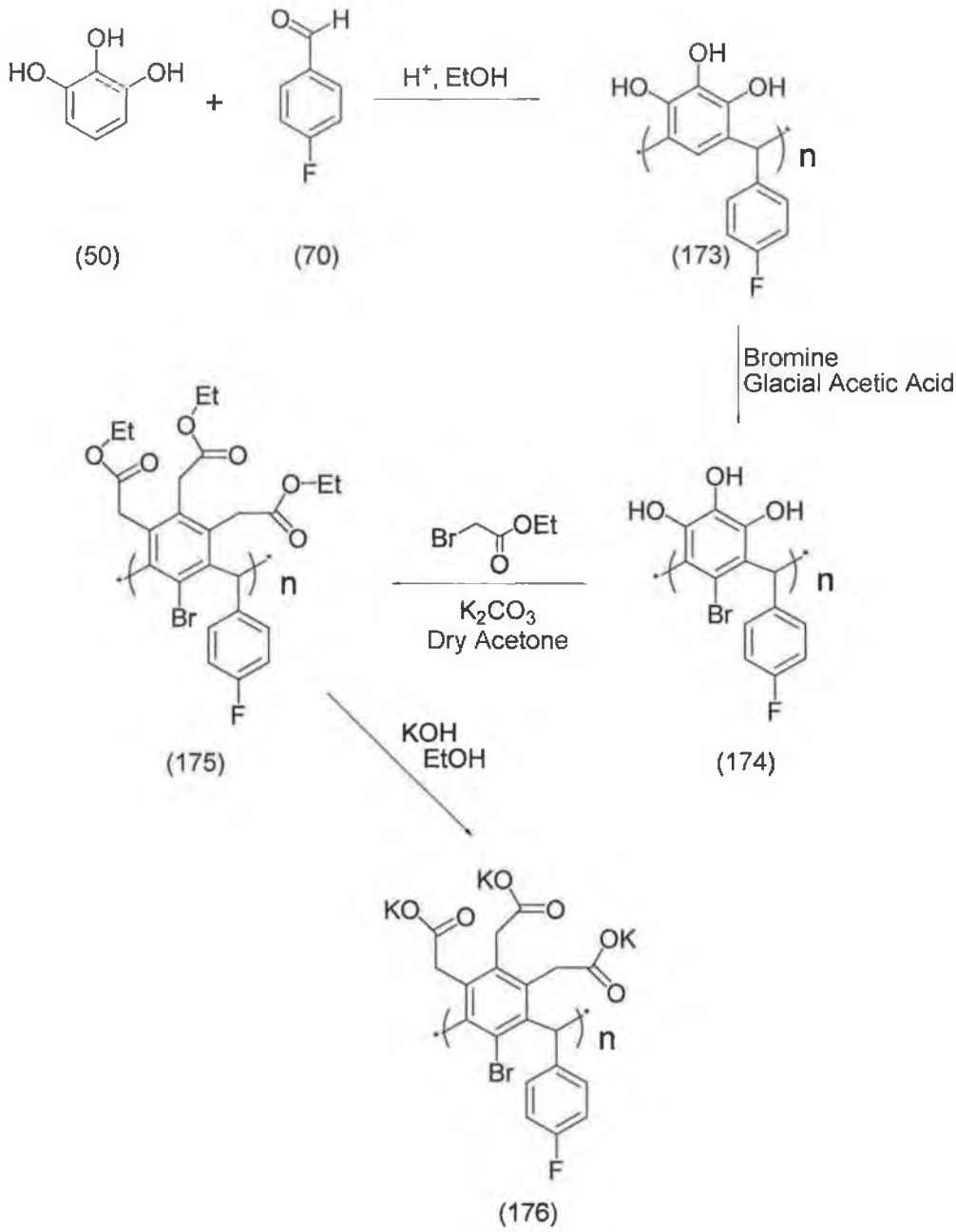

Scheme 36: *Formation of bioactive polymer.*

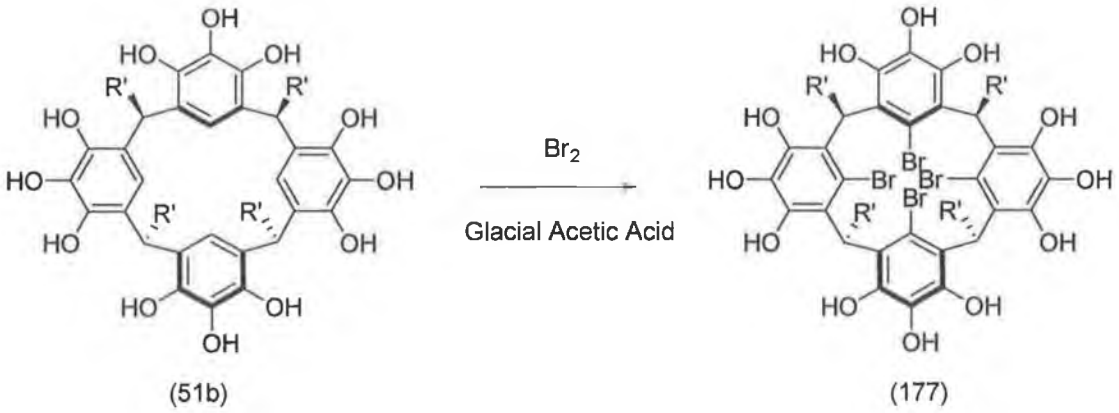

Scheme 37: *Bromination step*

Experimental

6.1: Large scale condensation of pyrogallol, 50, with 4-fluorobenzaldehyde, 70.

100 g scale: It was observed that this reaction is very exothermic upon addition of all reagents and that it is independent of the order of addition of reagents. A viscous solution was generated after 1 hour of reaction time and this did make stirring of the mixture somewhat problematic. The reaction mixture was worked up using the described method, and the isolated red product was washed with ethanol/water 4:1. It was found that further washing with ethanol removed most of the red colour to give a somewhat colourless product. 20 grams of product, **173** were isolated.

6.2: Bromination of product 173 to form 174.

The same procedure involved suspending 14.4 grams of the polymer in 150 mL of glacial acetic acid. To this solution was added dropwise bromine and the reaction mixture was allowed to stir at room temperature. Upon addition of bromine the reaction mixture turned from light red to purple. After 48 hours the reaction mixture

was worked up by filtering through a glass frit. The collected product, **174** was then washed with water until the filtrate was colourless and was then dried at room temperature for three days.

6.3: Alkylation of 174 with ethylbromoacetate to give 175.

The same procedure as described above (alkylation) was employed on a 8-gram scale of **174** starting material.

6.4: Base Hydrolysis of 175 to give 176.

Same procedure used above was employed on 8 grams of **175** that was prepared above. The product was further purified by dissolving the product in water and precipitating the product with methanol. The precipitate was then collected by centrifugation and washed with methanol. This procedure was carried out again until a nonsticky light red powder was obtained.

Chapter 7

Analytical and Biological Investigations

7.1 Introduction:

It has been reported that polyanionic species can act as gp120 inhibitors[66]. We believe this is also the case for the alkylated pyrogallol[4]arenes which possess negative charges. ELISA (Enzyme-Linked Immunosorbent Assay) studies indicate that pyrogallolarenes inhibit the binding of gp120 to CD4 cells, by binding to the cellular receptor on the virus binding site as well as binding to the fusion site on gp120. Pyrogallolarenes were also found to be specific and they do not inhibit reverse transcriptase, proteases or clotting proteins.

7.2 Results and Discussion:

The screening assay was carried out by Dr Shattock's group at St. George's Hospital in London and is based on the immobilization of infectious virions to 96 well plates. Three separate conditions were used, as shown in figure 40.

a), Virus is pretreated with titrated compound (detecting direct antiviral activity)

b), Target Cells are pretreated with titrated compound (detecting direct antiviral activity)

c), Titrated compound, virus and target cell are all incubated together.

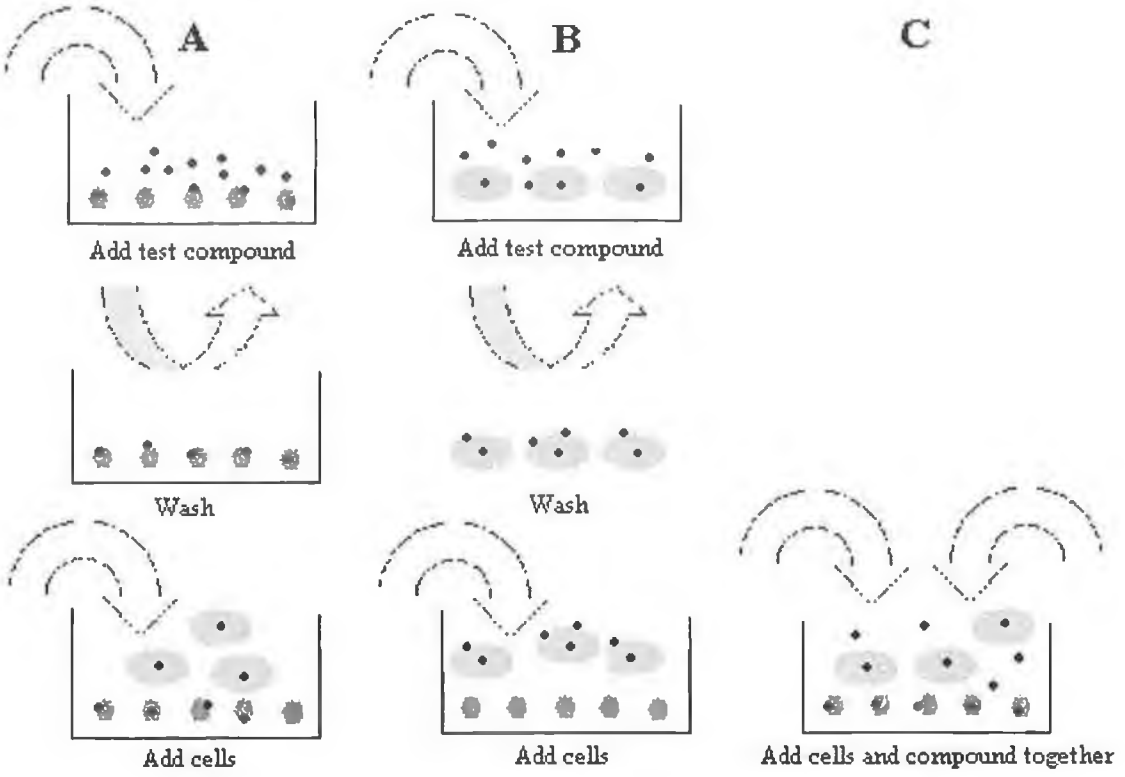

Figure 40: *Screening Method*

Figure 41 shows the various pyrogallolarenes that were used in biological testing and table 12 outlines the assay results (also see appendix 2).

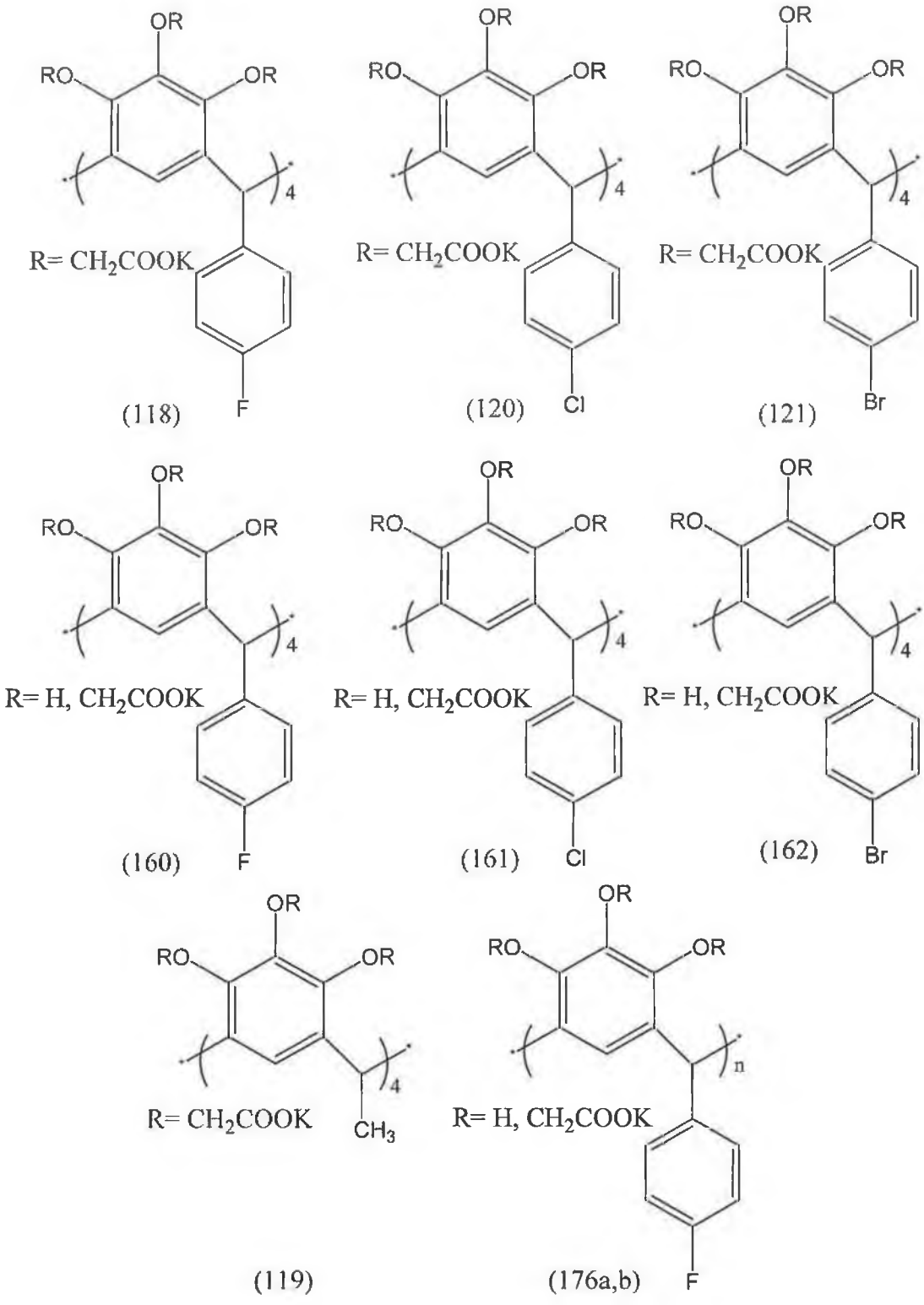

Figure 41: *Pyrogallolarenes that were sent for GP120 inhibition activity*

Compound Number	Description	EC-50	TC-50	Selectivity Index
176a	Polymer	0.015	350	23333
176b	Polymer	0.012	350	29166
118	Tetra-4-fluorophenyl pyrogallol [4]arene dodeca acetate salt.	8.683	2812	334.33
121	Tetra-4-bromophenyl pyrogallol [4]arene dodeca acetate salt.	0.494	195.6	400.89
120	Tetra-4-chlorophenyl pyrogallol [4]arene dodeca acetate salt.	2.65	868.19	335.54
160	Tetra-4-fluorophenyl pyrogallol [4]arene partially alkylated acetate salt.	12.01	1131.09	88.49
162	Tetra-4-bromophenyl pyrogallol [4]arene partially alkylated acetate salt.	2.64	1375.65	526.72
161	Tetra-4-chlorophenyl pyrogallol [4]arene partially alkylated acetate salt.	0.247	1015	4158.4
119	Tetramethyl pyrogallol[4]arene dodeca acetate salt (*rctt* chair).	0.228	1172.5	5203.4

Table 12: *GP120 inhibition results.*
EC-50 =molar concentration of an agonist, which produces 50% of the maximum possible response for that agonist.
TC-50 = molar concentration of an agonist, which kills 50% of uninfected cells

There are some definitive trends in the biological activity of the macrocycles tested. The first interesting trend to be observed is to do with charge. It is suggested by the mechanism of action that charge (i.e. the numbers of anionic groups) is related to bioactivity. However, it is seen that partially alkylated pyrogallol[4]arenes, **161**, have a far higher (by a factor of 12) selectivity index then that of the completely alkylated counterpart, **120**. This discrepancy would suggest that perhaps activity is independent

of charge. This result has also been reported recently in the case of sulphonated naphthyl porphyrins[79]. In this study a number of porphyrins with varying degrees of alkylation were tested for their biological activity against HIV-1. It was found that the partially sulphonated porphyrins had a greater activity than the completely alkylated adducts.

Why are the partially alkylated derivatives more active than the completely alkylated derivatives? It would appear as mentioned in Chapter 1 that charge may not be the sole factor for biological activity. By the nature of these compounds being partially alkylated, they therefore possess 'redox active' phenol groups. Phenol groups can undergo redox chemistry as outlined in scheme 38[80].

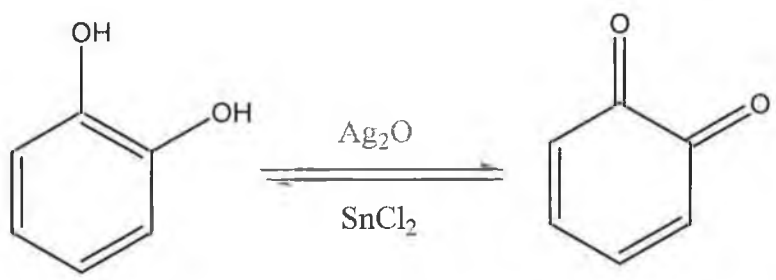

Catechol, (178) o-benzoquinone, (179)

Scheme 38: *Redox Chemistry of Phenols*

We believe that it may be possible that the remaining phenol/quinone groups in our macrocyles could be interfering with PDI, a redox active enzyme. If this is indeed occurring then the required conformational change of gp-120 may be inhibited and it is this that is preventing viral entry.

We also discovered a new lead structure from this work, which is a polymer derivative (**176a** and **176b**). It was found by ^{1}H-NMR that this polymer is 50% alkylated.[65] The polymer is far larger than the macrocycles, it also contains possibly hundreds of phenols along with acetate groups. Furthermore we believe that this polymer is partially oxidised since it was treated with bromine prior to alkylation. The polymer prepared in this work possesses ten times the biological activity of the partially alkylated macrocycle species. We believe that two possible explanations could be given to explain these results. The first is that negatively charged polymeric species have shown superior activity with other systems[65], but this does not eliminate the possibility that interference with PDI may also be occurring.

To determine if size is an issue with all compounds tested we decided to investigate possible promiscuous effects. Promiscuous drugs, (i.e. those that have promiscuous effects) as opposed to selective drugs, can be just as potent. The promiscuity relates to the ability of a drug to form larger complexes or clusters in solution. The formation of these clusters is typically caused by hydrogen bonding or electrostatic interactions. In these cases it is the complex or cluster that is biologically active and not the individual drug molecule. The size of these aggregates/particles in aqueous solution would have an effect on the biological activity. It has been reported that pyrogallol[4]arenes form highly symmetrical spherical clusters in solution[43,44], (although there was no particle size data to back up this proposal). To that end, we decided to carry out a PCS (Photon Correlation Spectroscopy) analysis on these compounds.

"PCS measures Brownian motion and relates it to the size to particles". Brownian motion is the random movement of particles due to the bombardment by solvent (or

gas) molecules that surround them. PCS can only measure particles with sizes below 1 micron, or more correctly particles with sufficiently low density, as above this size particles are generally affected by processes such as gravity – causing sedimentation – thus eliminating Brownian motion and therefore can not be measured by PCS[81].

PCS measures light intensities that change in time relative to the sizes of particles (small particles move quickly and therefore light intensity changes quickly at the detector, whereas large particles move slowly and hence light intensity changes at the detector are slow) being "viewed" by the detector.

PCS uses a correlation function to aid in deciphering the particle size. Large particles have a slow changing correlation function whereas small particles have a fast changing correlation function. This correlation function is then fitted to a straight line, the slope of which is related to the Z-average particle size, or the intensity of the averaged particle diameter. This is known as the cumulant analysis and it gives a single mean value for particle size[81].

The results of the PCS analysis are outlined in table 13. Five different compounds were analysed for their particle/cluster size in an aqueous matrix. 'Z-Ave' is the average size of the various different sized clusters in solution. Poly-dispersal Index, (PDI) is a measure of how many different sized clusters are present. For mono-dispersed system (i.e. only one size of cluster) the PDI should be lower than 0.3.

Record Number	Sample Name	Z-Ave. (nm)	PDI	Peak 1 Area Intensity	Peak 2 Area Intensity
72	4-Fluoro Salt	393.7	0.564	64	35
74	4-Chloro Salt	411.9	0.528	74	25
116	4-Chloro partial Salt	486.3	0.535	62	37
73	Methyl salt – sc1	**103.4**	**0.31**	98	1
73 (Different Batch)	Methyl salt – pg1	**103.3**	**0.193**	100	0
125b	Polymer	**74.61**	0.513	100	0

Table 13: *PCS Data*

For macrocycles **118** and **120**, which showed poor biological activity, the PCS data gives a high PDI value, indicating a number of different sized clusters present in solution. The average sizes of these clusters are quite high, 394nm and 412nm respectively

For macrocycle **119**, two separate batches of this compound were analysed and gave similar results. Both have acceptable PDI values and both only have one size cluster. The size of the cluster is far lower than the **118** and **120**, at 103nm. This compound also has good biological activity.

The polymer sample **176a**, has the highest biological activity of all samples tested. The average size of the polymer cluster is also the lowest of all the samples, at 74nm. This suggests that the size of the cluster and not the actual molecule plays an important role in the biological activity.

The partially alkylated derivative of the tetra-4-chlorophenyl pyrogallol[4]arene, **161**, is the exception to the trend. Despite the good biological activity, its PCS data makes it comparable to **118** and **120** which both displayed poor biological activity. The average size of the cluster is 486nm and the PDI is 0.535. This indicates that there are a few different cluster sizes in the aqueous matrix. This is probably owing to the fact that there exists a mixture of partially alkylated compounds in the sample. Perhaps there is one cluster comparable in size to those other biologically active compounds and that is why the EC_{50} for this compound is so high, at 5.4μg/ml. The only solution here would be to try and separate the different molecules in the sample. This has been attempted in the past and to no avail.

7.21 Stereoisomers:

It would have been of great interest to observe the difference (if any) in the biological activity of two different stereoisomers of the same pyrogallol[4]arene. As mentioned in Chapter 2, we successfully isolated both the chair *rctt* and the cone *rccc* isomers of tetramethylpyrogallol[4]arene. We had hoped to convert these into the respective water-soluble dodeca acetate salts and compare their biological activities. However as discussed in Chapter 5, it was not possible to alkylate the cone *rccc* isomer, therefore such a comparison was not possible to carry out.

7.2.2. Drug Delivery Vehicles: Synergy Studies.

In combination studies the lead compound mixtures have shown potent synergy with non-nucleotide reverse transcriptase inhibitor (NNRTI) TMC-120 (Tibotec PLC lead compound Average of Combination Indices calculated at EC50, EC75 and EC90 from three separate experiments was 0.454 suggesting good synergy with both compounds[61].

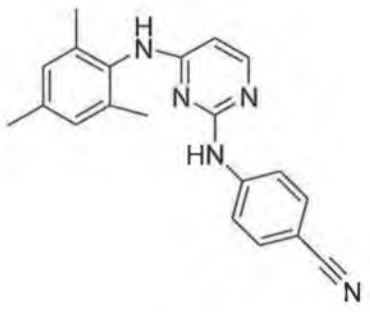

TMC-120

Figure 42: *Structure of TMC-120.*

The question is why do the macrocycles show a synergy with these NNRTI's? The mechanism of action of all compounds reported in this thesis involves the inhibition of viral replication at the early stages in the viral life-cycle. (either binding with the V3 loop of gp-120 or inhibition of PDI or both). However the enhancement of preformance of an NNRTI would not be expected, but if we look at the solubility properties of the NNRTI that acts synergistically with our leads we will note that all molecules are hydrophobic with poor water solubility. We believe that our macrocycles are solubilising these compounds, in essence they are behaving as drug delivery vehicles.

Shown in figure 43 is a proposed mechanism as to how hydrophobic NNRTI may bind with our macrocycles. Each macrocycle possesses a 'hydrophobic clip', we believe that sections of the NNRTI can fit into or weakly associate *via* π-π stacking with these clips. as a result an inclusion complex is formed and it takes on the solubility properties of the macrocycle, the whole complex is thus water soluble. Due to time constraints a complete physical analysis of this phenomena could not be determined and included in this work. I would propose a series of physical studies including differential scanning calorimetry, phase solubility testing, hydrophobic dye extractions and aqueous ^{1}H NMR titrations to prove this effect as a mechanism of action.

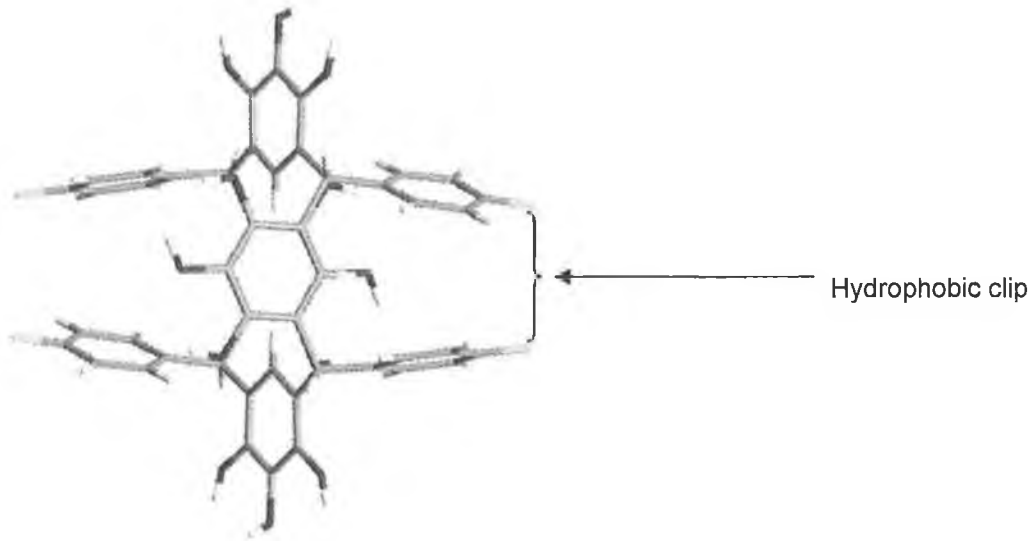

Figure 43: *Hydrophobic clip*

The biological results of this synergistic effect are quite exciting, these macrocycles can be readily used in the formulation of NNRTI's, not only do they possess a biological activity but they also can act as a drug delivery vehicles making them a

very valuable compounds. Furthermore these compounds are quite inexpensive to make, thus they can compete with other delivery vehicles.

7.3. HPLC Method Development

As mentioned above, we desired to isolate each component in the tested mixtures. We already attempted selective synthesis of these mixtures, unfortunately this endeavour failed. We turned our attention to developing an HPLC method that could separate these mixtures, such a method would not only be of value for separation and isolation but is also required if we wish to obtain quantitative data of *in vivo* bioavailability and performance.

An HPLC method had been previously developed by an industrial partner TopChem laboratories®, the method is outlined below in table 14:

TopChem Laboratories® Analytical Method					
Column	***Wavelength***	***Mobile Phase***	***Flow Rate***	***Sample Concentration***	***Run Time***
C18	210nm	0.05M KH_2PO4 (pH3)	0.5ml/min	26mg/ml	60mins

Table 14: *TopChem Laboratories® Analytical Method*

There are many problems with the shown method:

1) The sample concentrations are 'ridiculous'-this concentration is far too high for it to be used practically for *in vivo* analysis. (Typical sample concentrations should range from 0.01mg/ml to 1mg/ml)

2) Separation of various substituted derivatives could not be achieved, furthermore this method was not very efficient in separating the unsubstituted pryrogallolarene from the ester and acid derivatives.
3) The run time is very long, which is not ideal for multiple injections.

We chose to redevelop this method in the hope to solve the above two problems.

In developing this method we needed to take the following into consideration:

1) Column selection.
2) Mobile phase.
3) Sample concentration and diluent.
4) Flow rates.

In terms of column selection we chose a Zorbax C18 column to start with, and the compounds used for analysis were the tetramer derivatives prepared from pyrogallol and acetaldehyde. In terms of mobile phase we had some limitations; we could not use a mobile phase with a pH below 4. This limitation came from instrument considerations here at DCU. Sample concentrations that we started with were quite high at 13mg/ml and we selected a detection wavelength at 210nm (optimum absorption).

The first method attempted is shown in table 15 and is referred to as method A. We initially decided to add an organic element to the mobile phase to increase the solvent strength and we also increased the pH of the mobile phase from 3 to 7. We believed that at pH 7 the acids would be deprotonated and would therefore have a faster retention time than either the ester or unsubstituted macrocycle.

On introducing methanol into the mobile phase, the retention time of the various compounds decreased significantly, so much so, that all derivatives of the pyrogallol[4]arenes were eluted in the first 4 minutes. It was also found that the sample peaks were quite intense on the chromatogram, as a result we decided to lower the sample concentration to 1.35mg/ml .

Analytical Method Development- Method A					
Column	***Wave-length***	***Mobile Phase***	***Flow Rate***	***Sample Concentration***	***Run Time***
C18	210nm	85:15 0.05M K_2PO_4:MeOH (pH7)	0.5ml/ min	1.35mg/ml	60mins

Table 15: *Analytical Method Development – Method A*

On repeated injections using this method, we noticed something peculiar. The intensity of the peaks increased with each injection. We believe this to be due to a "column saturation effect". We believe that our analyte is absorbing onto the polar sites on the column and after multiple runs all the polar sites on the column are 'eliminated'. This conclusion makes sense since our analytes are polar in nature and are capable of binding tightly to any available silyloxy/silylhydroxy sites which are remaining on the surface. What we have discovered also explains the required high sample concentrations of the TopChem® method since most of the injected sample has been eliminated by absorption, therefore, only traces of the original sample after injection are eluting from the column. To ensure complete column saturation multiple injections at high concentration were carried out overnight.

Confident that column saturation was complete we began lower the sample concentration. The next concentration prepared was at 0.5 mg/ml, again we observed

a capped peak (off scale), the sample was further diluted to 0.25mg/ml again peak capping was observed, we continued to dilute the acid sample until we reached an optimum concentration of 0.0625mg/ml, (figure 44) in effect we have decreased the concentration by a factor of 416 from the original industrial method.

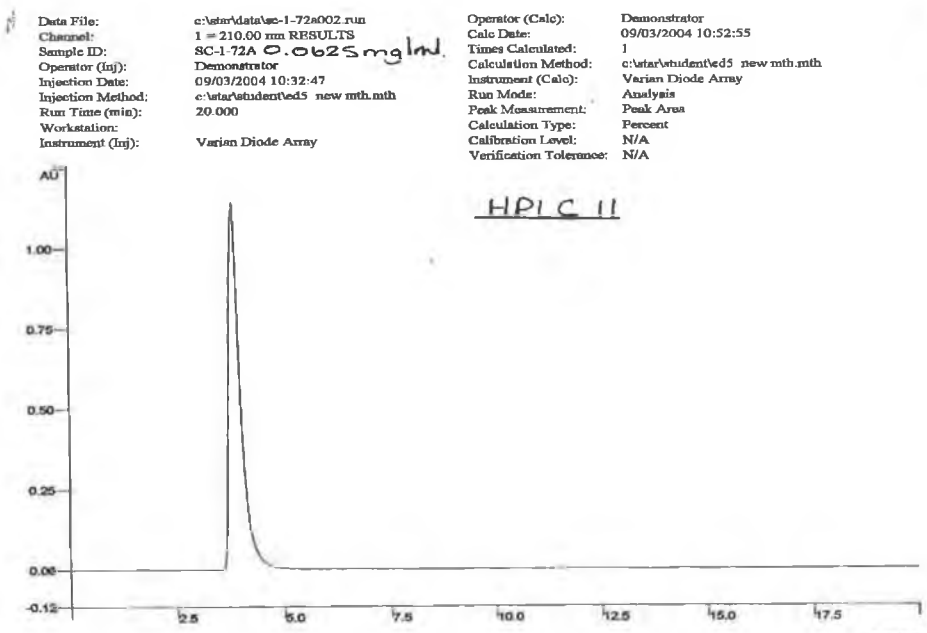

Peak No	Peak Name	Result 0	Ret. Time (min)	Time Offset (min)	Area (counts)	Rel Ret Time	Sep. Code	Width 1/2 (sec)	Status Codes	Group
1		99.6713	3.843	0.000	114626752	0.00	BB	16.8		0
2		0.0225	10.880	0.000	25861	0.00	BB	25.0		0
3		0.2567	14.464	0.000	295196	0.00	BB	29.8		0
4		0.0292	16.069	0.000	33570	0.00	BB	35.5		0
5		0.0203	19.240	0.000	23379	0.00	BB	0.0		0
	Totals	**100.0000**		**0.000**	**115004752**					

Figure 44: *HPLC of the salt at concentration 0.0625mg/ml.*

After solving the concentration problem we carried out single injections of the tetramer, ester, acid and salt using method A and the results are shown in table 16.

Compound	**Retention time (minutes)**
Salt	3.824
Pyrogallol acetaldehyde tetramer	4.784
Ester	3.981 and 4.456
Acid	3.843

Table 16: *Retention Times under Method A*

All compounds were then mixed together at 0.125 mg/mL and injected, however only two resolved peaks were observed in the chromatogram at 3.835 and 4.784 minutes, indicating overlap of peaks (figure 45).

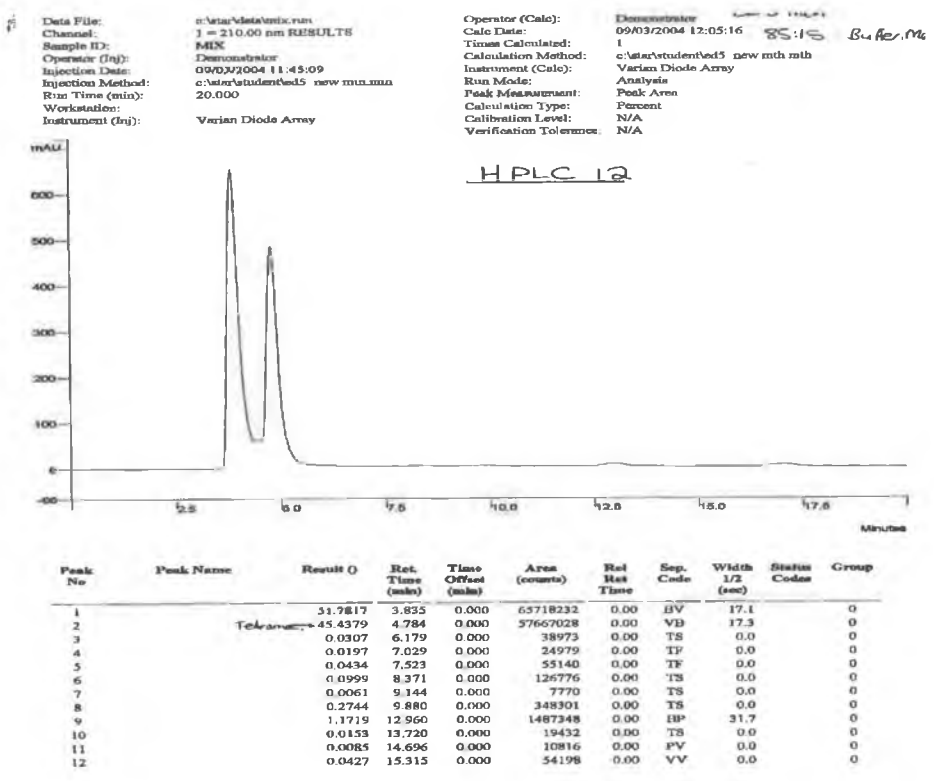

Figure 45. *Mixed injection of unsubstituted macrocycle, dodecaester, dodeca salt.*

To try and solve this problem we decided to lower the pH of the mobile phase to 5 and to lower the organic content to 10% (table 17 Method B).

Analytical Method Development- Method B					
Column	***Wave-length***	***Mobile Phase***	***Flow Rate***	***Sample Concentration***	***Run Time***
C18	210nm	90:10 0.05M K_2PO_4:MeOH (pH5)	0.3ml/ min		20mins

Table 17 : *Analytical Method Development- Method B*

Before running this method we noticed a carryover problem, the base line was drifting and becoming noisy, we believe that some of the absorbed acid was eluting off the column. A cleaning method had to be developed to eliminate this problem and is outlined as follows:

1) flush 30 mL of 90:10 H_2O:MeOH followed with 30 mL 50:50 H_2O:MeOH (this had little effect)
2) 25 mL 95% H_20/ACN followed by 25 mL THF followed by 95% ACN/H_2O (this procedure worked)

(Note that we found the column to be sufficiently saturated for sample injection after column washing.)

A fresh mobile phase was then prepared using 90% KH_2PO_4: 10% MeOH pH 5, four separate samples were prepared of the acid, ester, salt and macrocycle and injected individually, their retention times are listed in table 18.

Compound	**Retention time (minutes)**
Salt	4.216 and 4.741
Pyrogallol acetaldehyde tetramer	4.771
Ester	4.717 (single peak)
Acid	8.848

Table 18: *Retention Time under Method B*

An acid and ester mixture was also injected, two peaks were observed one at 4.685 minutes and the other at 8.912 minutes (large peak tailing).

We also decided to increase the pH of the mobile phase to 9.3, however this had little effect on the retention times and resolution could not be achieved.

Conclusions- Method development.

At the onset of the HPLC development work it was essential to develop a method that could detect at lower concetrations, this was achieved by column saturation. Also an

effective column cleaning method was developed to prevent compound carry over after multiple injections. We believe that this method is effective for analysis of *in vivo* samples.

However attempts at developing a method that can properly resolve the peaks of the unsubstituted macrocycle from the ester, acid/salt could not be achieved. Obviously separation of the partially substituted ester derivatives would be impossible at this point in time. However separation of the ester from the acid could be accomplished, this is quite useful in determining if conversion of esters to acids/salts (saponification step) is complete and could be used as a synthetic impurity method in the future.

Outlined below we believe to be the optimum method that can be used for detection/quantitation of acids/salt:

1) System set-up

Analytical Method Development- Method B					
Column	***Wave-length***	***Mobile Phase***	***Flow Rate***	***Sample Concentration***	***Run Time***
C18	210nm	85:15 0.05M K_2PO_4:MeOH (pH7)	0.3ml/ min	0.5mg/ml	15mins

2) Overnight multiple injections for column saturation.
3) Sample standard preparation for calibration 0.0625mg/mL.
4) Inject samples, followed by column flushing using the cleaning procedure described above.
5) Continue injection of samples.

7.4 Experimental:

1.0 HPLC Method Development

The following HPLC methods were developed to separate the different derivatives of pyrogallol[4]arenes. All compounds are derived from tetra-4-fluorophenyl pyrogallol[4]arene.

1.1 TopChem Laboratories® Analytical Development.

Instrument: Not Available

Column: C18

Wavelength: 210nm

Mobile Phase: 100% 0.05M KH_2PO_4, pH = 3

Flow Rate: 0.5ml/min

Sample Prep: 26mg/ml

Run Time: 60mins

1.2 Analytical Development; Method A

Instrument: Varian 9012, using the Varian Pro Star PDA Detector and a model 410 Varian Pro Star Autosampler.

Column: Zorbax, RX - C18 4.6mm x 150mm, 5µm

Wavelength: 210nm

Mobile Phase: 85% 0.05M KH_2PO_4, 15% Methanol, pH = 7

Flow Rate: 0.5ml/min

Sample Prep: 1.35mg/ml

Run Time: 60mins

1.3 Analytical Development; Method B

Instrument: Varian 9012, using the Varian Pro Star PDA Detector and a model 410 Varian Pro Star Autosampler.

Column: Zorbax, RX - C18 4.6mm x 150mm, 5µm

Wavelength: 210nm

Mobile Phase: 85% 0.05M KH_2PO_4, 15% Methanol, pH = 7

Flow Rate: 0.3ml/min

Sample Prep: 0.5mg/ml

Run Time: 15mins

Chapter 8

Structural Diversity,

Condensation with Dialdehydes

8.1 Introduction:

As a final section of this research, we wanted to exploit the structural possibilities of this new class of macrocycle. We began to explore the possibility of making more sophisticated macrocycles. On analysis of the *rctt* chair isomer of pyrogallol[4]arene we noticed that if we could bridge the two pendant aryl groups on the methylene bridges (derived from the aldehyde), we would have a macrocycle with three molecular rings. This new marcocycle could open up possibilities in receptor chemistry, self assembly, drug delivery and even nano-technology. Figure 46 shows the crystal structure of tetra-4-fluorophenyl pyrogallol[4]arene, **65,** highlighting the two pendant groups and how they could be linked.

Figure 46: *Crystal Structure of tetra-4-fluoro phenyl pyrogallol[4]arene,**30**, with pendant R-group linked to form a more sophisticated macrocycle.*

8.2 Results and Discussion:

Our first synthetic strategy to prepare these macrocycles, involved the condensation of an aryl dialdehyde with pyrogallol to form the target product (scheme 39).

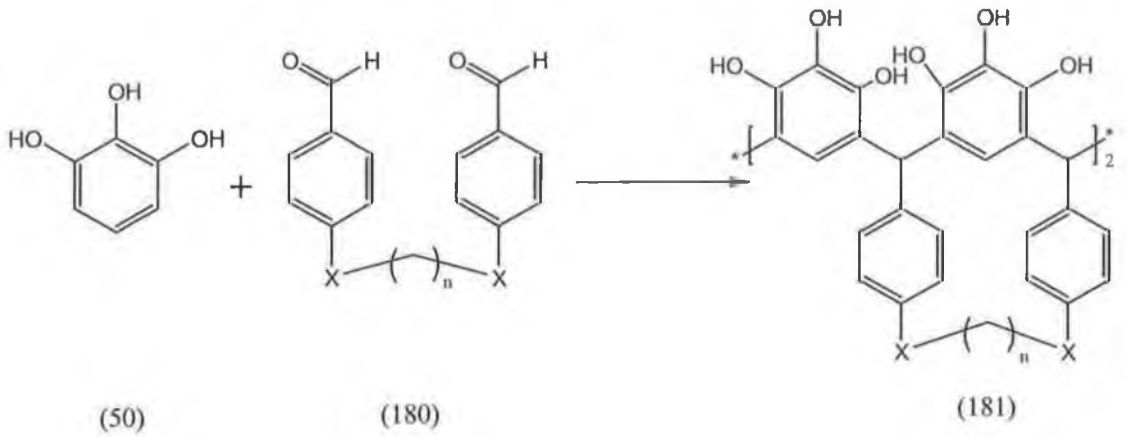

(50) (180) (181)

Scheme 39: *Condensation of pyrogallol with a dialdehyde*

The first approach we attempted is outlined in scheme 40, and involved the conversion of *p*-bromomethyl benzyl bromide, **182**, to the ethyl ester, **183**, which was to be reduced to the aldehyde, **184** and subsequently protected. Then **185,** (using ethane-1,2-diol – glycol, **71**), would be converted into a Grignard, **186,** and condensed with the other half of the protected aldehyde, **185**. This would be then followed by a simple deprotection reaction to form the target product, **188**.

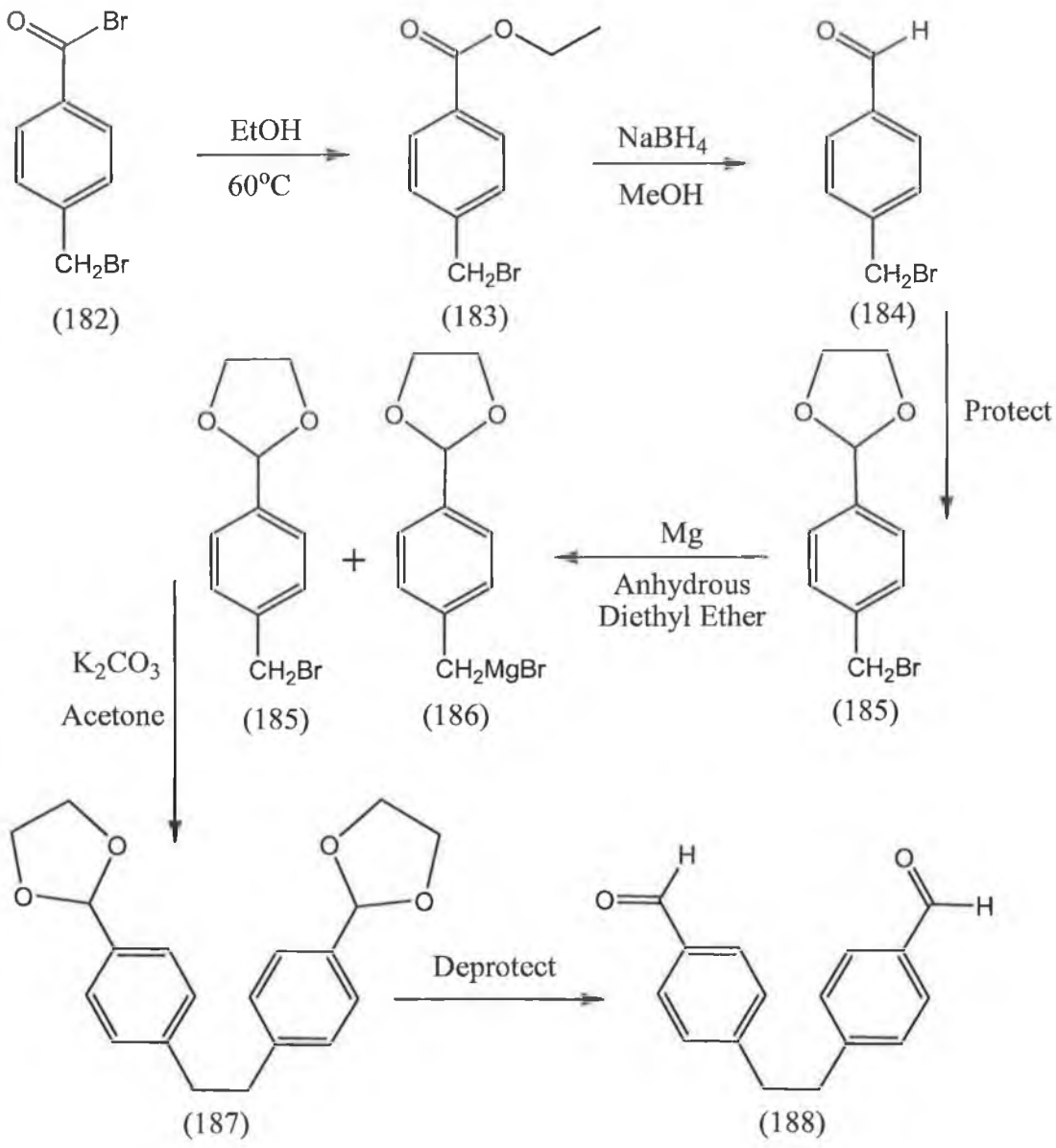

Scheme 40: *First attempt at synthesising the dialdehyhe system.*

This attempt failed in the first step, where the bromomethyl group on the 4 position of the benzene ring was also alkylated to give the ether ester, **183,** (figure 47). This was verified by ^{1}H-NMR and mass spectrometry. This is not a surprising result as the bromomethyl group is also susceptible to alkylation. We had hoped that by using stiochiometric control we would be able to alkylate the acid bromide group in the 1 position only, as it is more likely to be alkylated.

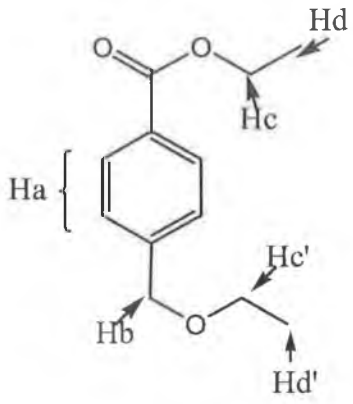

(183)

Figure 47: *Product from the first step of attempt 1, p-(ethyl ether) ethyl benzoate,131.*

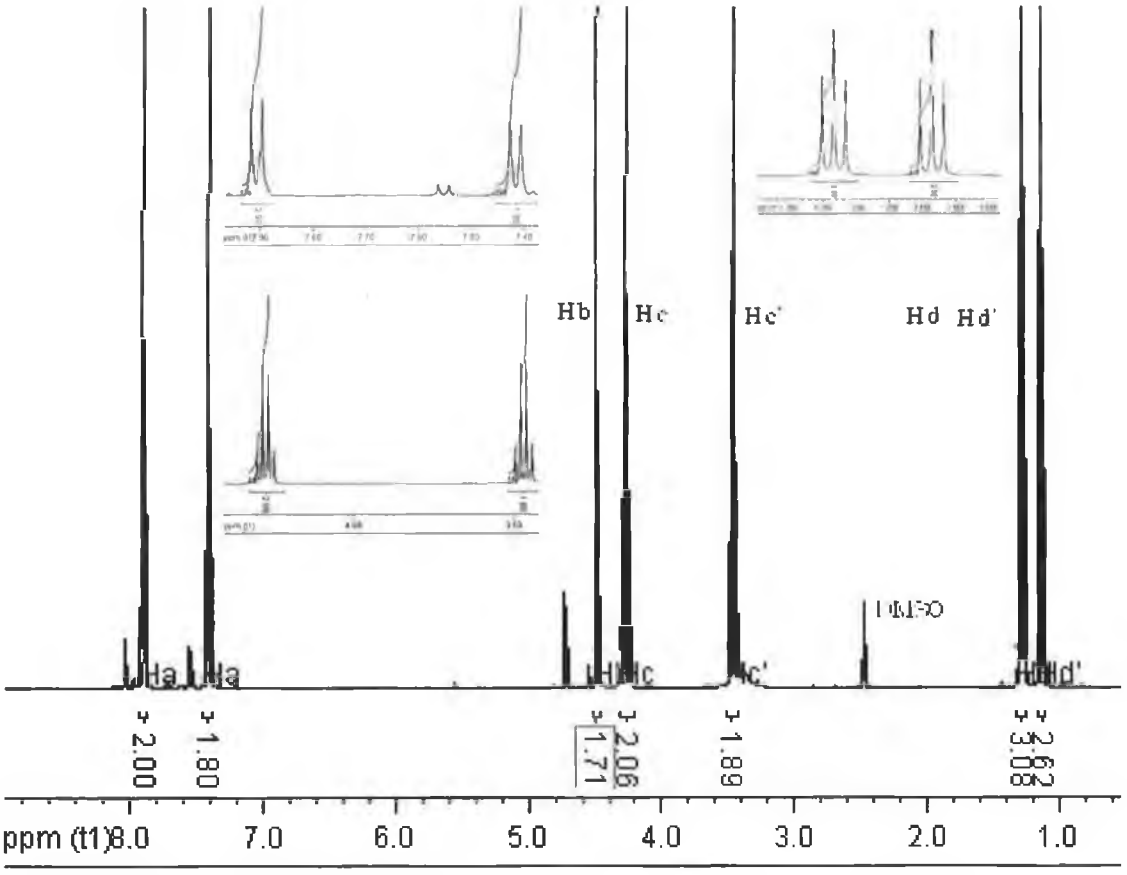

Figure 48: *^{1}H-NMR (DMSO-D_6) of p-(ethyl ether) ethyl benzoate*

The proton ^{1}H-NMR of *p*-(ethyl ether) ethyl benzoate, **183** (figures 47 & 48) gave a doublet of doublets at 7.2 and 7.5ppm which can be assigned to the 1,4-disubstituted phenyl ring (Ha) and the singlet at 4.25ppm represents the CH_2 group (Hb) on the 4

position of the phenyl ring. The ester protons are present as a quartet at 4.15ppm (Hc) and a triplet at 1.15ppm (Hd). The ether protons are a quartet at 3.25ppm (Hd'), and a triplet at 1.05ppm (Hd'). The ester protons are slightly shifted down field in comparison to the ether proton owing to the carbonyl group of the ester.

This synthetic plan was abandoned in favour of attempt 2 outlined in scheme 41. This plan involved the condensation of *p*-bromomethyl benzoic acid, **189** with glycol, **71,** to form the diacid, **190** this would then be reduced to form the dialdehyde, **191**. This reaction could lead to a mixture of six compounds, which would have to be separated by column chromatography.

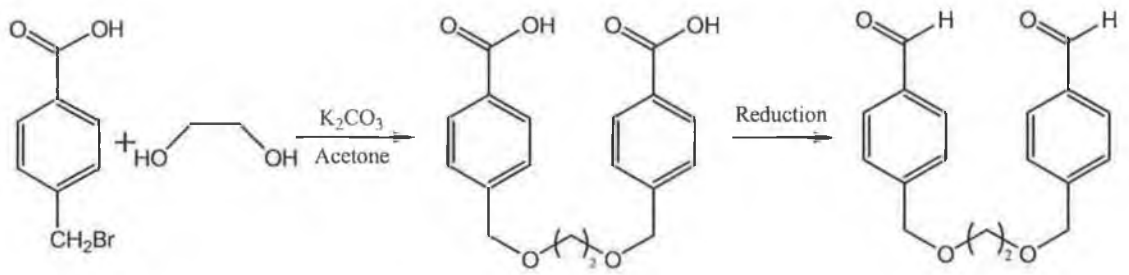

(189) (71) (190) (191)

Scheme 41: *Attempt 2 at synthesising the dialdehyde system.*

The first reaction was left to react for 3 days and yielded a mixture of starting material, monoalkylated and dialkylated adducts (analysis by ^{1}H-NMR and TLC). The reaction was then repeated for 6 days with extra equivalents of potassium carbonate added each day. This reaction yielded the same mixture as before, and this plan was abandoned in favour of attempt 3, (scheme 42).

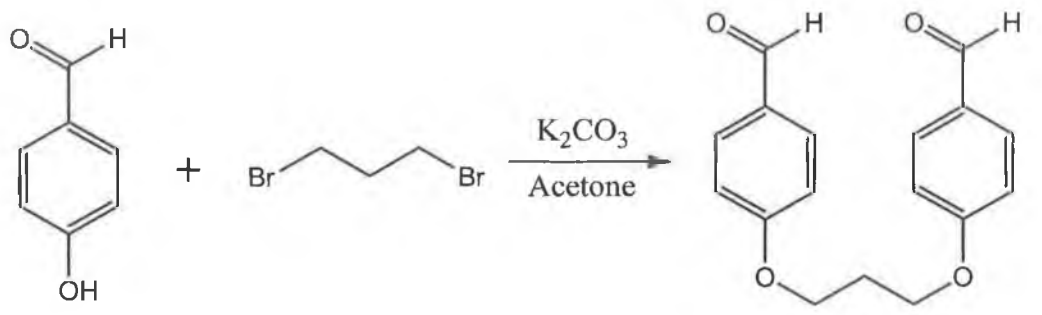

(192) (193) (194)

Scheme 42: *Attempt 3 at preparing the dialdehyde system.*

In this attempt 4-hydroxybenzaldehyde, **192,** was treated with 1,3-dibromopropane to give the dialdehyde, **194**. This was verified by ^{1}H-NMR. The product was recrystallised from hot methanol and was recovered in 35% yield. After the dialdehyde moiety was synthesised the next step was to proceed in making our desired macrocycle, **196,** as shown in scheme 43.

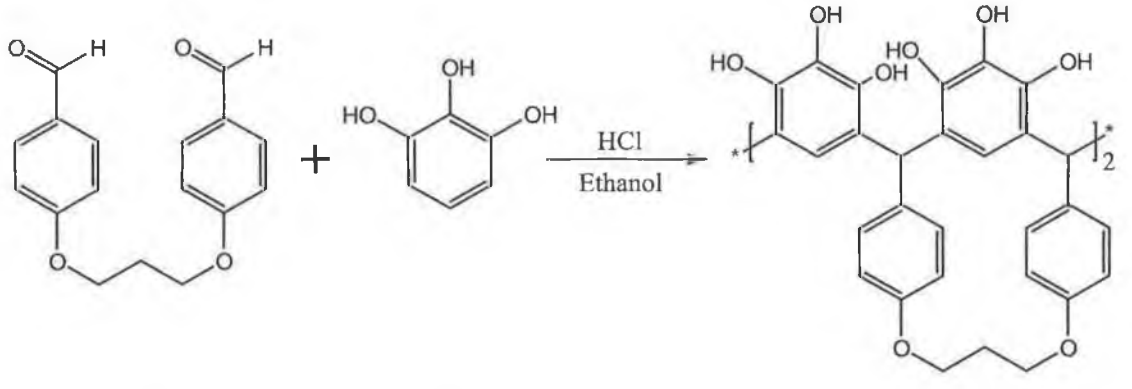

(195) (50) (196)

Scheme 43: *Condensation of dialdehyde system, **142**, with pyrogallol, **2**.*

The first attempt yielded a red precipitate after 24hours. This precipitate was found to be completely insoluble in all solvents and therefore it was not possible to attain ^{1}H-NMR data. The sample was sent for microanalysis and the results are outlined in table 19.

	%C	%H
Theoretical	69.59	4.83
Actual	64.44	4.53
Difference	5.15	0.30

Table 19: *Microanalysis Results from dialdehyde condensation reaction.*

It is clear from this table that the desired product was not obtained. Due to the poor solubility in many different solvents, it was presumed that this product is a cross linked polymer.

In an attempt to inhibit polymer formation a series of reactions was set up, where the concentrations of the reactants were progressively decreased. Keeping the original concentration (100%) as a positive control and decreasing the concentration to 5%, unfortunately this had no effect on the reaction outcome, (concentrations are displayed in table 20), all six different concentrations gave the same insoluble red precipitate.

Reaction No.	Conc.	Pyrogallol	Dialdehyde	HCl	Ethanol
8.4.1-A	100%	0.50g (71mg/ml)	0.56g (80mg/ml)	2ml	5ml
8.4.1-B	50%	0.50g (36mg/ml)	0.56g (40mg/ml)	4ml	10ml
8.4.1-C	25%	0.25g (18mg/ml)	0.28g (20mg/ml)	4ml	10ml
8.4.1-D	10%	0.10g (7.1mg/ml)	0.112g (8mg/ml)	4ml	10ml
8.4.1-E	5%	0.05g (3.6mg/ml)	0.056g (4mg/ml)	4ml	10ml

Table 20: *Concentration study.*

The next attempt at driving this reaction involved changing the condensation conditions, from hydrochloric acid to a weaker acid, acetic acid. Again this attempt was to no avail as the same insoluble red precipitate was produced.

The fourth and final attempt at this condensation involved a series of reactions whereby the HCl acid concentration was progressively lowered. Taking the lowest concentration (Reaction 8.4.1-E - 5%, table 20) from the previous concentration study the acid volume was initially halved and then progressively lowered from 2ml to 0.02ml and then even to 1 drop.

Once again these eight reactions gave the same product. This attempt was then abandoned in favour of the alkylation outlined in scheme 44.

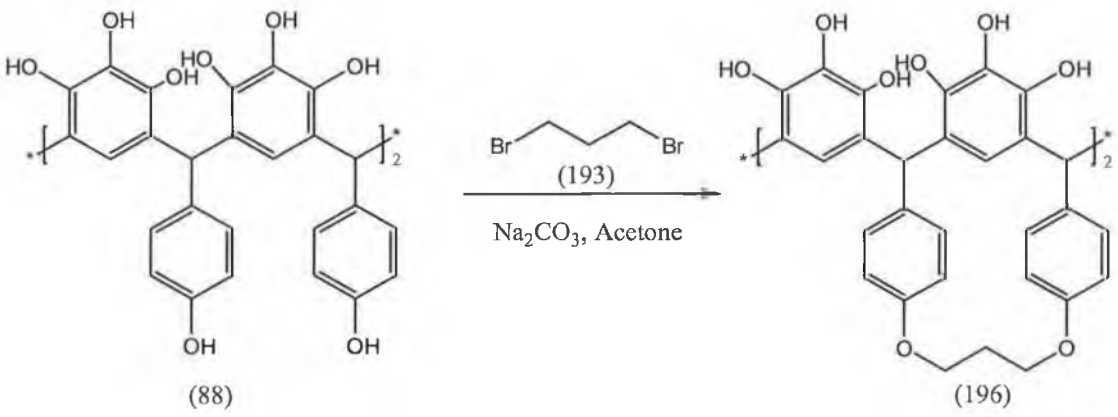

Scheme 44: *Dialkylation of tetra-4-hydroxyphenyl pyrogallol[4]arene with 1,3-dibromopropane.*

This reaction gave a large mixture of compounds as mono-alkylation occurred along with alkylations of the pyrogallol hydroxyl groups. The only way this reaction would proceed is if the pyrogallol hydroxyl groups were alkylated, however it is difficult to

do this without alkylating the lower rim hydroxyl groups as well. A synthetic plan for this reaction is currently being investigated in our research group as in scheme 45.

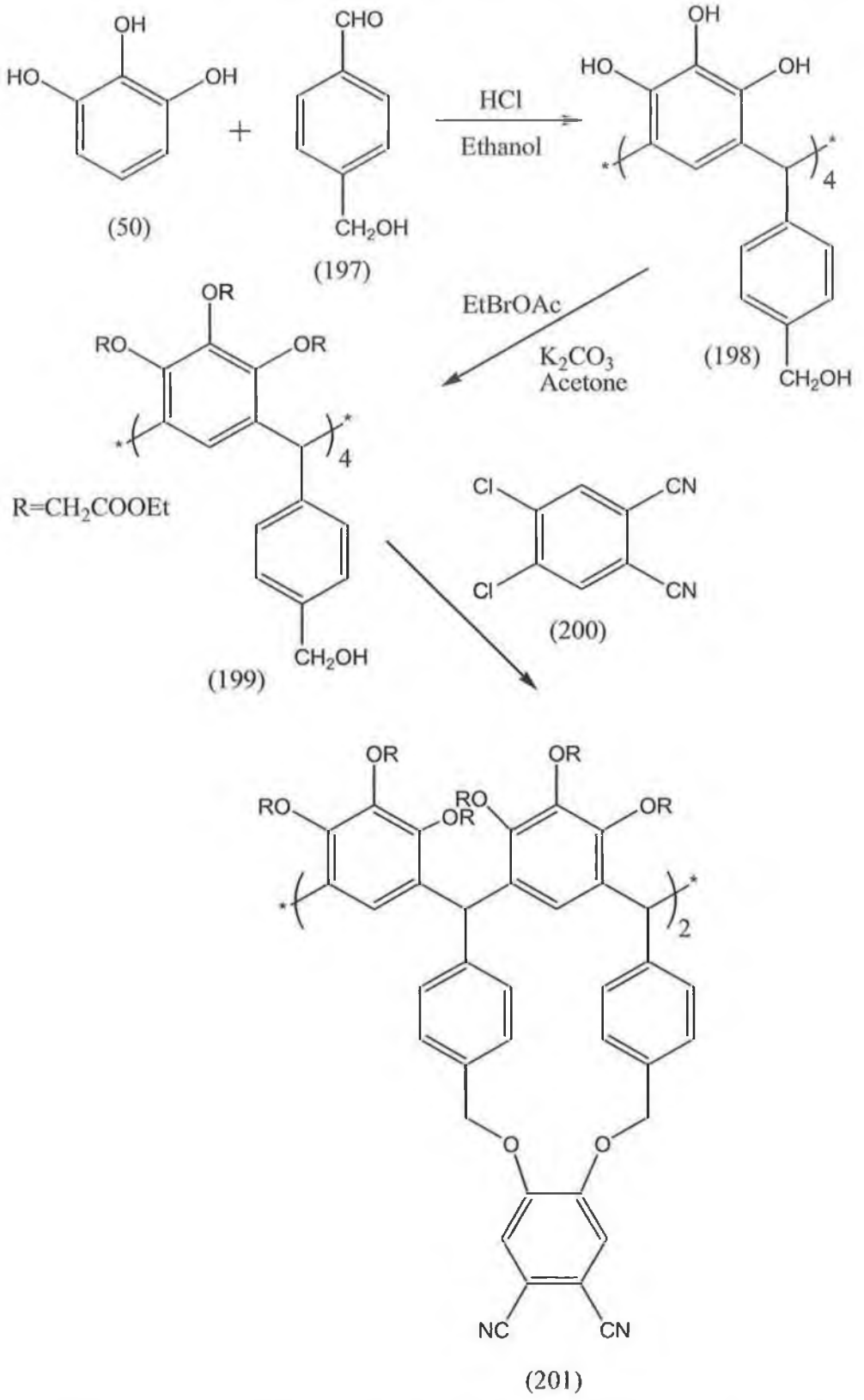

Scheme 45: *Current investigation into synthesis of sophisicated macrocycle.*

8.3 Experimental:

8.3.1 Alkyaltion of *p*-bromomethyl benzylbromide, 182, with Ethanol

3.6mmol (1.0g) of *p*-bromomethyl benzylbromide, **182**, was added to 3.5ml of Ethanol and the reaction was heated to 60°C and was stirred overnight under an inert atmosphere. The reaction mixture had turned to a straw yellow colour upon which solvent was removed under reduced pressure. The resulting yellow oil was recrystallised from ethyl acetate and was washed with water via liquid-liquid extraction. The resulting dry oil was analysed by ^{1}H-NMR and Mass Spectrometry and was found to be the dialkylated adduct, **183**.

^{1}H-NMR- (400MHz) δ (DMSO-D_6) [ppm]

1.05ppm (3H, triplet, J=6.4Hz, Ar-CH_2-O-$CH_2C\mathbf{H}_3$), 1.15ppm (3H, triplet, J=6.4Hz, Ar-C(=O)-O-$CH_2C\mathbf{H}_3$), 3.25ppm (2H, quartet, J=6.8Hz, Ar-CH_2-O-$C\mathbf{H}_2CH_3$), 4.1ppm (2H, quartet, J=6.8Hz, Ar-C(=O)-O-$C\mathbf{H}_2CH_3$), 4.25ppm (2H, s, Ar-$C\mathbf{H}_2$-OR), 7.2ppm (2H, d, J=7.2Hz, Ar-**H**), 7.45ppm (2H, d, J=7.2Hz, Ar-**H**).

Mass Spec: M/Z: 231 (M+Na)

8.3.2 Condensation of *p*-bromomethyl benzoic Acid, 189, with Glycol, 71.

4.65mmol (1.0g) of *p*-bromomethyl benzoic acid, **189** and 1.86mmol (0.12g, 0.104ml) of glycol, **71** (ethan-1,2-diol) were treated with 7.44mmol (1.03g) of potassium carbonate in 5ml of acetone. The reaction was refluxed at 60°C for 3-6 days. On completion, the solvent was removed under reduced pressure, and dilute HCl was

added to neutralise excess potassium carbonate, 0.33g of a white product precipitated. This was analysed by ^{1}H-NMR and found to be a mixture of products.

^{1}H-NMR- (400MHz) δ (DMSO-D_6) [ppm]

4.55ppm (1H, s, Ar-CH_2-O-C**H**$_2$R), 4.65ppm (1H, s, Ar-CH_2-O-C**H**$_2$R), 4.8ppm (1H, s, Ar-CH_2-O-C**H**$_2$R), 5.45ppm (2H, multiplet, Ar-C**H**$_2$-O-CH_2R), 7.5ppm (4H, multiplet, Ar-**H**), 8.0ppm (4H, multiplet, Ar-**H**).

8.3.3 Condensation of *p*-hydroxybenzaldehyde with 1,3-dibromopopane.

8.2mmol (1.0g) of *p*-hydroxybenzaldehyde, **192,** and 4.1mmol (0.82g, 0.41ml) of 1,3-dibromopropane, **193,** were treated with 12.3mmol (1.70g) of potassium carbonate in 10ml of acetone. The reaction was allowed to reflux for 6 days. The reaction mixture was filtered and exhaustively washed with acetone. The filtrates were collected and the solvent removed under reduced pressure, to leave an off-white solid. This solid was then recrystallised from hot methanol to yield 0.40g (1.44mmol , 35%) of a white powder, which was found to be the desired dialdhyde system, **194.**

^{1}H-NMR- (400MHz) δ (DMSO-D_6) [ppm]

2.25ppm (2H, quartet, J=6.4Hz, Ar-O-CH_2-C**H**$_2$R), 4.30ppm (4H, Triplet, J=6.8Hz Ar-O-C**H**$_2$-CH_2R), 7.15ppm (4H, d, J=7.2Hz Ar-**H**), 7.90ppm (4H, d, J=7.2Hz Ar-**H**), 9.90ppm (2H, s, Ar-COO**H**).

Mass Spec: M/Z: 303 (M+Na)

8.3.4 Condensation of Dialdehyde system, 195, with Pyrogallol, 50.

2.0mmol (0.25g) of pyrogallol, **50**, and 1.0mmol (0.28g) of dialdehyde, **195**, were treated with 1ml of hydrochloric acid in 2.5ml of ethanol at 80°C overnight. The reaction mixture was filtered to yield an insoluble red solid. The insoluble solid was sent for microanalysis.

Microanalysis: $C_{58}H_{48}O_{16}$: Theoretical: %C – 69.59; %H – 4.83; Actual: %C - 64.44; %H – 4.53

8.3.4.1 Concentration Study of 8.4

A series of reactions were carried out as in Experiment 8.4, with the concentration of reactants being progressively decreased as outlined in table 21.

Reaction No.	Conc	Pyrogallol	Dialdehyde	HCl	Ethanol
8.4.1 -A	100%	0.50g (71mg/ml)	0.56g (80mg/ml)	2ml	5ml
8.4.1–B	50%	0.50g (36mg/ml)	0.56g (40mg/ml)	4ml	10ml
8.4.1–C	25%	0.25g (18mg/ml)	0.28g (20mg/ml)	4ml	10ml
8.4.1–D	10%	0.10g (7.1mg/ml)	0.112g (8mg/ml)	4ml	10ml
8.4.1–E	5%	0.05g (3.6mg/ml)	0.056g (4mg/ml)	4ml	10ml

Table 21: *Concentration study.*

8.3.4.2: Condensation of Dialdehyde system with Pyrogallol, using a weaker acid.

The reaction was carried out as in Experiment **8.4** using 0.8mmol (0.1g) of pyrogallol, **50**, 0.04mmol (0.112g) and 4ml of acetic acid in 10ml in ethanol. As in Experiment **3.2** the reaction yielded an insoluble red solid.

8.3.4.3: Acid Concentration Study

A series of reactions was set up as in Experiment 8.4.1-E, with the concentration of acid halved initially and then being progressively decreased as described in table 22.

Reaction No.	Pyrogallol	Dialdehyde	HCl (Conc.)	Ethanol
8.4.3 –A	0.05g	0.056g	2ml (0.167ml/ml)	10ml
8.4.3–B	0.05g	0.056g	1ml (0.091ml/ml)	10ml
8.4.3–C	0.05g	0.056g	0.5ml (0.048ml/ml)	10ml
8.4.3–D	0.05g	0.056g	0.25ml (0.024ml/ml)	10ml
8.4.3–E	0.05g	0.056g	0.1ml (0.010ml/ml)	10ml
8.4.3–F	0.05g	0.056g	0.05ml (0.005ml/ml)	10ml
8.4.3–G	0.05g	0.056g	0.02ml (0.002ml/ml)	10ml
8.4.3–H	0.05g	0.056g	1 drop (<0.001ml/ml)	10ml

Table 22: *Acid concentration study.*

Once again the insoluble red solid was formed, in all cases.

8.3.5 Alkylation of tetra-4-hydroxyphenyl pyrogallol[4]arene, 88, with 1,3-dibromopropane, 193.

1.09mmol (1.0g) of tetra-4-hydroxyphenyl pyrogallol[4]arene, **88**, and 2.18mmol (0.44g, 0.22ml) of 1,3-dibromopropane, **193**, were treated with 6.54mmol (0.69g) of sodium carbonate in 60ml of acetone. The reaction was refluxed at 60°C for 3 days. A brown precipitate was filtered and washed with acetone, and the resulting product was analysed by ^{1}H-NMR. The ^{1}H-NMR was found to be poorly resolved and this is due to a large mixture of compounds. The filtrate was also retained and the solvents were removed under reduced pressure and the resulting yellow product was also analysed by ^{1}H-NMR, however there was no NMR signal. This product is presumed to be excess bromine salts.

8.4 Thesis Conclusion:

After completing all the above work, and revisiting our initial seven research proposals, we can conclude the following:

The yield of the pyrogallol[4]arene condensation can be improved. A series of optimisation experiments was carried out and we have now reported the optimum condensation conditions, with reproducible yields of up to 93% depending on the aldehyde used.

The stereochemistry of the pyrogallol[4]arenes was thoroughly investigated and discussed. The predominent stereoisomer derived from aryl aldehydes is the *rctt* chair isomer, and from alkyl aldehydes is the *rccc* cone conformation. There are, however, some exceptions to this rule.

Biological investigations have shown us that the lead compounds are in fact mixtures of partially alkylated derivatives, The problem, however, lies in the development of a reproducible synthetic method to form partially alkylated derivatives. To date all we have been able to do is produce "enriched" samples of partially alkylated derivatives.

With regard to specific structural limitations, for biological performance, the derivative needs to be partially alkylated (there may be some oxidation/reduction chemistry occurring with the residual hydroxy groups). There is a size effect issue also. The particle size in an aqueous solution of some of these compounds was measured using PCS and a correlation was observed between the biologically active

compounds and those of smaller particle size. Finally our inability to alkylate a *rccc* cone stereoisomer leaves this investigation incomplete.

We have also developed an analytical HPLC method to detect these molecules. The method uses a low sample concentration and therefore is suitable for potential *in vivo* studies in the future.

The final element of the research was an attempt to develop a more sophisticated class of pyrogallolarene and perhaps a new lead structure. We still believe that this is possible, however more work is required in the area.

Bibliography

1. Niederl, J.; Vogel, H.; *J. Am. Chem. Soc.*, **1940**, *62*, 2512.

2. a) Erdtman, H; Högberg, S; Abarhamsson, S; Nilsson, B; *Tetrahedron Lett.* 1968, 1679: b) Nilsson, B.; *Acta Chem. Scand.*, **1968**, *22*, 732.

3. Gutsche, C.; *Calixarenes, Monographs in Supramol. Chem.*; Stoddart, J., Ed.; Royal Society of Chemistry: Cambridge, **1989**; Vol. 1.

4. Vicens, J; Bömher, V.; Eds. *Calixarenes: A Versatile Class of Macrocyclic Compounds*; Kluwer Academic Press: Dordrecht, **1991**.

5. Egberink, R.; Cobben, P.; Verboom, W; Harkema, S; Reinhoudt, D.; *J.Inclusion Phenom.*, **1992**, *12*, 151.

6. Tunstad, L.; Tucker, J.; Dalcanale, E; Weiser, J; Bryant, J.; Sherman, J.; Helgeson, R.; Knobler, C.; Cram, D.; *J. Org. Chem.*, **1989**, *54*, 1305.

7. Cram, D.; Karbach,S; Kim, H.; Knobbler, C.; Maverick, E.; Ericson, J.; Helgeson, R.; *J. Am. Chem. Soc.*, **1988**, *110*, 2229.

8. Schneider, U; Schneider, H.; *Chem. Ber.*, **1994**, *127*, 2455.

9. Thoden van Velzen, E.; Engbersen, J.; Reinhoudt, D.; *J. Am. Chem. Soc.*, **1994**, *116*, 3597.

10. Högberg, A.; *J. Org. Chem.*, **1980**, *45*, 4498.

11. Kobayashi, K; Asakawa, Y; Kato, Y; Aoyama, Y.; *J. Am. Chem. Soc.*, **1992**, *114*, 10307 and references cited therein.

12. Ma, B.; Zhang, Y.; Coppen, P.; *Crystal Growth and Design, Communications*, **2005**, *0, 0*, 1. http://harker.chem.buffalo.edu./group/publication/CEC2.pdf, 15 November 2005

13. Palmer,K.; Wong, R.; Jurd, L.; Stevens, K.; *Acta Crystallogr., Sect. B,* **1976**, *32*, 847.

14. Abis, L.; Dacanale, E.; Du Vosel, A.; Spera, S.; *J. Org. Chem.*, **1988**, *53*, 5475.

15. Högberg, A.; *J. Am. Chem. Soc.,* **1980,** *45*, 4498.

16. Palmer, L.; Rebek, J.; *Org. Lett.,* **2005**, *7*, 5.

17. Cometti, C,; Dalcanale, E.; Du Vosel, A., Levelut, A.; *J. Chem. Soc., Chem Commun.,* **1990**, 163.

18. Kalchenko, V.; Rudkevich, D.; Shivanyuk, A.; Pirozenko, V.; Tsymbal, I.; Markovsky, L.; *Russ. J. Gen. Chem.*, **1994**, *64*, 731.

19. Hu, W.; Rourke, J.; Vital, J.; *Inorg. Chem.*, **1995**, *34*, 323.

20. Kalchenko, V.; Solov'yov, A.; Gladun, N.; Shivanyuk, A.; Atamas, L.; Pirozenko, V.; Markovsky, L.; Lipkowski, Yu A.; Simonov, A.; *Supramol. Chem.*, **1997**, *8*, 269.

21. Neda, I.; Sidentop, T.; Vollbreact, A.; Theonessen, H.; Jones, P.; Schmutzler, R.; Naturforsch, Z.; *Chem. Sci.*, **1998**, *53*, 841.

22. Yamakawa, Y.; Ueda, M.; Nagahata, R.; Takeuchi, T.; Asai, M.; *J. Chem, Soc. Perkin Trans*, *1*, **1998**, 4135.

23. Fransen, J.; Dutton, P.; *Can. J. Chem.*, **1995**, *73*, 2217.

24. Mislin, G.; Graf, E.; Hosseine, M.; De Cian, A.; Kyritsakas, N.; Fisher, J.; *Chem. Commun.*, **1998**, 2545.

25. Schneider, U.; Schneider, H.; *Chem. Ber.*, **1994**, *127*, 2455.

26. Leigh, D.; Linnane, P.; Pitchard, R.; Jackson, G.; *J. Chem.Soc., Chem Commun.*, **1994**, 389.

27. Linanne, P.; Shinkai, S.; *Tetrahedron Lett.*, **1995**, *36*, 3865.

28. Buckley, B.; Page, P.; Heaney, H.; Sampler, E.; Carley, S.; Brocke, C.; Brimble, M.A.; *Tetrahedron*, **2005**, *61*, 5876.

29. Schneider, H.; Güttes, D.; Schneider, U.; *J. Am. Chem. Soc.*, **1988**, *110*, 6449.

30. For a related case of this geometrical disposition, see: Saenger, W; Betzel, C; Hingerty, B.; Brown, G.; *Angew. Chem.* **1983**, *95*, 908: *Angew. Chem., Int. Ed. Engl.*, **1983**, *22*, 883.

31. Schneider, H.; Schneider, U.; *J. Org. Chem.*, **1987**, *52*, 1613 and references cited therein.

32. Schneider, H.; Güttes, D.; Schneider, U.; *Angew. Chem.*, **1986**, *98*, 635; *Agnew. Chem., Int. Ed. Engl.*, **1986**, *25*, 647.

33. Schneider, H.; *Thesis, I. Agnew. Chem.*, **1989**, *101*, 757; *Angew. Chem., Int. Ed. Engl.*, **1989**, *28*, 753.

34. Lippmann, T.; Wilde, H.; Pink, M.; Schäfer, A.; Hesse, M.; Mann, G.; *Angew. Chem.*, **1993**, *105*, 1258; *Angew. Chem., Int. Ed. Engl.*, **1993**, *32*, 1195.

35. Shivanyuk, A.; Rebek, J.Jr., *Proc Nat Acad Sci USA,* **2001**, *98*, 7662.

36. Moran, J.; Karback, S.; Cram, D. J., *J. Am. Chem. Soc.*, **1982**, *104*, 5826.

37. Cram, D.;Stewart, K.; Goldberg, I.; Trueblood, K.; *J. Am. Chem. Soc.*, **1985**, *107*, 2574.

38. Xu, W.; Rarke, J.; Jadagese, S.;Puddephatt, R., *J. Chem. Soc., Chem. Commun.*, **1993**, 145.

39. Pons, M.; Millet, O., *Progress in Nuclear Magnetic Resonance Spectroscopy*, **2001**, *38*, 267.

40. Holmes, J.; Tasker, P.; EP0400773, A3, B1, *EP19900301815 19900220,* **1990**.

41. Matsushita, Y.; Matsui; T. *Tetrahedron Lett.,* **1993**, *34,* 7433.

42. Gutsche, C.; *Calixarenes*; *first edition*, Washington University, **1989©**

43. Högberg, A.; *J. Am. Chem. Soc.,* **1980,** *102*, 6046.

44. Atwood, J.; Barbour, L.; Jerga, A.; *J. Supramol. Chem.*, **2001**, *1*, 131.

45. Gerkensmeier, T.; Iwanek, W.; Agena, C.; Frohlich, R.; Kotila, S.; Mattay, J.; *Eur. J. Org. Chem.*, **1999**, 2257.

46. Wu, L.; Gerard, N.; Wyatt, R.; Choe, H.; Parolin, C.; Ruffing, N.; Borsetti, A.; Cardosa, A.; Desjardin, E.; Newman, W.; *Nature*, **1996**, *384*, 179.

47. MacGillivray, L.; Atwood, J.; *Nature*, **1997**, *389*, 169.

48. Eds.; Billups, W.; Ciufolini, M.; *Buckminsterfullerenes*, VCH: New York, **1993.**

49. Murakami, Y.; Ohno, T.; Hayashida, O.; Hisaeda, Y.; *J. Chem. Soc., Chem. Commun.*, **1991**, 950.

50. Kobayashi, K.; Tominaga, M.; Asakawa, Y.; Aoyama, Y.; *Tetrahedron Lett.*, **1993**, *34*, 5121.

51. Kobayashi, K.; Asakawa, Y.; Kikuchi, Y.; Toi, H.; Aoyama, Y.; *J. Am. Chem. Soc.*, **1992**, 114.

52. Nishio, M.; Hirota, M.; *Tetrahedron*, **1989**, *45*, 7201.

53. www.howstuffworks.com/health/diseases/AIDS, 23 April 2004.

54. www.andrew.cmu.edu/ user/weit/reserved/hiv.jpg, 6 May 2004.

55. Kwong, P.; Wyatt, R.; Robinson, J.; Sweet, R.; Sodroske, J.; Hendnekson, W.; *Nature*, **1998**, *393*, 648.

56. Robey, W.; Safai, B.; Oroszian, S.; Arthur, L.; Gnda, M., Gallo, R.; Fishinger, P.; *Science*, **1985**, *228*, 593.

57. Moore, J.; *Science*, **1997**, *276*, 51.

58. Speck, R.; Wehrly, K.; Platt, E.; Atchison, R.; Charo, I.; Kabot, D.; Chesebro, B.; Goldsmith, M.; *J. Virol.*, **1997**, *71*, 7139.

59. Wyatt, R.; Kwong, P.; Robinson, J.; Sweet, R.; Sodroski, J.; Hendricks, W.; *Nature*, **1998**, *393*, 705.

60. Gallo, S.; Finnegan, C.; Viard, M.; Raviv, Y.; Dimitrov, A.; Blumenthal, R.; *Biochemica et Biophysica Acta*, **2003**, *1614*, 36.

61. Consultation with Dr. Robin Shatock, St. Georges Hospital, London.

62. Ryser, H.; Fluckiger, R.; *DDT*, **2005**, *10*, *16*, 1086.

63. Biscone, M.; Pierson, T.; Doms, R.W.; *Current Opinion in Pharmacology*, **2002**, *2*, 529.

64. De Clercq, E; *Biochemica et Biophysica Acta,* **2002**, *1587*, 258.

65. Watson, K.; Goodeham, N.; Davies, D.; Edwards, R.; *Biochem Pharm,* **1999**, *57*, 775.

66. Santhosh, K.; Paul, G.; Pannecouque, C.; Witurouw, M.; Loftus, T.; Turpin, J.; Buckleit, R.; Cushman, M.; *J. Med. Chem.* **2001**, *44*, 703.

67. http://www.who.int/hiv/topics/microbicides/microbicides/en/, 15 May 2004.

68. Aids Care Pharma, *TopChem Laboratories,* Analytical Report, **Nov. 2002.**

69. Harris, S.; *Calixarene-Based Compounds having Antibacterial, Antifungal, Anticancer-HIV Activity*, **WO9519974 - 1995-07-27**.

70. Böhmer, V.; Shivanyuk, A.; Paulus, E.; Vogt, W.; *Angew Chem. Int. Ed. Engl.* **1997**, *36*, No. 12. 1301.

71. Thompson, M.; Busch, D.; *J. Am. Chem. Soc*, **1964,** *86*, 3651.

72. http://wulfenite.fandm.edu/Data%20/Table_22.html, 12 March 2005.

73. Thondorf, I.; Brenn, J.; Böhmer, V.; *Tetrahedron*, **1998**, *54*, 12823.

74. http://www.chem.ucalgary.ca/courses/351/Carey/Ch12/ch12-11.html, 21 April 2005.

75. Ph.D. Thesis, S. O' Malley, Dublin City University, **2006.**

76. Ph.D. Thesis, Rachel Wall, Dublin City University, **2002.**

77. Budka, J.; Lhoták, P.; Michlová, V.; Stibor, I.; *Tetrahedron Lett.* **2001**, *42*, 1583.

78. Dudic, M.; Colombo, A.; Sansone, F.; Casnati, A.; Donofrio, G.; Ungaro, R.; *Tetrahedron*, **2004**, *60*, 11613.

79. Dixon, D.; Gill, A.; Giribabu, L.; Vzorov, A.; Alam, A.; Compans, R.; *Journal of Inorganic Biochemistry,* **2005**, *99*, 813.

80. Mc Murry, J.; *Organic Chemistry*; *Third edition*, Cornell University, **1992©**

81. Rawle, A.; *PCS in 30 Minutes*, www.malvern.com, April 2004.

82. Crystallography carried out Dr. Helge Müller-Bunz in U.C.D. Sept 2004.

Appendices

Appendix 1:

X-ray crystal structure data for tetra-4-fluoro pyrogallol[4]arene[82].

Table 1. Crystal data and structure refinement for kno06.

Identification code	kno06
Empirical formula	$C_{68}\ H_{88}\ O_{22}\ F_4\ S_8$
Molecular formula	$C_{52}\ H_{36}\ O_{12}\ F_4$ x 8 $C_2\ H_6\ O\ S$ x 2 $H_2\ O$
Formula weight	1589.86
Temperature	100(2) K
Wavelength	0.71073 Å
Crystal system	Triclinic
Space group	P–1 (#2)
Unit cell dimensions	a = 10.6871(10) Å α= 62.7760(10)°. b = 14.0609(13) Å β= 72.812(2)°. c = 15.2198(15) Å γ = 70.779(2)°.
Volume	1891.6(3) Å^3
Z	1
Density (calculated)	1.396 Mg/m^3
Absorption coefficient	0.318 mm^{-1}
F(000)	836
Crystal size	1.60 x 0.80 x 0.80 mm^3
Theta range for data collection	2.05 to 26.00°.
Index ranges	–13<=h<=13, –17<=k<=17, –18<=l<=18
Reflections collected	29403
Independent reflections	7410 [R(int) = 0.0222]
Completeness to theta = 26.00°	99.8 %
Absorption correction	Semi–empirical from equivalents
Max. and min. transmission	0.7850 and 0.6430
Refinement method	Full–matrix least–squares on F^2
Data / restraints / parameters	7410 / 14 / 530
Goodness–of–fit on F^2	1.030
Final R indices [I>2sigma(I)]	R1 = 0.0366, wR2 = 0.0966
R indices (all data)	R1 = 0.0401, wR2 = 0.0988
Largest diff. peak and hole	0.434 and –0.318 e.Å^{-3}

Table 2. Atomic coordinates (x 10^4) and equivalent isotropic displacement parameters ($Å^2$x 10^3)
for kno06. U(eq) is defined as one third of the trace of the orthogonalized U^{ij} tensor.

Atom	x	y	z	U(eq)
C(1)	3488(1)	–246(1)	3945(1)	15(1)
C(2)	3514(2)	973(1)	3458(1)	17(1)
C(3)	4232(2)	1366(1)	3799(1)	24(1)
C(4)	4268(2)	2465(1)	3380(1)	26(1)
C(5)	3599(2)	3167(1)	2594(1)	26(1)
F(1)	3642(1)	4253(1)	2169(1)	36(1)
C(6)	2915(2)	2821(2)	2207(2)	36(1)
C(7)	2854(2)	1719(2)	2662(1)	29(1)
C(8)	2902(2)	–543(1)	3329(1)	15(1)
C(9)	3725(2)	–782(1)	2523(1)	16(1)
O(1)	5052(1)	–769(1)	2325(1)	21(1)
C(10)	3194(2)	–1020(1)	1929(1)	17(1)
O(2)	4043(1)	–1271(1)	1144(1)	22(1)
C(11)	1829(2)	–1007(1)	2135(1)	16(1)
O(3)	1283(1)	–1243(1)	1573(1)	21(1)
C(12)	970(2)	–692(1)	2895(1)	15(1)
C(13)	1534(2)	–488(1)	3490(1)	16(1)
C(14)	–540(2)	–548(1)	3022(1)	15(1)
C(15)	–999(2)	–1622(1)	3552(1)	18(1)
C(16)	–265(2)	–2574(1)	4192(1)	25(1)
C(17)	–775(2)	–3519(2)	4715(1)	35(1)
C(18)	–2006(2)	–3478(2)	4581(2)	40(1)
F(2)	–2494(2)	–4411(1)	5097(1)	65(1)
C(19)	–2764(2)	–2558(2)	3955(2)	36(1)
C(20)	–2246(2)	–1630(2)	3437(1)	26(1)
C(21)	–1353(1)	243(1)	3522(1)	14(1)
C(22)	–1469(2)	1365(1)	2970(1)	16(1)
O(4)	–807(1)	1720(1)	1998(1)	21(1)
C(23)	–2279(2)	2117(1)	3382(1)	17(1)
O(5)	–2417(1)	3206(1)	2739(1)	24(1)

C(24)	–2927(2)	1744(1)	4380(1)	16(1)
O(6)	–3763(1)	2447(1)	4818(1)	21(1)
C(25)	–2779(1)	618(1)	4963(1)	15(1)
C(26)	–1999(1)	–110(1)	4521(1)	15(1)
O(7)	6711(1)	9555(1)	10545(1)	25(1)
S(1)	7620(1)	8432(1)	10648(1)	23(1)
C(27)	7440(2)	8202(2)	9638(1)	32(1)
C(28)	9287(2)	8646(2)	10203(2)	32(1)
O(8)	7457(1)	2589(1)	–638(1)	37(1)
S(2)	6265(1)	2714(1)	152(1)	28(1)
C(29)	6494(2)	3718(2)	468(2)	34(1)
C(30)	6586(2)	1539(2)	1280(2)	33(1)
O(9A) [a]	–663(2)	5740(1)	1207(1)	26(1)
S(3A) [a]	453(1)	5250(1)	1826(1)	24(1)
C(31A) [a]	272(8)	6175(6)	2380(5)	35(1)
C(32A) [a]	–85(3)	4146(2)	2926(2)	36(1)
O(9B) [b] [e]	75(14)	5300(11)	1267(9)	82(4)
S(3B) [b]	–656(5)	5647(3)	2138(3)	69(2)
C(31B) [b] [e]	540(30)	6040(30)	2420(30)	41(8)
C(32B) [b] [e]	–722(17)	4438(11)	3212(11)	59(4)
O(10A) [c]	6493(2)	4607(1)	3661(1)	32(1)
S(4A) [c]	5965(1)	5828(1)	3103(1)	30(1)
C(33A) [c]	5754(5)	6035(4)	1909(3)	36(1)
C(34A) [c]	4260(5)	6117(4)	3631(4)	73(2)
O(10B) [d] [e]	5848(8)	4532(6)	3632(6)	44(2)
S(4B) [d]	4693(3)	5372(2)	3153(2)	40(1)
C(33B) [d] [e]	5650(40)	6070(30)	2016(17)	113(13)
C(34B) [d] [e]	4107(14)	6301(12)	3709(12)	29(3)
O(11)	9710(2)	3750(1)	822(1)	40(1)

[a] s.o.f = 0.804(2) [b] s.o.f. = 0.196(2) [c] s.o.f = 0.776(2) [d] s.o.f. = 0.224(2) [s.o.f.: site occupation factor; the sums of the s.o.f.'s a) and b) as well as c) and d) are constrained to be 1] [e] only isotropic temperature factors could be refined.

Table 3. Bond lengths [Å] and angles [°] for kno06.

C(1)–C(8)	1.525(2)
C(1)–C(25)#1	1.527(2)
C(1)–C(2)	1.530(2)
C(1)–H(1A)	1.0000
C(2)–C(7)	1.386(2)
C(2)–C(3)	1.393(2)
C(3)–C(4)	1.385(2)
C(3)–H(3A)	0.9500
C(4)–C(5)	1.370(2)
C(4)–H(4A)	0.9500
C(5)–C(6)	1.367(3)
C(5)–F(1)	1.3700(19)
C(6)–C(7)	1.393(3)
C(6)–H(6A)	0.9500
C(7)–H(7)	0.9500
C(8)–C(13)	1.391(2)
C(8)–C(9)	1.391(2)
C(9)–O(1)	1.3640(18)
C(9)–C(10)	1.399(2)
O(1)–H(1)	0.8400
C(10)–O(2)	1.3827(18)
C(10)–C(11)	1.395(2)
O(2)–H(2)	0.8400
C(11)–O(3)	1.3656(18)
C(11)–C(12)	1.396(2)
O(3)–H(3)	0.8400
C(12)–C(13)	1.393(2)
C(12)–C(14)	1.524(2)
C(13)–H(13)	0.9500
C(14)–C(15)	1.520(2)
C(14)–C(21)	1.524(2)
C(14)–H(14)	1.0000
C(15)–C(16)	1.387(2)
C(15)–C(20)	1.398(2)
C(16)–C(17)	1.396(3)
C(16)–H(16)	0.9500

C(17)–C(18)	1.369(3)
C(17)–H(17)	0.9500
C(18)–F(2)	1.369(2)
C(18)–C(19)	1.369(3)
C(19)–C(20)	1.382(3)
C(19)–H(19)	0.9500
C(20)–H(20)	0.9500
C(21)–C(22)	1.389(2)
C(21)–C(26)	1.396(2)
C(22)–O(4)	1.3695(18)
C(22)–C(23)	1.394(2)
O(4)–H(4)	0.8400
C(23)–O(5)	1.3752(19)
C(23)–C(24)	1.396(2)
O(5)–H(5)	0.8400
C(24)–O(6)	1.3747(18)
C(24)–C(25)	1.398(2)
O(6)–H(6)	0.8400
C(25)–C(26)	1.389(2)
C(25)–C(1)#1	1.527(2)
C(26)–H(26)	0.9500
O(7)–S(1)	1.5211(13)
S(1)–C(28)	1.7819(18)
S(1)–C(27)	1.7824(18)
C(27)–H(27A)	0.9800
C(27)–H(27B)	0.9800
C(27)–H(27C)	0.9800
C(28)–H(28A)	0.9800
C(28)–H(28B)	0.9800
C(28)–H(28C)	0.9800
O(8)–S(2)	1.4971(14)
S(2)–C(30)	1.782(2)
S(2)–C(29)	1.7892(19)
C(29)–H(29A)	0.9800
C(29)–H(29B)	0.9800
C(29)–H(29C)	0.9800
C(30)–H(30A)	0.9800
C(30)–H(30B)	0.9800

C(30)–H(30C)	0.9800
O(9A)–S(3A)	1.5212(16)
S(3A)–C(31A)	1.784(5)
S(3A)–C(32A)	1.784(2)
C(31A)–H(31A)	0.9800
C(31A)–H(31B)	0.9800
C(31A)–H(31C)	0.9800
C(32A)–H(32A)	0.9800
C(32A)–H(32B)	0.9800
C(32A)–H(32C)	0.9800
O(9B)–S(3B)	1.528(12)
S(3B)–C(32B)	1.743(12)
S(3B)–C(31B)	1.773(15)
C(31B)–H(31D)	0.9800
C(31B)–H(31E)	0.9800
C(31B)–H(31F)	0.9800
C(32B)–H(32D)	0.9800
C(32B)–H(32E)	0.9800
C(32B)–H(32F)	0.9800
O(10A)–S(4A)	1.5156(16)
S(4A)–C(34A)	1.755(5)
S(4A)–C(33A)	1.776(4)
C(33A)–H(33A)	0.9800
C(33A)–H(33B)	0.9800
C(33A)–H(33C)	0.9800
C(34A)–H(34A)	0.9800
C(34A)–H(34B)	0.9800
C(34A)–H(34C)	0.9800
O(10B)–S(4B)	1.495(8)
S(4B)–C(34B)	1.725(12)
S(4B)–C(33B)	1.750(15)
C(33B)–H(33D)	0.9800
C(33B)–H(33E)	0.9800
C(33B)–H(33F)	0.9800
C(34B)–H(34D)	0.9800
C(34B)–H(34E)	0.9800
C(34B)–H(34F)	0.9800
O(11)–H(1O)	0.79(3)

O(11)–H(2O)	0.82(3)
C(8)–C(1)–C(25)#1	111.28(12)
C(8)–C(1)–C(2)	111.59(12)
C(25)#1–C(1)–C(2)	113.26(12)
C(8)–C(1)–H(1A)	106.8
C(25)#1–C(1)–H(1A)	106.8
C(2)–C(1)–H(1A)	106.8
C(7)–C(2)–C(3)	117.50(15)
C(7)–C(2)–C(1)	122.16(14)
C(3)–C(2)–C(1)	120.33(14)
C(4)–C(3)–C(2)	121.82(15)
C(4)–C(3)–H(3A)	119.1
C(2)–C(3)–H(3A)	119.1
C(5)–C(4)–C(3)	118.18(16)
C(5)–C(4)–H(4A)	120.9
C(3)–C(4)–H(4A)	120.9
C(6)–C(5)–F(1)	118.99(16)
C(6)–C(5)–C(4)	122.53(16)
F(1)–C(5)–C(4)	118.46(16)
C(5)–C(6)–C(7)	118.23(16)
C(5)–C(6)–H(6A)	120.9
C(7)–C(6)–H(6A)	120.9
C(2)–C(7)–C(6)	121.65(16)
C(2)–C(7)–H(7)	119.2
C(6)–C(7)–H(7)	119.2
C(13)–C(8)–C(9)	118.25(13)
C(13)–C(8)–C(1)	121.82(13)
C(9)–C(8)–C(1)	119.67(13)
O(1)–C(9)–C(8)	118.42(13)
O(1)–C(9)–C(10)	121.18(13)
C(8)–C(9)–C(10)	120.39(14)
C(9)–O(1)–H(1)	109.5
O(2)–C(10)–C(11)	120.90(13)
O(2)–C(10)–C(9)	118.99(13)
C(11)–C(10)–C(9)	120.11(14)
C(10)–O(2)–H(2)	109.5

O(3)–C(11)–C(10)	121.41(13)
O(3)–C(11)–C(12)	118.28(13)
C(10)–C(11)–C(12)	120.23(14)
C(11)–O(3)–H(3)	109.5
C(13)–C(12)–C(11)	118.20(13)
C(13)–C(12)–C(14)	122.51(13)
C(11)–C(12)–C(14)	119.26(13)
C(8)–C(13)–C(12)	122.57(14)
C(8)–C(13)–H(13)	118.7
C(12)–C(13)–H(13)	118.7
C(15)–C(14)–C(12)	113.94(12)
C(15)–C(14)–C(21)	110.76(12)
C(12)–C(14)–C(21)	112.29(12)
C(15)–C(14)–H(14)	106.4
C(12)–C(14)–H(14)	106.4
C(21)–C(14)–H(14)	106.4
C(16)–C(15)–C(20)	118.98(15)
C(16)–C(15)–C(14)	122.31(14)
C(20)–C(15)–C(14)	118.59(14)
C(15)–C(16)–C(17)	120.11(17)
C(15)–C(16)–H(16)	119.9
C(17)–C(16)–H(16)	119.9
C(18)–C(17)–C(16)	118.48(19)
C(18)–C(17)–H(17)	120.8
C(16)–C(17)–H(17)	120.8
C(17)–C(18)–F(2)	117.9(2)
C(17)–C(18)–C(19)	123.45(17)
F(2)–C(18)–C(19)	118.6(2)
C(18)–C(19)–C(20)	117.56(18)
C(18)–C(19)–H(19)	121.2
C(20)–C(19)–H(19)	121.2
C(19)–C(20)–C(15)	121.42(18)
C(19)–C(20)–H(20)	119.3
C(15)–C(20)–H(20)	119.3
C(22)–C(21)–C(26)	118.01(13)
C(22)–C(21)–C(14)	119.29(13)
C(26)–C(21)–C(14)	122.71(13)
O(4)–C(22)–C(21)	118.56(13)

O(4)–C(22)–C(23)	120.59(14)
C(21)–C(22)–C(23)	120.81(14)
C(22)–O(4)–H(4)	109.5
O(5)–C(23)–C(22)	115.78(13)
O(5)–C(23)–C(24)	124.13(14)
C(22)–C(23)–C(24)	120.05(14)
C(23)–O(5)–H(5)	109.5
O(6)–C(24)–C(23)	122.54(14)
O(6)–C(24)–C(25)	117.37(13)
C(23)–C(24)–C(25)	120.04(14)
C(24)–O(6)–H(6)	109.5
C(26)–C(25)–C(24)	118.53(13)
C(26)–C(25)–C(1)#1	123.14(13)
C(24)–C(25)–C(1)#1	118.33(13)
C(25)–C(26)–C(21)	122.44(14)
C(25)–C(26)–H(26)	118.8
C(21)–C(26)–H(26)	118.8
O(7)–S(1)–C(28)	105.40(8)
O(7)–S(1)–C(27)	105.34(8)
C(28)–S(1)–C(27)	98.85(10)
S(1)–C(27)–H(27A)	109.5
S(1)–C(27)–H(27B)	109.5
H(27A)–C(27)–H(27B)	109.5
S(1)–C(27)–H(27C)	109.5
H(27A)–C(27)–H(27C)	109.5
H(27B)–C(27)–H(27C)	109.5
S(1)–C(28)–H(28A)	109.5
S(1)–C(28)–H(28B)	109.5
H(28A)–C(28)–H(28B)	109.5
S(1)–C(28)–H(28C)	109.5
H(28A)–C(28)–H(28C)	109.5
H(28B)–C(28)–H(28C)	109.5

O(8)–S(2)–C(30)	106.44(9)
O(8)–S(2)–C(29)	104.30(9)
C(30)–S(2)–C(29)	98.65(9)
S(2)–C(29)–H(29A)	109.5
S(2)–C(29)–H(29B)	109.5
H(29A)–C(29)–H(29B)	109.5
S(2)–C(29)–H(29C)	109.5
H(29A)–C(29)–H(29C)	109.5
H(29B)–C(29)–H(29C)	109.5
S(2)–C(30)–H(30A)	109.5
S(2)–C(30)–H(30B)	109.5
H(30A)–C(30)–H(30B)	109.5
S(2)–C(30)–H(30C)	109.5
H(30A)–C(30)–H(30C)	109.5
H(30B)–C(30)–H(30C)	109.5
O(9A)–S(3A)–C(31A)	106.3(3)
O(9A)–S(3A)–C(32A)	105.31(11)
C(31A)–S(3A)–C(32A)	98.8(2)
O(9B)–S(3B)–C(32B)	106.3(8)
O(9B)–S(3B)–C(31B)	105.8(13)
C(32B)–S(3B)–C(31B)	96.9(13)
S(3B)–C(31B)–H(31D)	109.5
S(3B)–C(31B)–H(31E)	109.5
H(31D)–C(31B)–	109.5

H(31E)	
S(3B)–C(31B)–H(31F)	109.5
H(31D)–C(31B)–H(31F)	109.5
H(31E)–C(31B)–H(31F)	109.5
S(3B)–C(32B)–H(32D)	109.5
S(3B)–C(32B)–H(32E)	109.5
H(32D)–C(32B)–H(32E)	109.5
S(3B)–C(32B)–H(32F)	109.5
H(32D)–C(32B)–H(32F)	109.5
H(32E)–C(32B)–H(32F)	109.5
O(10A)–S(4A)–C(34A)	106.03(19)
O(10A)–S(4A)–C(33A)	107.47(17)
C(34A)–S(4A)–C(33A)	98.1(3)
O(10B)–S(4B)–C(34B)	107.4(6)
O(10B)–S(4B)–C(33B)	96.9(14)
C(34B)–S(4B)–C(33B)	102.6(14)
S(4B)–C(33B)–H(33D)	109.5
S(4B)–C(33B)–H(33E)	109.5
H(33D)–C(33B)–H(33E)	109.5
S(4B)–C(33B)–	109.5

H(33F)	
H(33D)–C(33B)–H(33F)	109.5
H(33E)–C(33B)–H(33F)	109.5
S(4B)–C(34B)–H(34D)	109.5
S(4B)–C(34B)–H(34E)	109.5
H(34D)–C(34B)–H(34E)	109.5
S(4B)–C(34B)–H(34F)	109.5
H(34D)–C(34B)–H(34F)	109.5
H(34E)–C(34B)–H(34F)	109.5
H(1O)–O(11)–H(2O)	109(3)

Symmetry transformations used to generate equivalent atoms:
#1 –x,–y,–z+1

Table 4. Anisotropic displacement parameters ($Å^2 x\ 10^3$) for kno06. The anisotropic displacement factor exponent takes the form: $-2\pi^2[\ h^2\ a^{*2}U^{11} + ...\ + 2\ h\ k\ a^*\ b^*\ U^{12}\ ]$

Atom	U^{11}	U^{22}	U^{33}	U^{23}	U^{13}	U^{12}
C(1)	12(1)	19(1)	15(1)	–8(1)	–2(1)	–3(1)
C(2)	14(1)	21(1)	14(1)	–8(1)	0(1)	–4(1)
C(3)	21(1)	24(1)	26(1)	–5(1)	–10(1)	–7(1)
C(4)	22(1)	26(1)	34(1)	–12(1)	–8(1)	–8(1)
C(5)	29(1)	17(1)	28(1)	–8(1)	–3(1)	–5(1)
F(1)	44(1)	18(1)	43(1)	–7(1)	–14(1)	–7(1)
C(6)	53(1)	23(1)	33(1)	–6(1)	–26(1)	–2(1)
C(7)	41(1)	24(1)	30(1)	–10(1)	–19(1)	–5(1)
C(8)	16(1)	16(1)	14(1)	–6(1)	–4(1)	–3(1)
C(9)	13(1)	17(1)	16(1)	–6(1)	–3(1)	–2(1)
O(1)	14(1)	35(1)	19(1)	–16(1)	1(1)	–6(1)
C(10)	16(1)	18(1)	16(1)	–9(1)	–2(1)	–1(1)
O(2)	18(1)	32(1)	20(1)	–17(1)	–2(1)	–1(1)
C(11)	18(1)	15(1)	17(1)	–7(1)	–6(1)	–3(1)
O(3)	17(1)	31(1)	24(1)	–20(1)	–3(1)	–3(1)
C(12)	14(1)	15(1)	16(1)	–6(1)	–3(1)	–4(1)
C(13)	16(1)	18(1)	14(1)	–8(1)	–2(1)	–3(1)
C(14)	15(1)	18(1)	14(1)	–7(1)	–3(1)	–4(1)
C(15)	20(1)	20(1)	18(1)	–12(1)	1(1)	–6(1)
C(16)	33(1)	22(1)	22(1)	–11(1)	–4(1)	–8(1)
C(17)	60(1)	22(1)	25(1)	–8(1)	–5(1)	–13(1)
C(18)	58(1)	34(1)	37(1)	–20(1)	14(1)	–32(1)
F(2)	95(1)	45(1)	63(1)	–19(1)	13(1)	–52(1)
C(19)	32(1)	41(1)	49(1)	–29(1)	6(1)	–21(1)
C(20)	23(1)	29(1)	36(1)	–20(1)	–2(1)	–9(1)
C(21)	11(1)	18(1)	17(1)	–8(1)	–5(1)	–2(1)
C(22)	14(1)	21(1)	14(1)	–7(1)	–3(1)	–7(1)
O(4)	26(1)	18(1)	16(1)	–7(1)	2(1)	–8(1)
C(23)	18(1)	16(1)	20(1)	–6(1)	–7(1)	–4(1)
O(5)	34(1)	16(1)	20(1)	–7(1)	0(1)	–5(1)

C(24)	13(1)	19(1)	19(1)	–11(1)	–4(1)	–2(1)
O(6)	24(1)	18(1)	21(1)	–11(1)	–2(1)	–2(1)
C(25)	12(1)	20(1)	14(1)	–8(1)	–5(1)	–4(1)
C(26)	13(1)	16(1)	16(1)	–6(1)	–5(1)	–3(1)
O(7)	23(1)	30(1)	22(1)	–14(1)	0(1)	–4(1)
S(1)	21(1)	27(1)	20(1)	–10(1)	–1(1)	–5(1)
C(27)	40(1)	29(1)	30(1)	–16(1)	–10(1)	–4(1)
C(28)	20(1)	37(1)	34(1)	–13(1)	–2(1)	–6(1)
O(8)	42(1)	44(1)	34(1)	–28(1)	5(1)	–12(1)
S(2)	22(1)	36(1)	32(1)	–20(1)	–5(1)	–4(1)
C(29)	43(1)	30(1)	31(1)	–19(1)	–1(1)	–6(1)
C(30)	38(1)	30(1)	35(1)	–15(1)	–3(1)	–11(1)
O(9A)	24(1)	36(1)	22(1)	–15(1)	–7(1)	–2(1)
S(3A)	23(1)	31(1)	20(1)	–11(1)	–3(1)	–7(1)
C(31A)	44(3)	40(2)	30(2)	–18(2)	–9(2)	–12(3)
C(32A)	39(2)	41(1)	27(1)	–7(1)	–6(1)	–18(1)
S(3B)	93(4)	49(2)	76(3)	–15(2)	–50(2)	–15(2)
O(10A)	49(1)	16(1)	27(1)	–8(1)	–7(1)	–4(1)
S(4A)	46(1)	16(1)	28(1)	–9(1)	–7(1)	–8(1)
C(33A)	53(2)	33(2)	18(1)	–3(1)	–8(1)	–15(1)
C(34A)	77(3)	32(2)	52(2)	–3(2)	24(2)	9(2)
S(4B)	53(2)	29(1)	42(1)	–20(1)	–2(1)	–10(1)
O(11)	65(1)	26(1)	24(1)	–10(1)	7(1)	–19(1)

Table 5. Hydrogen coordinates (x 10^4) and isotropic displacement parameters (Å^{2}x 10^3)
for kno06.

Atom	x	y	z	U(eq)
H(1A)	4445	–669	3946	18
H(3A)	4710	867	4333	28
H(4A)	4744	2725	3630	31
H(6A)	2493	3318	1642	43
H(7)	2348	1474	2421	35
H(1)	5383	–724	1737	32
H(2)	3864	–755	597	33
H(3)	1897	–1584	1259	32
H(13)	961	–303	4026	19
H(14)	–758	–202	2330	18
H(16)	586	–2583	4275	29
H(17)	–278	–4176	5154	43
H(19)	–3616	–2559	3880	43
H(20)	–2747	–983	2992	32
H(4)	–855	2397	1775	31
H(5)	–2814	3600	3065	36
H(6)	–3724	3097	4424	32
H(26)	–1903	–876	4913	18
H(27A)	6505	8180	9715	47
H(27B)	8035	7500	9643	47
H(27C)	7680	8798	9001	47
H(28A)	9331	9249	9537	48
H(28B)	9914	7973	10159	48
H(28C)	9533	8832	10667	48
H(29A)	7385	3485	652	50
H(29B)	5800	3793	1036	50
H(29C)	6422	4427	–110	50
H(30A)	6567	883	1214	50
H(30B)	5894	1633	1842	50
H(30C)	7473	1454	1406	50

H(31A)	547	6845	1862	53
H(31B)	841	5826	2896	53
H(31C)	–670	6363	2686	53
H(32A)	–971	4423	3260	53
H(32B)	564	3825	3383	53
H(32C)	–144	3583	2739	53
H(31D)	1313	5418	2603	61
H(31E)	130	6267	2982	61
H(31F)	847	6656	1831	61
H(32D)	–1267	4034	3156	88
H(32E)	–1127	4616	3801	88
H(32F)	191	3983	3282	88
H(33A)	6637	5886	1503	54
H(33B)	5281	6797	1571	54
H(33C)	5226	5536	1994	54
H(34A)	3791	5664	3569	110
H(34B)	3857	6895	3279	110
H(34C)	4179	5953	4342	110
H(33D)	5046	6699	1587	169
H(33E)	6138	5575	1677	169
H(33F)	6285	6338	2146	169
H(34D)	4806	6688	3560	43
H(34E)	3876	5911	4437	43
H(34F)	3305	6834	3446	43
H(1O)	9890(30)	3900(20)	240(20)	66(9)
H(2O)	9330(30)	4310(20)	920(20)	56(8)

Table 6. Torsion angles [°] for kno06.

C(8)–C(1)–C(2)–C(7)	10.9(2)
C(25)#1–C(1)–C(2)–C(7)	–115.58(17)
C(8)–C(1)–C(2)–C(3)	–168.13(14)
C(25)#1–C(1)–C(2)–C(3)	65.36(18)
C(7)–C(2)–C(3)–C(4)	1.4(3)
C(1)–C(2)–C(3)–C(4)	–179.46(15)
C(2)–C(3)–C(4)–C(5)	–1.5(3)
C(3)–C(4)–C(5)–C(6)	–0.7(3)
C(3)–C(4)–C(5)–F(1)	–179.33(16)
F(1)–C(5)–C(6)–C(7)	–178.51(17)
C(4)–C(5)–C(6)–C(7)	2.9(3)
C(3)–C(2)–C(7)–C(6)	0.8(3)
C(1)–C(2)–C(7)–C(6)	–178.25(17)
C(5)–C(6)–C(7)–C(2)	–2.9(3)
C(25)#1–C(1)–C(8)–C(13)	37.17(19)
C(2)–C(1)–C(8)–C(13)	–90.41(17)
C(25)#1–C(1)–C(8)–C(9)	–148.78(14)
C(2)–C(1)–C(8)–C(9)	83.64(17)
C(13)–C(8)–C(9)–O(1)	175.90(13)
C(1)–C(8)–C(9)–O(1)	1.6(2)
C(13)–C(8)–C(9)–C(10)	–3.6(2)
C(1)–C(8)–C(9)–C(10)	–177.81(13)
O(1)–C(9)–C(10)–O(2)	1.6(2)
C(8)–C(9)–C(10)–O(2)	–178.99(14)
O(1)–C(9)–C(10)–C(11)	–178.73(14)
C(8)–C(9)–C(10)–C(11)	0.7(2)
O(2)–C(10)–C(11)–O(3)	0.2(2)
C(9)–C(10)–C(11)–O(3)	–179.53(14)
O(2)–C(10)–C(11)–C(12)	–176.40(14)
C(9)–C(10)–C(11)–C(12)	3.9(2)
O(3)–C(11)–C(12)–C(13)	177.87(13)
C(10)–C(11)–C(12)–C(13)	–5.4(2)
O(3)–C(11)–C(12)–C(14)	–4.2(2)
C(10)–C(11)–C(12)–C(14)	172.49(13)
C(9)–C(8)–C(13)–C(12)	1.9(2)
C(1)–C(8)–C(13)–C(12)	176.04(14)

C(11)–C(12)–C(13)–C(8)	2.6(2)
C(14)–C(12)–C(13)–C(8)	–175.31(14)
C(13)–C(12)–C(14)–C(15)	–103.86(16)
C(11)–C(12)–C(14)–C(15)	78.29(17)
C(13)–C(12)–C(14)–C(21)	23.1(2)
C(11)–C(12)–C(14)–C(21)	–154.75(13)
C(12)–C(14)–C(15)–C(16)	23.9(2)
C(21)–C(14)–C(15)–C(16)	–103.89(16)
C(12)–C(14)–C(15)–C(20)	–160.22(14)
C(21)–C(14)–C(15)–C(20)	72.03(17)
C(20)–C(15)–C(16)–C(17)	–0.4(2)
C(14)–C(15)–C(16)–C(17)	175.54(15)
C(15)–C(16)–C(17)–C(18)	–0.2(3)
C(16)–C(17)–C(18)–F(2)	179.87(16)
C(16)–C(17)–C(18)–C(19)	0.4(3)
C(17)–C(18)–C(19)–C(20)	0.0(3)
F(2)–C(18)–C(19)–C(20)	–179.45(17)
C(18)–C(19)–C(20)–C(15)	–0.6(3)
C(16)–C(15)–C(20)–C(19)	0.8(2)
C(14)–C(15)–C(20)–C(19)	–175.26(15)
C(15)–C(14)–C(21)–C(22)	–155.79(13)
C(12)–C(14)–C(21)–C(22)	75.56(17)
C(15)–C(14)–C(21)–C(26)	23.86(19)
C(12)–C(14)–C(21)–C(26)	–104.79(16)
C(26)–C(21)–C(22)–O(4)	178.10(13)
C(14)–C(21)–C(22)–O(4)	–2.2(2)
C(26)–C(21)–C(22)–C(23)	–4.1(2)
C(14)–C(21)–C(22)–C(23)	175.55(13)
O(4)–C(22)–C(23)–O(5)	3.5(2)
C(21)–C(22)–C(23)–O(5)	–174.24(13)
O(4)–C(22)–C(23)–C(24)	–178.68(13)
C(21)–C(22)–C(23)–C(24)	3.6(2)
O(5)–C(23)–C(24)–O(6)	–0.8(2)
C(22)–C(23)–C(24)–O(6)	–178.41(13)
O(5)–C(23)–C(24)–C(25)	176.77(14)
C(22)–C(23)–C(24)–C(25)	–0.9(2)
O(6)–C(24)–C(25)–C(26)	176.50(13)
C(23)–C(24)–C(25)–C(26)	–1.2(2)

O(6)–C(24)–C(25)–C(1)#1	–3.2(2)
C(23)–C(24)–C(25)–C(1)#1	179.10(13)
C(24)–C(25)–C(26)–C(21)	0.6(2)
C(1)#1–C(25)–C(26)–C(21)	–179.71(13)
C(22)–C(21)–C(26)–C(25)	2.1(2)
C(14)–C(21)–C(26)–C(25)	–177.60(13)

Symmetry transformations used to generate equivalent atoms:
#1 –x,–y,–z+1

Table 7. Hydrogen bonds for kno06 [Å and °].

D–H...A	d(D–H)	d(H...A)	d(D...A)	<(DHA)
O(11)–H(2O)...O(9B)#2	0.82(3)	2.11(3)	2.724(13)	131(3)
O(11)–H(2O)...O(9A)#2	0.82(3)	2.24(3)	2.992(2)	152(3)
O(11)–H(1O)...O(9B)#3	0.79(3)	2.03(3)	2.798(13)	163(3)
O(11)–H(1O)...O(9A)#3	0.79(3)	1.99(3)	2.772(2)	170(3)
O(6)–H(6)...O(10B)#4	0.84	1.80	2.613(8)	163.5
O(6)–H(6)...O(10A)#4	0.84	1.95	2.787(2)	171.2
O(5)–H(5)...O(10B)#4	0.84	1.89	2.705(8)	162.6
O(5)–H(5)...O(10A)#4	0.84	1.86	2.694(2)	171.2
O(4)–H(4)...O(11)#4	0.84	1.95	2.7267(18)	153.3
O(3)–H(3)...O(8)#5	0.84	1.89	2.6584(16)	152.2
O(2)–H(2)...O(7)#6	0.84	1.87	2.7107(17)	173.8

O(1)–H(1)...O(7)#7	0.84	1.91	2.6933(16)	154.4

Symmetry transformations used to generate equivalent atoms:

#1 –x,–y,–z+1 #2 x+1,y,z #3 –x+1,–y+1,–z

#4 x–1,y,z #5 –x+1,–y,–z #6 –x+1,–y+1,–z+1

#7 x,y–1,z–1

Appendix 2:

Cmpd Number	Concentration (ug/ml)	Syncytia (+/-)	Estimated % Control I	Estimated Cell Growth % of Control infected	Estimated Cell Growth % of Control uninfected	EC50	TC50	Selectivity Index
1151C	400	-		73	69	0.25	500	2000
Harris	80	-		105	100			
Comp.	16	-		92				
	3.2	-		92				
	0.64	ST-/+	17	72				
	0.128	ST-/+	63	30				
	0.0256	+		28				
04-002	400	TC50		41	42	0.015	350	23333
	80	-		93	94			
	16	-		99				
	3.2	-		104				
	0.64	-		101				
	0.128	-	14	100				
	0.0256	ST-/+	30	46.5				
04-003	400	TC50		44	45	0.012	350	29166
	80	-		100	100			
	16	-		96				
	3.2	-		100				
	0.64	-		100				
	0.128	-	0	100				
	0.0256	ST-/+	25	55				
04-004	400	T40		41	41	0.32	350	1100
	80	-		100	100			
	16	-		100				
	3.2	-		94				
	0.64	ST-/+	27	70				
	0.128	ST+/-	99	34				
	0.0256	+		29				
AC-	200	T		16	16	8	30	3.75
	40	T25		29	31			
	8	ST-/+	54	58	98			
	1.6	+	99	27	100			
	0.32	+		27				
	0.64	+		24				
AZT	2	-		100	100	0.016	>1000	>62500
	0.016	ST+/-	51	49				

Cmpd Number	Concentration (ug/ml)	Syncytia (+/-)	Estimated % Control I	cell growth U	gp120 % Control	Estimated % Inhibition	EC50	TC50	Selectivity Index	Comments
SC 103A	10000	T	10.69	9.63			190	4600	24.21	IC 17.3%
	2000	T30-	55.32	69.20	22.40	77.60	ug/ml	ug/ml		
	400	NT-/+	63.55	91.04	30.48	69.52				
	80	+	50.95	96.75	61.15	38.85				
	16	+	32.36	104.70	72.67	27.33				
SC 103B	400	T50-	52.18	41.10			10.8	320	29.63	IC 17.3%
	80	T20-	78.39	77.16	15.01	84.99	ug/ml	ug/ml		
	16	ST-/+	91.66	89.84	19.26	80.74				
	3.2	+	48.99	92.72	95.89	4.11				
	0.64	+	32.64	88.58	98.28	1.72				
SC 103C	2000	T50-	58.73	41.21			58	1420	24.48	IC 17.3%
	400	T30-	75.59	65.96	17.35	82.65	ug/ml	ug/ml		
	80	ST-/+	81.80	89.03	22.75	77.25				
	16	+	51.57	108.29	102.61	0.00				
	3.2	+	35.05	103.25	97.67	2.33				
SC 103D	2000	T50-	42.85	45.50	4.52	95.48	283	1850	6.54	IC 24%
	400	NT-/+	64.50	92.90	10.18	89.82	ug/ml	ug/ml		
	80	+	42.25	99.80	89.90	0.00				
	16	+	30.90	85.40	93.19	6.81				
SC 103E	10000	T-	17.80	19.30			57.8	2250	38.93	IC 24%
	2000	T50-	54.55	51.10			ug/ml	ug/ml		
	400	T40-	64.60	55.30	3.38	96.62				
	80	ST-	77.65	76.50	3.07	96.93				
	16	NT+	56.10	90.70	103.57	0.00				
	3.2	+	28.90	83.10	85.59	14.41				
SC 103F	2000	T50-	43.30	43.10			5.4	1660	307.41	IC 24%
	400	T30-	73.55	75.30			ug/ml	ug/ml		
	80	T10-	74.50	78.50	6.04	93.96				
	16	NT-/+	29.05	84.70	33.64	66.36				
	3.2	+	27.70	85.30	53.31	0.00				
	0.64	+	25.65	93.60	75.79	24.21				
SC 103N	10000	T-	14.25	11.70			9.5	4700	494.74	IC 24%
	2000	T50-	72.20	69.10			ug/ml	ug/ml		
	80	ST-/+	55.00	78.60	42.46	57.54				
	16	NT-/+	22.90	85.40	45.41	54.59				
	3.2	-/+	18.00	87.00	54.43	45.57				
	0.64	+	17.30	95.50	61.31	38.69				
	Control			**100**	**100**	**0**	—	----	----	

IC - Infected control

U - Uninfected control

T - Compound Toxic

ST - Slightly Toxic

NT - Non Toxic

Dilutions of compounds in 50 uls, are mixed with T-cells C8166, 40,000/well.

Virus HIV-1 111B is added at M.O.I of 0.01 and incubated for 5 days.

Syncytia observed from days 3-5

Cell viability by XTT-Formazan method at day 5.